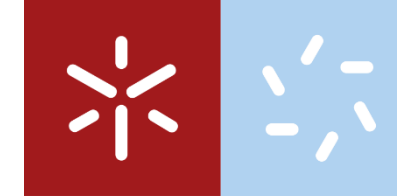




Bruna Daniela Rodrigues da Silva

**Synthesis of fused heteroaromatic N
and S compounds and antitumor
evaluation in human tumor cell lines**





Universidade do Minho

Escola de Ciências

Bruna Daniela Rodrigues da Silva

**Synthesis of fused heteroaromatic N
and S compounds and antitumor
evaluation in human tumor cell lines**

Dissertação de Mestrado

Bioquímica Aplicada

Especialização em Biomedicina

Trabalho efetuado sob a orientação da

**Professora Doutora Maria João Ribeiro
Queiroz**

e da

**Professora Doutora Maria Helena
Vasconcelos**

DIREITOS DE AUTOR E CONDIÇÕES DE UTILIZAÇÃO DO TRABALHO POR TERCEIROS

Este é um trabalho académico que pode ser utilizado por terceiros desde que respeitadas as regras e boas práticas internacionalmente aceites, no que concerne aos direitos de autor e direitos conexos.

Assim, o presente trabalho pode ser utilizado nos termos previstos na licença abaixo indicada.



Atribuição-NãoComercial-SemDerivações

CC BY-NC-ND

AGRADECIMENTOS

A realização desta dissertação de mestrado agora concluída só foi possível graças a diversos incentivos e apoios fulcrais ao longo de um ano de muito trabalho e esforço.

À **Professora Doutora Maria João Queiroz** agradeço a confiança que depositou em mim ao aceitar-me como sua aluna mesmo sabendo que não era da sua área. Agradeço igualmente todas as opiniões e críticas dadas durante o trabalho desenvolvido e por todas as dúvidas que por mais simples que fossem nunca se recusou a explicar-me. São poucos os orientadores que “perdem” tempo a explicar coisas básicas aos seus alunos. Por isso, pelo apoio quando mais precisei e por tudo o que pude aprender de novo, muito obrigada!

À **Professora Doutora Maria Helena Vasconcelos** estou grata por me ter dado a oportunidade de fazer metade do meu projeto num centro de investigação de referência onde não só pude aprender muitas novas técnicas que reforçaram muito a minha formação base que é Biologia como também tive contato com outros investigadores, seminários e cursos igualmente enriquecedores, e claro, por me ter me aceite como sua aluna sem me conhecer.

Quero também agradecer-te **Juliana** por tudo que me ensinaste no laboratório para fazer os meus compostos e a ti **Patrícia** pela ajuda e paciência para quem pouco sabia sobre um laboratório de Química. Acolheram-me muito bem e sempre foram minhas amigas. E ainda tivemos mega casório pelo meio!!! A ambas, pelo companheirismo, pela paciência e pela força nos dias menos positivos, obrigada.

Da mesma forma, serei para sempre grata a ti **Cristina Xavier** por tudo o que fiz e aprendi na parte biológica desta dissertação. Criámos logo uma empatia muito bonita e natural e devote tudo o que sei hoje desde ao nível prático das técnicas à análise e discussão de resultados e sei que vamos ficar amigas depois disto tudo. Alguns membros do CDR dizem que és uma máquina no laboratório e eu concordo, sabes muito e fazes muito (e muitas vezes não só por ti nem só pelo teu próprio benefício...). És uma referência para mim!

Aos restantes **membros do CDR**, muito obrigada por me terem recebido de braços abertos, por serem tão sociáveis, pelos bolos de grupo e pelos almoços mensais em sítios fantásticos que me deram a conhecer um bocadinho do Porto...obrigada. Dirijo um especial agradecimento a ti, **Diana**, pelas palavras e força que sempre soubeste dar quando mais precisei.

Dirijo um especial agradecimento a ti **Mãe** e a ti **Justin**, pelo apoio que me deram, pela calma que sempre souberam transmitir quando eu chegava a casa depois de um dia menos bom, pelo incentivo “Está quase!”, “Vai compensar!”, pelo constante encorajamento de prosseguir e pelo carinho e maminho que sempre me dão diariamente. Obrigada por me fazerem sentir que vale a pena todo o esforço e abdicar de certas (muitas) coisas, e que vou conseguir tudo aquilo que sempre sonhei, seja por um caminho mais direto ou outro.

A ti **Pai**, obrigada por me protegeres e iluminares, és o meu anjo da guarda e certamente estás orgulhoso de eu ter concluído mais uma etapa! “Storms make trees take deeper roots”.

Ao resto dos **meus familiares**, obrigada por indireta ou diretamente terem contribuído para que tudo isto se realizasse e pela confiança e orgulho que depositam em mim.

Finalmente, **aos meus verdadeiros amigos** que não chegava uma folha de agradecimentos para vos agradecer um a um da forma única que realmente merecem, mas em especial a ti **Patrícia** e a ti **Jú**, a ti **André** e a ti **Cate** e também a ti **Cris**, obrigada por toda a força dada, por todas as risadas que me fizeram dar quando eu mais precisei nesta fase da minha vida e por me lembrarem que sou capaz e que vou conseguir tudo aquilo que tanto ambiciono nas minhas metas a atingir. Obrigada por todos os “confia no processo, tudo vai correr bem, tudo vai ficar bem, tu consegues, tu és capaz, está quase...”. Obrigada por toda a paciência que tiveram para as minhas crises de ansiedade e por ser nessas alturas que me transmitiram a maior tranquilidade e força que tinham para me oferecer! Obrigada por me fazerem acreditar nisto e acima de tudo acreditar em mim e naquilo que valho nesta área e em tudo o resto que vocês sabem. Obrigada por serem realmente verdadeiros amigos, estão lá para os bons momentos, mas, acima de tudo, para os momentos menos bons e serão para sempre meus amigos, tenho a certeza!

STATEMENT OF INTEGRITY

I hereby declare having conducted this academic work with integrity. I confirm that I have not used plagiarism or any form of undue use of information or falsification of results along the process leading to its elaboration.

I further declare that I have fully acknowledged the Code of Ethical Conduct of the University of Minho.

Síntese de compostos N e S fundidos heteroaromáticos e avaliação antitumoral em linhas celulares tumorais humanas

RESUMO

Atualmente, devido ao *cancer burden*, a seleção de novos compostos sintéticos como potenciais antitumorais e a exploração de alguns dos seus possíveis mecanismos de ação têm sido objeto de contínuo interesse no combate ao cancro. Assim, o principal objetivo deste trabalho foi sintetizar novos compostos e avaliar o seu potencial antitumoral.

Novas tieno[3,2-*b*]piridinas funcionalizadas foram sintetizadas por acoplamento-cruzado C-C de Suzuki-Miyaura catalisado por Pd, usando o 3-bromotieno[3,2-*b*]piridina-2-carboxilato de metilo, também preparado, e (het)aril pinacolboranos, sais de trifluoropotássio de boro ou ácidos borónicos, e foram completamente caracterizadas (pf, ^1H , ^{13}C -RMN, Espectrometria de Massa de Alta Resolução ou Análise Elementar). O potencial antitumoral dos compostos foi avaliado em linhas celulares tumorais: pancreáticas (PANC1 e BxPC3), pulmão de células não pequenas (NCI-H460) e mama triplo negativo (MDA-MB-231 e MDA-MB-468) – pelo ensaio Sulforodamina B. Os mais promissores foram estudados quanto a possíveis efeitos no ciclo celular e no nível de expressão de algumas proteínas relacionadas com ciclo celular, apoptose e danos no DNA.

A série de 3-(het)ariltieno[3,2-*b*]piridina-2-carboxilatos de metilo foi preparada com fenilo ou arilos com dadores (OMe, Me) ou retiradores de eletrões (halogénio (Cl), nitrilo (CN), CF_3) na posição *para*, ou com heteroarilos, piridina, deficiente em eletrões, ou furano, rico em eletrões, com rendimentos moderados a altos. Nos ensaios biológicos três compostos inibiram o crescimento apenas nas linhas celulares de cancro da mama: o composto com *p*-Cl inibiu o crescimento das células MDA-MB-231, enquanto os compostos com *p*-CN e furano o das MDA-MB-468. Curiosamente, estes compostos apresentaram pouco ou nenhum efeito no crescimento das células não tumorais MCF-12A. Apesar de serem necessários mais ensaios, o derivado furano alterou o ciclo celular das células MDA-MB-468, aumentando a fase G2/M com conseqüente diminuição da fase G0/G1 e expressão aumentada de p21. Por outro lado, o composto *p*-Cl induziu dano no DNA e diminuiu o tamanho dos tumores xeno enxertados das células MDA-MB-231 no ensaio CAM (Chick Chorioallantoic Membrane) *in vivo*. Finalmente, o derivado *p*-CN não alterou o ciclo celular nem induziu apoptose nas concentrações testadas.

PALAVRAS-CHAVE: Acoplamento de Suzuki-Miyaura; Avaliação biológica; Cancro; Tienopiridinas.

Synthesis of fused heteroaromatic N and S compounds and antitumor evaluation in human tumor cell lines

ABSTRACT

Nowadays, due to cancer burden, the screening for new potential antitumoral synthetic compounds and the knowledge about some of their possible mechanisms of action have been object of continuing interest to tackle cancer. Thus, the main aim of this work was the synthesis of novel compounds and the evaluation of their potential antitumoral activity.

Novel functionalized thieno[3,2-*b*]pyridines were synthesized by C-C Pd-catalyzed Suzuki-Miyaura cross-coupling of methyl 3-bromothieno[3,2-*b*]pyridine-2-carboxylate, also prepared, with (het)aryl pinacol boranes, trifluoro potassium boronate salts or boronic acids, and were fully characterized (m.p., ¹H, ¹³C NMR, HRMS or Elemental Analysis). Their antitumoral potential was evaluated in human tumor cell lines - pancreatic (PANC1 and BxPC3), non-small cell lung (NCI-H460) and triple negative breast (MDA-MB-231 and MDA-MB-468) - by Sulforhodamine B assay. The most promising compounds were further studied concerning possible effects on cell cycle profile and expression levels of some proteins related with cell cycle, apoptosis and DNA damage.

The series of methyl 3-(het)arylthieno[3,2-*b*]pyridine-2-carboxylates was prepared with a phenyl ring or an aryl bearing electron donating (OMe, Me) or withdrawing (halogen (Cl), nitrile (CN), CF₃) groups, in the *para* position or with heteroaryl rings, pyridine, electron-deficient, or an furan, electron-rich, in moderate to high yields. The biological studies showed that three of the synthesized compounds caused growth inhibition only in breast cancer cell lines: *p*-Cl inhibited the growth of MDA-MB-231 cells while the *p*-CN and furan derivatives inhibited the growth of MDA-MB-468. Interestingly, these compounds had little or no effect in the growth of the non-tumorigenic MCF-12A cells. Although further assays are necessary, the furan derivative altered the cell cycle profile of MDA-MB-468 cells by increasing the G2/M phase with concomitant decrease in G0/G1 phase and increased expression of p21. On the other hand, the compound *p*-Cl induced DNA damage and decreased tumor size of xenografted MDA-MD-231 cells evaluated by the *in vivo* CAM (Chick Chorioallantoic Membrane) assay. Finally, *p*-CN derivative did not alter the cell cycle-profile nor induced apoptosis, at the concentrations tested.

KEYWORDS: Cancer; Screening; Suzuki-Miyaura coupling; Thienopyridines.

INDEX

DIREITOS DE AUTOR E CONDIÇÕES DE UTILIZAÇÃO DO TRABALHO POR TERCEIROS.....	ii
Agradecimentos.....	iii
STATEMENT OF INTEGRITY.....	v
Resumo.....	vi
Abstract	vii
Abbreviations List	xi
Index of Figures.....	xv
Index of Tables	xvii
Index of scheme.....	xviii
I – INTRODUCTION.....	1
1. Cancer.....	2
1.1 Types of cancer cells tested in this dissertation: pancreatic ductal adenocarcinoma, non-small cell lung cancer and triple negative breast cancers	5
1.1.1 PANCREATIC DUCTAL ADENOCARCINOMA.....	5
1.1.2 NON-SMALL LUNG CANCER	6
1.1.3 TRIPLE NEGATIVE BREAST CANCER	7
2. Screening of new compounds	9
2.1 Study of the activity of potential novel drugs in apoptosis and cell cycle	9
3. Thienopyridine derivatives and some of their biological properties.....	11
3.1 Thienopyridines and Cancer	12
3.1.1 Earlier work developed with thieno[3,2- <i>b</i>]pyridine derivatives in the scope of synthesis and biological studies in our research group	15
3.1.1.1 C-C SUZUKI COUPLING MOST PROMISSING PRODUCTS.....	17
3.1.1.2 C-C SONOGASHIRA COUPLING MOST PROMISSING PRODUCTS.....	18
3.1.1.3 C-N BUCHWALD-HARTWIG COUPLING MOST PROMISSING PRODUCTS.....	20
3.2 Other biological properties of thienopyridines	21
4. Rationale and aims.....	22

II - RESULTS AND DISCUSSION.....	24
1. Chemical Synthesis.....	25
1.1 Synthesis of starting materials	25
1.1.1 Synthesis of methyl 3-aminothieno[3,2- <i>b</i>]pyridine-2-carboxylate (1)	25
1.1.2 Synthesis of methyl 3-bromothieno[3,2- <i>b</i>]pyridine-2-carboxylate (2).....	26
1.2 C-C Suzuki-Miyaura cross-coupling	27
1.2.1 Introduction.....	27
1.2.1.1 Catalytic cycle.....	29
1.2.2 Synthesis of methyl 3-(het)arylthieno[3,2- <i>b</i>]pyridine-2-carboxylates (3-10) by C-C Suzuki-Miyaura cross-coupling.....	30
2. Biological Studies	35
2.1 Screening of the synthesized compounds against several human tumor cell lines	35
2.2 Effect of the selected compounds in the growth of non-tumorigenic cells.....	39
2.3 Effect of the selected compounds on viable cell number of cancer cell lines.....	41
2.4 Effect of the selected compounds on cell cycle profile	43
2.5 Effect of the selected compounds on the expression levels of some proteins related with cell cycle, apoptosis and DNA damage	45
2.6 Antitumoral effect of compound 7 by the Chick Chorioallantoic Membrane (CAM) assay <i>in ovo</i> inoculated with MDA-MB-231 cells	48
III - CONCLUSION.....	51
1. Final Remarks.....	52
2. Future Perspectives	53
IV - EXPERIMENTAL.....	55
1. Chemical Synthesis.....	56
1.1 Synthesis: General Procedure.....	56
1.1.1 Synthesis of starting materials	57
1.1.1.1 Methyl 3-aminothieno[3,2- <i>b</i>]pyridine-2-carboxylate (1).....	56

1.1.1.2 Methyl 3-bromothieno[3,2- <i>b</i>]pyridine-2-carboxylate (2).....	56
1.2 Synthesis of the C-C Suzuki-Miyaura coupling products	58
1.2.1 General procedure	58
1.2.1.1 Methyl 3-phenylthieno[3,2- <i>b</i>]pyridine-2-carboxylate (3).....	59
1.2.1.2 Methyl 3-(<i>p</i> -tolyl)thieno[3,2- <i>b</i>]pyridine-2-carboxylate (4)	60
1.2.1.3 Methyl 3-(4-methoxyphenyl)thieno[3,2- <i>b</i>]pyridine-2-carboxylate (5)	61
1.2.1.4 Methyl 3-(4-(trifluoromethyl)phenyl)thieno[3,2- <i>b</i>]pyridine-2-carboxylate (6)	62
1.2.1.5 Methyl 3-(4-chlorophenyl)thieno[3,2- <i>b</i>]pyridine-2-carboxylate (7)	63
1.2.1.6 Methyl 3-(4-cyanophenyl)thieno[3,2- <i>b</i>]pyridine-2-carboxylate (8)	64
1.2.1.7 Methyl 3-(pyridin-4-yl)thieno[3,2- <i>b</i>]pyridine-2-carboxylate (9)	65
1.2.1.8 Methyl 3-(furan-3-yl)thieno[3,2- <i>b</i>]pyridine-2-carboxylate (10)	66
2. Biological Studies	67
2.1 Reagents and Compounds.....	67
2.2 Cell culture	67
2.3 Trypan Blue Exclusion Assay.....	68
2.4 Sulforhodamine B (SRB) assay	68
2.5 Flow Cytometry for cell cycle analysis with Propidium Iodide	70
2.6 Expression of specific proteins	70
2.6.1 Extraction of total protein.....	70
2.6.2 Protein quantification	71
2.6.3 Western blot assay	71
2.7 Chick Chorioallantoic Membrane (CAM) assay.....	73
2.8 Statistical analysis of the results.....	74
 V - REFERENCES.....	 75
1. References	76

ABBREVIATIONS LIST

A

AKT1 – Enzyme (serine/threonine-protein kinase) V-akt murine thymoma viral oncogene homolog 1, in humans is codified by gene *AKT1*)

APS – Ammonium persulfate

B

BRAF - Human gene that encodes the protein B-Raf (a serine/threonine-protein kinase), a proto-oncogene

BSA- Bovine serum albumin

BxPC₃ – Pancreatic human tumor cell line

C

CAM assay - Chick Chorioallantoic Membrane assay

CDCl₃ - Deuterated chloroform

CH₃CN – Acetonitrile

c-Met - Tyrosine-protein kinase Met or hepatocyte growth factor receptor (HGFR)

COSY- COrelated SpectroscopY

CuBr₂ - Copper(II) bromide

D

d – Duplet

dd – Double duplet

DME – 1,2-Dimethoxyethane

DMEM - Dulbecco's Modified Eagle Medium

DMF - Dimethylformamide

DMSO-*d*₆ – Hexa deuterated dimethyl sulfoxide

E

EDTA - Ethylenediaminetetraacetic acid

EGFR - Epidermal growth factor receptor

EI – Electron ionization

equiv. - Equivalent

ESI – Electrospray ionization

F

FBS – Fetal bovine serum

FDA - Food and Drug Administration

FGFR - Fibroblast growth factor receptors

G

GI₅₀ - Concentration of drug to cause 50% reduction in cell proliferation (growth)

H

HCC – Hepatocellular carcinoma human tumor cell line

HCT15 - Colorectal cancer human tumor cell line

HCV – Hepatitis C virus

HeLa - Henrietta Lacks human tumor cell line of cervical cancer

HepG₂ – Human liver cancer cell line

HMBC - Heteronuclear multiple-bond correlation spectroscopy

HRMS – High resolution mass spectrometry

HSQC - Heteronuclear single-quantum correlation spectroscopy

I

IARC - International Agency for Research on Cancer

J

J – Coupling constant

K

KRAS - Kirsten RA_t Sarcoma virus

M

m/z – Mass to charge ratio

m - Multiplet

M⁺ - Molecular radical cation

MAPK/Erk – Pathway made by a chain of proteins in the cell that communicates a signal from a receptor on the surface of the cell to the DNA

MCF-7 - Breast cancer cell line

MDA-MB-231 - Triple negative breast cancer cell line, ER (estrogen receptor), PR (progesterone receptor) and HER2 (Human Epidermal growth factor Receptor 2) negative

MDA-MB-468 - Triple negative breast cancer cell line, ER, PR and HER2 negative

MEK - Mitogen-activated protein kinase

m.p. – Melting point

MS – Mass spectrometry

MTA – Microtubule targeting agents

N

NCI-H460 – Non-small cell lung human tumor cell line

NSCLC – Non-small cell lung cancer

P

PANC-1 – Pancreatic cancer cell line

PARP-1 - Poly (ADP-ribose) polymerase 1

PBS- Phosphate buffered saline

PBS-T - Phosphate buffered saline-teen

PDAC - Pancreatic ductal adenocarcinoma

PdCl₂(dppf).CH₂Cl₂- 1,1'-Bis(diphenylphosphino)ferrocene]dichloropalladium(II), complex with dichloromethane

PdCl₂(PPh₃)₂- Bis(triphenylphosphine)palladium chloride

PI(3)K-mTOR – Intracellular signalling pathway important in regulating the cell cycle

ppm – Parts per million

R

Rac-BINAP - Racemic 2,2'-bis(diphenylphosphino)-1,1'-binaphthyl

RET – Proto-oncogene which encodes a tyrosine kinase receptor

RPMI - Roswell Park Memorial Institute (RPMI) 1640 Medium

ROS1- Proto-oncogene tyrosine-protein kinase ROS is an enzyme that in humans is encoded by the *ROS1* gene

S

s – Singlet

SAR - Structure–activity relationship

SDS - Sodium dodecyl sulphate polyacrylamide

S_NAr - Nucleophilic aromatic substitution

SRB - Sulforhodamine B

T

t-BuONO - *tert*-Butyl Nitrite

TCA – Trichloroacetic acid

TE - trypsin/EDTA Solution

TEMED – Tetramethylethylenediamine

TMS - Tetramethylsilane

TNBC – Triple negative breast cancer

V

VEGFR-2 - Vascular endothelial growth factor receptor 2

W

WB – Western blot

δ - chemical deviation

γ-H2A.X – In the presence of DNA double-strand break (DSB) the histone H2A variant, H2AX, becomes almost instantly phosphorylated at serine 139 - termed γ-H2AX.

INDEX OF FIGURES

Figure 1. Hallmarks and Enabling Characteristics of cancer, the ten biological characteristics of human tumors and possible therapeutic targets. (<i>Adapted from</i> ³)	4
Figure 2. Subtypes of breast cancers based on expression of key proteins, like HER-2, estrogen and progesterone receptors, Ki67, claudins, EGFR and others. (<i>Adapted from</i> ^{1,2}).....	8
Figure 3. Scaffolds of nitrogen-based heterocycles relevant for cancer treatment.....	11
Figure 4. Structure of thiophene.....	11
Figure 5. Six isomeric thienopyridine structures.....	12
Figure 6. Structure of the (3-amino-6-thien-2-yl-thieno[2,3- <i>b</i>]pyridine-2-yl)arylmethanones derivatives with antitumoral potential.	12
Figure 7. 7-(Indol-5-yl)aminothieno[3,2- <i>b</i>]pyridines, inhibitors of VEGFR-2.....	13
Figure 8. Structures of the best 7-[(2,4-dichloro-5-methoxyphenyl)amino]thieno[3,2- <i>b</i>]pyridine-6-carbonitriles, Scr inhibitors.	13
Figure 9. 7-Arylethers of thieno[3,2- <i>b</i>]pyridine phenylacetylthioureas substituted in the thiophene ring with imidazoles as potent inhibitors of VEGFR-2 and c-Met.	14
Figure 10. Thieno[3,2- <i>c</i>]pyridine ureas, potent inhibitors of VEGFR-2.....	14
Figure 11. Most promising compounds of the C-C Suzuki Miyaura products.	17
Figure 12. C-C Sonogashira coupling products.....	18
Figure 13. Most promising compound obtained by C-C Sonogashira coupling on the thiophene ring.....	19
Figure 14. Most promising C-N Buchwald-Hartwig coupling compounds as potential antitumoral products.	20
Figure 15. Aminodi(hetero)arylamines synthesized by C-N Buchwald-Hartwig coupling.	20
Figure 16. Examples of some of the most popular types boron reagents used as coupling components in the Suzuki reaction.....	28
Figure 17. A) ¹ H (CDCl ₃ , 400MHz)- ¹³ C (CDCl ₃ , 100.6MHz) HSQC correlations (expansion between 120 ppm and 163 ppm), B) ¹⁹ F- NMR (CDCl ₃ , 376.5 MHz) and C) of ¹³ C-NMR (CDCl ₃ , 100.6 MHz) of compound 6.....	33
Figure 18. Microscopic images of the different tumor cell lines used in the SRB assay.....	37
Figure 19. Morphology of MCF-12A cells (non-tumorigenic cell line) visualized under a Microscope.....	40

Figure 20. Effects of compound 7 on MDA-MB-231 viable cell number.	42
Figure 21. Cells cycle effects of compound 7 on MDA-MB-231 cells (panels A and B), and of compound 8 (panels C and D) and 10 (panels E and F) on MDA-MB-468 cells, analysed by Flow Cytometry following incubation with Propidium Iodide (PI).	44
Figure 22. Expression levels of PARP-1 and γ -H2AX in MDA-MB-231 cells, following treatment with compound 7, analysed by Western blot.	46
Figure 23. Expression levels of PARP-1 and p21 in MDA-MB-468 cells, following treatment with compounds 8 or 10, analysed by Western blot.	47
Figure 24. Chick Embryo Chorioallantoic membrane (CAM) assay. MDA-MB-231 cells were injected in the eggs, which and, after 24 h, were treated with vehicle or compound 7 at GI_{50} concentration, for 48 h.	50
Figure 25. Layout of the plates used for the screening with the SRB assay.	69
Figure 26. Layout of the 6-well plates for the Cell cycle and Western Blot experiments performed in MDA-MB-231 and MDA-MB-468 human tumor cell lines.	73
Figure 27. Illustration of CAM (Chick Chorioallantoic Membrane) assay procedure.	74

INDEX OF TABLES

Table 1. Compounds with the thienopyridine moiety with different biological properties....	21
Table 2. Synthesis of compounds 3-10 by C-C Suzuki-Miyaura cross-coupling using compound 2 and (het)aryl BF ₃ K salts, boronic acids and/or pinacol esters. The yields (%) and reaction time (h) are shown for each compound.....	30
Table 3. Features of the different cancer cell lines used in the SRB assay (origin, cancer type, tissue, morphology and common mutations) ¹²³	36
Table 4. GI ₅₀ concentrations (GI ₅₀) in different human tumor cell lines, using SRB the assay.	38
Table 5. Molecular classification, immune-profile and typical features of the breast cancer cell lines MDA-MB-231 and MDA-MB-468 ^{40, 124-126}	39
Table 6. Evaluation of the toxicity of the most promising compounds in the non-tumorigenic cell line MCF-12A.....	40
Table 7. Number of cells per mL plated, for each cell line, for the SRB assays.	68

INDEX OF SCHEMES

Scheme 1. Synthesis of thieno[3,2- <i>b</i>]pyridine by C-C Suzuki and Sonogashira couplings and C-N Buchwald Hartwig coupling in the Queiroz <i>et al.</i> research group.....	16
Scheme 2. Synthesis of the methyl 3-aminothieno[3,2- <i>b</i>]pyridine-2-carboxylate (1).	25
Scheme 3. Mechanism for the synthesis of compound 1.	26
Scheme 4. Synthesis of the methyl 3-bromothieno[3,2- <i>b</i>]pyridine-2-carboxylate (2) from (1).	26
Scheme 5. Synthesis of aryl bromo compounds from arylamines using alkyl nitrites and Cu(II) salts.....	26
Scheme 6. General scheme for the C-C Suzuki-Miyaura cross-coupling used in this work.....	27
Scheme 7. Self-coupling, the secondary product most common of the C-C Suzuki-Miyaura coupling.	28
Scheme 8. Catalytic cycle of Pd-catalyzed Suzuki-Miyaura coupling, applied to a boronic acid.	29

CHAPTER I

INTRODUCTION

1. CANCER

Cancer is the disease of the century and the second major cause of death worldwide, just after cardiovascular diseases⁴. In fact, in 2018, an estimated 9.6 million people died from cancer⁵. Thus, research for new therapies is an area of tremendous interest and joins the scientific community together in a great effort to better understanding and combating cancer.

Unfortunately, cancer may affect everybody and may appear in any part of the body⁵. Generally, cancer arises from mutations in a normal cell⁶ but carcinogenesis is a much more complex and slow process in which the cell accumulates genetic and epigenetic alterations over time, that together contribute to the malignant phenotype⁷. Carcinogenesis is a multistep process divided into three main phases: initiation, promotion and progression. Initiation involves at least one stable cellular change arising spontaneously or induced through exposure to a carcinogen; in promotion the transformed (already initiated) cell can continue harmless until stimulated to undergo further proliferation; finally, the progression phase of this multistep process gives rise to progressively malignant sub-populations⁸.

Given the ability that tumors have to spread through lymphatic or blood vessels to other sites of the body⁹, metastasis is the most life threatening event of cancer¹⁰.

The aggressiveness of cancer is due to its typical features known as “Hallmarks of Cancer” (**Figure 1**), which are groups of ten characteristics and abilities acquired during the multistep development of human tumors¹¹. From the Medicinal Chemistry point of view, the understanding of the Hallmarks of Cancer uncovers molecular targets, thus leading drug development in oncology. This is particularly important, given the limited efficacy of current drugs mainly due to Drug Resistance and/or high cytotoxic effects¹².

In 2000, Hanahan and Weinberg¹³ published the initial six Hallmarks of Cancer, which a decade later were updated to 8 “Hallmarks of Cancer” and 2 “Enabling Characteristics”³, which are the following¹⁴:

- Hallmarks of cancer: self-sufficiency in growth signals, insensitivity to anti-growth signals, evading apoptosis, limitless replicative potential, sustained angiogenesis, tissue invasion and metastasis, reprogramming energy metabolism and evading immune response;

- Enabling Characteristics: genome instability and mutation, and tumor-promoting inflammation.

The first Hallmark provides cancer cells with proliferative advantage due to the fact of the usually tightly regulated cell cycle is disrupted¹⁵. This occurs together with alterations in signalling pathways¹⁶. Furthermore, cancer cells do not respond to anti-growth signals, which gives them a great proliferation potential, given their capacity to inactivate tumor suppressor genes such as TP53¹⁷. Another ability that makes cancer difficult to tackle is the evasion from apoptosis, due to insensitivity to abnormal signals such as DNA damage in the case of TP53 being inactivated¹⁸, contributing also for the increase in the number of cancer cells¹⁹. Another hallmark confers cancer limitless replicative potential. The angiogenesis, tissue invasion and metastasis, as already mentioned, culminate in the systemic dissemination of cancer. The reprogramming of cellular energy metabolism allows cancer cells to survive under conditions in which normal cells would not survive, which is a crucial feature to support the continuous cell growth and proliferation in cancer²⁰. Cancer cells also have capacity to evade the immune response. In normal conditions, the immune system can detect pathogens and destroy unhealthy cells to protect the organism but cancer can escape the immune surveillance²¹. Finally, not only the instability of the genome and mutations play an important role in the development of cancer, but also the tumor microenvironment which includes surrounding blood vessels, the extracellular matrix, signalling molecules, endothelial cells and immune cells, strongly contributes to cancer progression²².

All these features combined make cancer a difficult disease to manage and a huge public health issue, which demands continuous research by the scientific community.

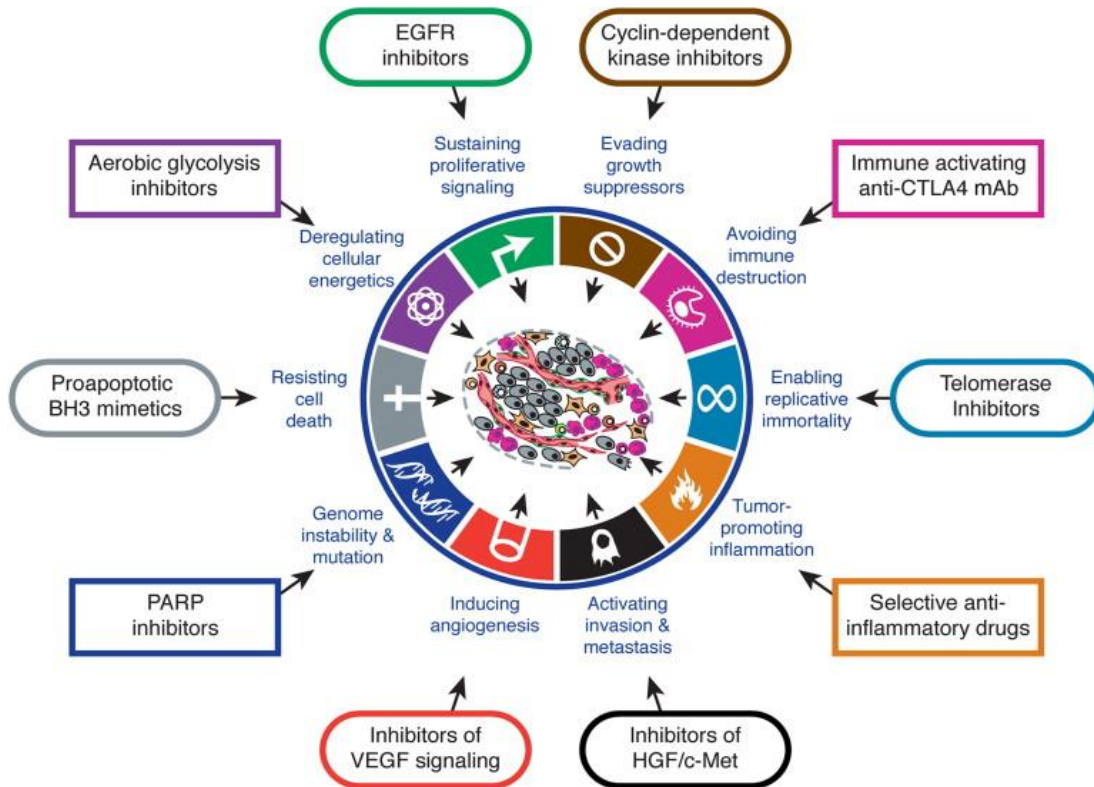


Figure 1. Hallmarks and Enabling Characteristics of cancer, the ten biological characteristics of human tumors and possible therapeutic targets. (Adapted from ³)

1.1 Types of cancer cells tested in this dissertation: pancreatic ductal adenocarcinoma, non-small cell lung cancer and triple negative breast cancers

1.1.1 PANCREATIC DUCTAL ADENOCARCINOMA

Pancreatic cancer is the fourth cancer related cause of death in the USA and it is estimated that in the year of 2030 it will be the second one, just before lung cancer deaths²³. Undeniably, there are some risk factors associated with this type of cancer contributing to the statistics like age, overweight, smoking, alcohol abuse and pre-existing chronic pancreatitis²⁴.

In terms of classification, tumors in the pancreas are divided into two main groups: non-endocrine (exocrine) and endocrine pancreatic tumors. The ductal adenocarcinoma accounts for >90% of all pancreatic malignancies, being considered exocrine tumors²⁴.

Pancreatic ductal adenocarcinoma (PDAC) is an aggressive type of pancreatic cancer that develops without symptoms. Therefore, when diagnosed it is already at an advanced stage. There are four main altered genes in PDAC: KRAS (Kirsten rat sarcoma), which is mutated in 70-95% of all cases^{25, 26}; the tumor suppressor gene TP53, being mutated in 75% of PDAC cases²⁷; CDKN2A (Cyclin dependent Kinase 2A) that is mutated or has promoter methylation in 95% of PDAC cases²⁸; and SMAD4 (Mothers against decapentaplegic homolog 4), that is mutated in 55% of PDAC cases²⁹.

The drugs approved by FDA for PDAC treatment are gemcitabine, erlotinib or nab-paclitaxel³⁰. Nevertheless, some patients have resistance to these drugs. Thus, given the lack of efficacy of the currently clinically used drugs, it is crucial to search for novel and more effective drugs to treat PDAC.

1.1.2 NON-SMALL LUNG CANCER

Lung cancer has become the number one killer among cancers worldwide, according to IARC in 2019 ³¹, being a public health concern. Therefore, the search for new treatments for lung cancer is essential.

Lung cancer is divided in two main histologically subtypes: non-small cell lung cancer (NSCLC) and small cell lung cancer (SCLC). The NSCLC accounts for 85% of all cases of lung cancer in the USA and in Europe is the biggest cancer killer – being responsible for 20% of all cancer related deaths ³².

NSCLC has “driver” mutations in oncogenes, namely in AKT1, ALK, BRAF, EGFR, HER2, KRAS, MEK1, MET, NRAS, PIK3CA, RET, and ROS1, being EGFR mutation the most predominant ³³.

There are subtypes of NSCLC: adenocarcinoma, squamous cell (epidermoid) carcinoma, large cell (undifferentiated) carcinoma and the sarcomatoid carcinomas, which are much less common ³⁴.

Concerning treatment, surgery resection is the most successful option for lung cancer patients. Unfortunately, 70% of the patients have locally advanced or metastatic disease when diagnosed, being chemotherapy the only treatment option. However, the use of targeted therapies is possible in some cases. For example, therapies against EGFR are used in patients who have overexpression of EGFR, which accounts for 40% of the cases. Indeed, EGFR inhibitors like erlotinib (that block the EGFR signal) are currently used in the clinic ³⁵.

Nowadays, some molecular tests are part of the diagnostic algorithm of lung adenocarcinoma, with the main aim being the discovery of the driver mutation(s) to be targeted by precise inhibitors ³⁶. These molecular tests are mainly for EGFR and for Alk (anaplastic lymphoma kinase) mutations. Nevertheless, there are also other driver mutations already mentioned – in KRAS, ROS1, RET, HER2, BRAF, PIK3CA, NRAS, AKT1, MET and MEK - which also affect important signalling pathways, such as the RTK/RAS/RAF, PI(3)K-mTOR and p53 pathways ³⁷. Therefore, a lot of research is still needed to find novel drugs to fight lung cancer.

1.1.3 TRIPLE NEGATIVE BREAST CANCER

Breast cancer is the most frequent diagnosed cancer and the main cause of cancer death in women ³⁸. The most aggressive, invasive and with poor prognosis type of breast cancer is the triple negative breast cancer (TNBC), which lacks expression of two hormone receptors - estrogen receptor and progesterone receptors - and lacks HER2 (Human Epidermal growth factor Receptor 2) amplification ³⁸.

Nowadays, since medicine is moving towards a personalized approach, the identification of different molecular subtypes capable of reflecting the biological diversity of breast cancer, namely the molecular and genetic characterization of the subtypes of the disease, has as main goal to improve effective targeted therapies and patient clinical outcomes³⁹. Consequently, due to new histopathologic classifications over the last decade, breast cancers are divided into different subtypes depending of the expression of key proteins, like HER-2, estrogen and progesterone receptors, Ki67, claudins, EGFR and others, being designed as luminal A, luminal B, HER2-enriched (+), basal-like and claudin-low ⁴⁰.

The claudin-low is one subtype of TNBC that has low expression of cell-cell adhesion molecules such as claudins 3,4, and 7, being of poor prognosis (**Figure 2**). The tumors of this subtype have an aggressive behaviour and a limited response to therapy and patient's outcomes are not similar ⁴¹. Another TNBC subtype is designed as the basal-like tumors subtype (**Figure 2**), due to the high presence of basal markers such as keratins 5/6 and 17, being characteristically less aggressive, more responsive to chemotherapy and common in women with mutated *BRCA1* gene ⁴².

On the other hand, luminal A cancers are classified as low-grade, with a typically slow growth rate and are the ones with better prognosis. The HER2(+) type grow faster than luminal A, thus having a worse prognosis; however, they may be targeted by therapies for the HER2 protein, such as Herceptin ⁴². Nonetheless, the claudin-low and basal tumors are a challenge to clinic nowadays since no targeted therapies exist ⁴³.

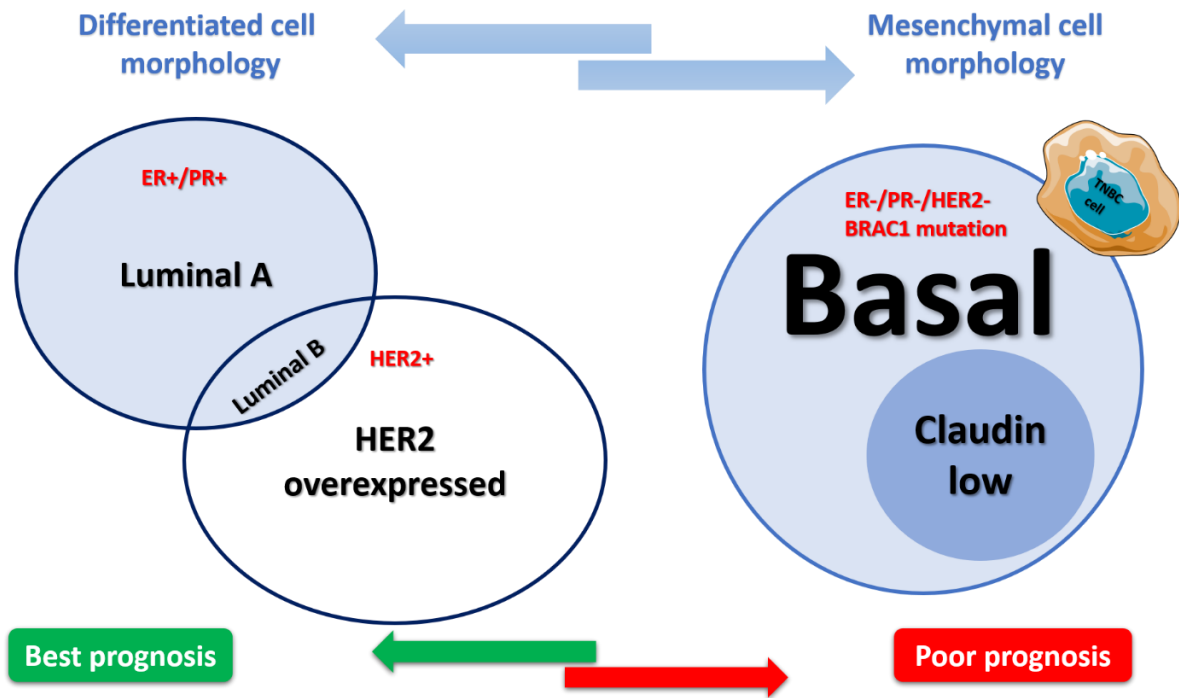


Figure 2. Subtypes of breast cancers based on expression of key proteins, like HER-2, estrogen and progesterone receptors, Ki67, claudins, EGFR and others. (Adapted from ^{1,2})

In conclusion, classification into subtypes concerning the morphological features and expression of certain key proteins and genes might help not only to distinguish between the different characteristics of these malignant neoplasms but are also crucial for a better knowledge about their clinical behaviour and, consequently, response to therapy^{39,41,44}. Thus, the molecular stratification of different subtypes of breast tumors might be a helpful tool for better prognosis of patients. However, since they are dependent of intrinsic genetic subtypes only accessed via gene expression analysis, is not feasible to all tumor samples in the clinical practice. As so, a combined classification was proposed by Cheang *et al.*, consisting not only of genetic profiling but also of immunohistochemistry testing to detect: ER, PR and HER-2 in order to distinguish between luminal (A or B), basal-like and HER-2(+); and the Ki67 proliferation marker which is used to distinguish Luminal A from Luminal B ⁴⁵.

2. SCREENING OF NEW COMPOUNDS

Earlier in the 90's, the National Cancer Institute initiated the so-called "disease-oriented" drug screening using around 60 human cancer cell lines derived from different types of cancer - brain, colon, leukaemia, lung, melanoma, ovarian, renal, breast, and prostate ⁴⁶. Nowadays, drug screening is widely used in the field of drug development for testing effects of several drugs or new synthesized compounds against numerous diseases, using numerous cell lines ⁴⁷.

Search for novel anticancer agents in primary cancer samples faces as major obstacle the low sample input ⁴⁸. Thus, conventional research in human cell lines *in vitro* using 2D culture is the best alternative, although 3D cultures better reproduce the physiological features of cells (e.g.: cell-cell contact, cell-matrix contact, polarity) compared to the traditional 2D cultures⁴⁹⁻⁵¹. Nonetheless, the original tumor features are not completely reproduced in a 3D screening ⁵⁰. Drug or compound screening in cell lines is a method with several advantages, providing a limitless source of material that is broadly accessible and can be easily propagated in culture, making cell lines appropriate to apply in drug development research⁵².

Since the compounds produced in this dissertation are new, testing them in different human tumor cell lines was considered a good first approach to verify if they had activity against human tumour cell line growth.

2.1 Study of the activity of potential novel drugs in apoptosis and cell cycle

The majority of chemotherapeutic agents cause DNA damage and trigger a complex signalling network, often causing cell cycle arrest and/or apoptosis ⁵³. Indeed, the cell cycle and apoptosis continue to attract the attention of researchers committed to develop new types of anticancer therapies ⁵⁴.

Cancer cells have the capacity to avoid apoptosis, ability known as one of the Hallmarks of Cancer ¹³, affecting the efficient elimination of cancer cells ⁵⁵. Therefore, induction of apoptosis in tumor cells may be a good strategy to kill some cancer cells ⁵⁶. Novel potent and

specific compounds that induce apoptosis in tumor cells, may be further studied regarding toxicity, for possible drug development.

The idea is identifying novel compounds that prime the apoptotic machinery to act as promising apoptosis-inducing agents. There are several examples of compounds that have such effect. For example, compounds targeting the antiapoptotic members of the Bcl-2 family (since this family is often overexpressed in cancer and contributes to chemotherapeutic resistance ⁵⁷) or targeting the IAP family (since several primary tumour biopsy samples presented high IAP expression levels ⁵⁸) are a good approach.

Regarding the possible activity of novel drugs as anticancer agents acting at the cell cycle, one of the aims is to induce cellular stress able to cause cell cycle arrest. Thus, currently approaches of drug screening include targeting checkpoints of the cell cycle with increase efficacy and, more importantly, selectivity compared to conventional chemotherapeutic treatments⁵⁹. As example, the Microtubule-Targeting Agents (MTA) are the most important antimitotic drugs used ⁶⁰. Other drugs being developed are inhibitors of the cyclin-dependent-kinases, proteins, that tightly regulate cell cycle progression and/or arrest ⁶¹.

To sum up, in the field of screening for novel anticancer drugs, studies concerning the activity in apoptosis and cell cycle are one of the possible approaches to discover new compounds to fight cancer. However, other hallmarks need be taken into account due to the complexity and heterogeneity of cancer⁶².

3. THIENOPYRIDINE DERIVATIVES AND SOME OF THEIR BIOLOGICAL PROPERTIES

The major class of heterocycles incorporated in chemotherapeutic drugs is dominated by nitrogen-based heterocycles (73%), followed by nitrogen-oxygen (15%) and compounds with sulphur that make part of 4% of all them ⁶³.

In fact, several authors have claimed that nitrogen-based heterocycles like quinoline ⁶⁴, piperidine and pyridine scaffolds (**Figure 3**), have a high clinical relevance in cancer treatment, the latter two being the most common heterocycles approved as drugs in Food and Drug Administration (FDA) ⁶⁵. Moreover, pyridine forms the nucleus of over 7000 existing drugs ⁶⁶ and, indeed, some platinum complexes covalently linked to organic intercalators of DNA, including pyridine, are used for cancer treatment ⁶⁷.

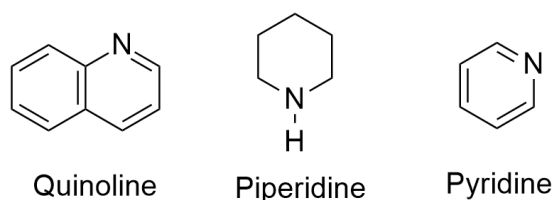


Figure 3. Scaffolds of nitrogen-based heterocycles relevant for cancer treatment.

On the other hand, other authors argue that thiophene (**Figure 4**), might be a good candidate to develop new anticancer agents. Thiophene derivatives have been described in the literature to have several pharmacological activities including anticancer activity ^{68, 69}, namely possessing cytotoxic activity against many type of cancers cells, such as leukaemia, ovarian, glioma, renal, and lung cancer by causing cell cycle arrest, apoptosis induction and affecting tubulin polymerization ^{70, 71}.

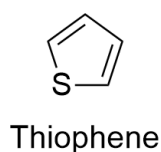


Figure 4. Structure of thiophene.

The thienopyridine unit is composed by a pyridine ring fused with a thiophene one. Six isomeric thienopyridines structures resulting by different ring fusion are possible (**Figure 5**).

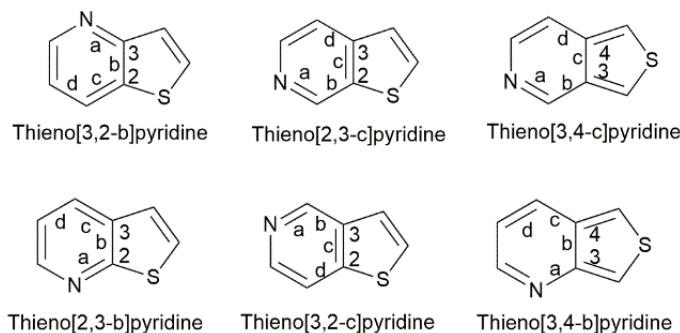


Figure 5. Six isomeric thienopyridine structures.

Several thienopyridine derivatives have been synthesized based on the high probability of having different biological properties ⁷². Hereafter, some examples from the literature are presented.

3.1 Thienopyridines and Cancer

Sugano *et al.* in 2004 reported that the (3-amino-6-thien-2-yl-thieno[2,3-*b*]pyridine-2-yl)arylmethanones (**Figure 6**) showed selectivity against the tumorigenic cell line WI-38 VA-13 subline 2RA (lung cancer cell line) at very low EC_{50} value (40 ng/mL) without cytotoxicity effect in the non-tumor cell line WI-38 (EC_{50} = 4000 ng/mL) ⁷³.

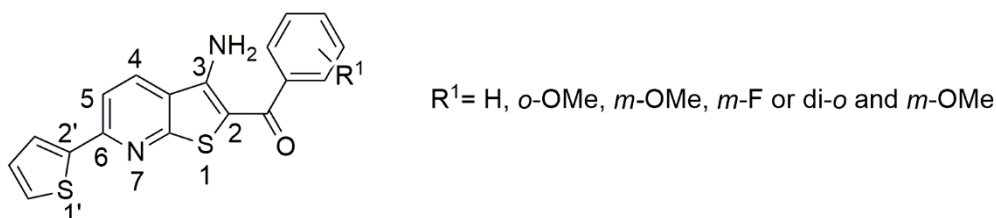


Figure 6. Structure of the (3-amino-6-thien-2-yl-thieno[2,3-*b*]pyridine-2-yl)arylmethanones derivatives with antitumoral potential.

In 2004, Munchhof *et al.* found that the substituted 7-(indol-5-yl)aminothieno[3,2-*b*]pyridines (**Figure 7**) have the potential to inhibit the Vascular Endothelial Growth Factor Receptor 2 (VEGFR-2) ⁷⁴. VEGFR-2 is a Receptor of Tyrosine Kinase (RTK) that, when is activated, autophosphorylates and triggers signalization pathways causing endothelial cell proliferation and angiogenesis ⁷⁵.

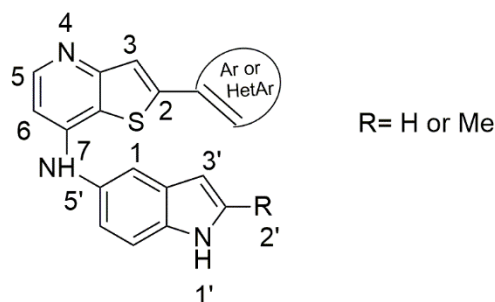


Figure 7. 7-(Indol-5-yl)aminothieno[3,2-*b*]pyridines, inhibitors of VEGFR-2.

2-Heteroaryl substituted 7-[(2,4-dichloro-5-methoxyphenyl)amino]thieno[3,2-*b*]pyridine-6-carbonitriles were described by Boschelli *et al.* in 2005, which act by inhibiting the non-receptor tyrosine kinase Src. This kinase has been implicated in cancer, osteoporosis and ischemic diseases when is overexpressed or overactivated ^{76, 77}. Studies also demonstrated that the compounds with a 3,5-disubstituted furan or a 2,5-disubstituted pyridine at C-2 (**Figure 8**) showed best activity in the cell based assays using c-Src transformed rat fibroblasts, with IC₅₀ ranging between 260 and 360nM, and in the enzymatic assay of inhibition of Src, with IC₅₀ values of 13 and 14nM, respectively ⁷⁸.

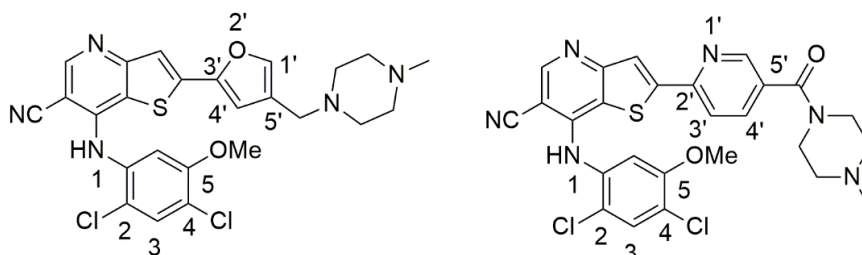


Figure 8. Structures of the best 7-[(2,4-dichloro-5-methoxyphenyl)amino]thieno[3,2-*b*]pyridine-6-carbonitriles, Src inhibitors.

In 2008, Claridge and co-authors showed that substituted 7-arylethers of thieno[3,2-*b*]pyridine phenylacetylthioureas were able to inhibit VEGFR-2 and c-Met receptors ⁷⁹. Furthermore, although the compounds tested by Claridge *et al.* were active inhibitors of the tyrosine kinase Src, the C-2 imidazole substituted compounds were the most potent in kinase inhibition assays against c-Met and VEGFR2, when tested *in vitro* (**Figure 9**). Specifically, the compound with R=1-methyl-1*H*-imidazol-4-yl were the most promising in various HGF- and VEGF-dependent cell-based assays. This compound was also studied *in vivo* for its

pharmacokinetic properties, showing antitumoral activity against several human tumor models ⁷⁹.

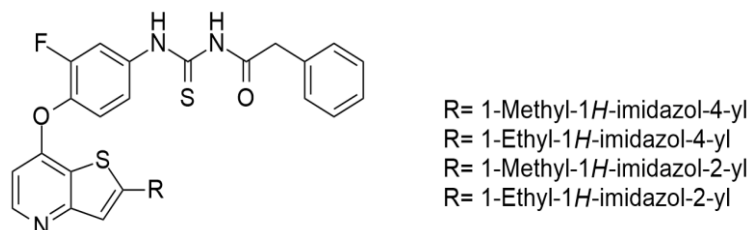


Figure 9. 7-Arylethers of thieno[3,2-*b*]pyridine phenylacetylthioureas substituted in the thiophene ring with imidazoles as potent inhibitors of VEGFR-2 and c-Met.

Heyman *et al.* in 2007 prepared a series of 1-[4-(4-aminothieno[3,2-*c*]pyridine-3-yl)phenyl]-3-(*p*-tolyl) ureas, which demonstrated to be potent inhibitors of the tyrosine kinase domain of VEGFR-2. The two most promising ones obtained by the authors were compounds **A** and **B** (Figure 10).

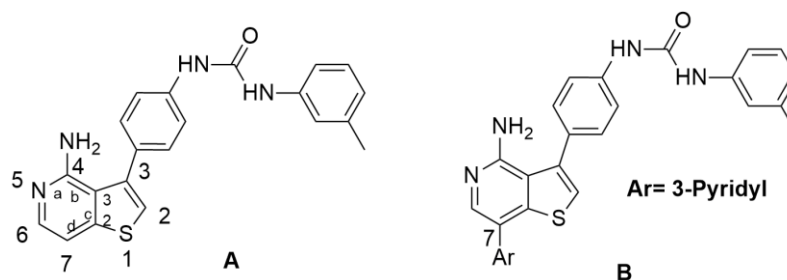


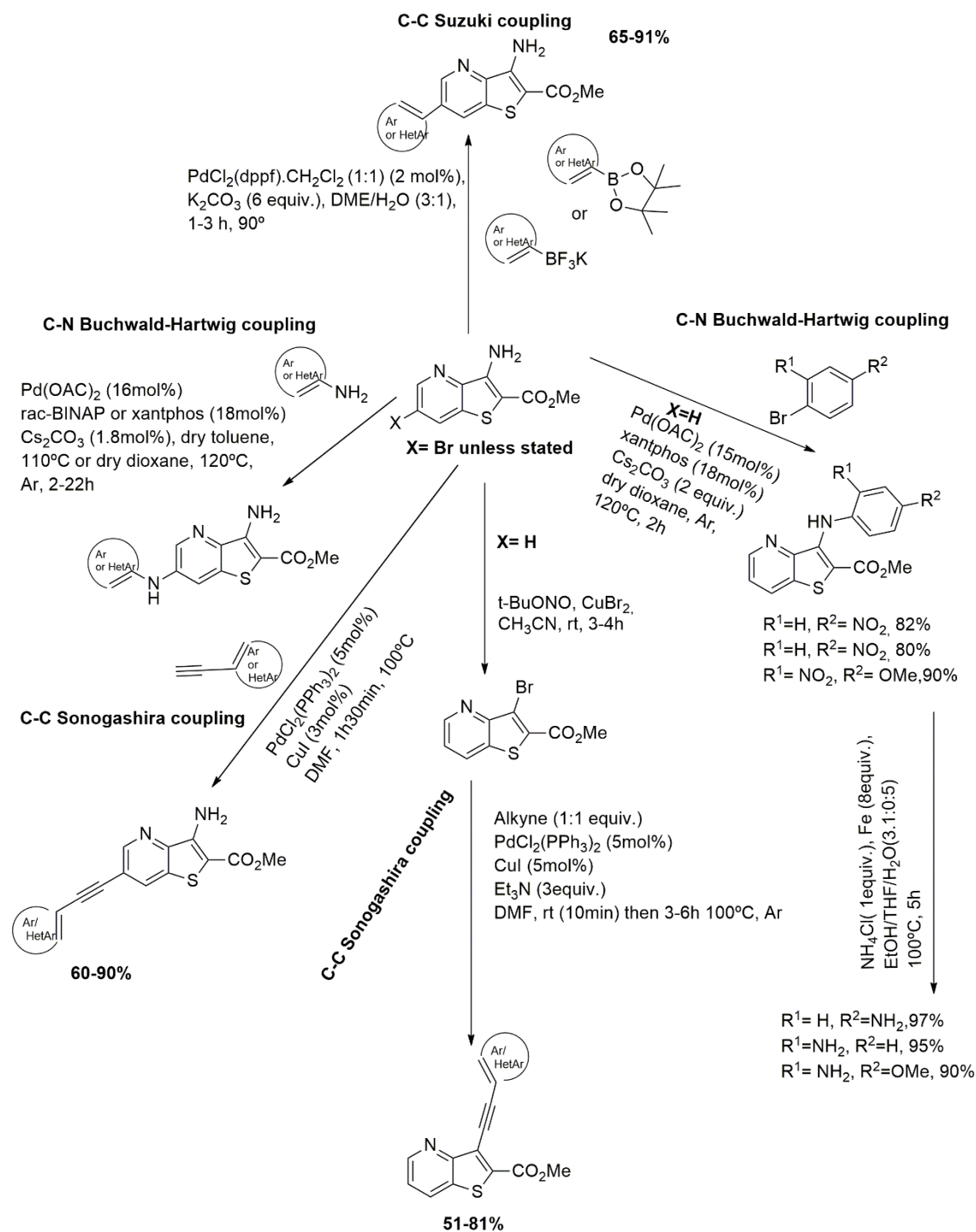
Figure 10. Thieno[3,2-*c*]pyridine ureas, potent inhibitors of VEGFR-2.

The selectivity of these two derivatives was shown to be much higher against VEGFR-2 than against Fibroblast Growth Factor Receptor (FGFR) or the cytosolic kinase Src. Compound **B** was the most potent inhibitor against VEGFR-2 (<10 nM) in both enzymatic and cellular assays ⁸⁰.

3.1.1 Earlier work developed with thieno[3,2-*b*]pyridine derivatives in the scope of synthesis and biological studies in our research group

Since 2010, the research group of Queiroz *et al.* of the University of Minho involved in the present work, have started the synthesis of thieno[3,2-*b*]pyridine derivatives functionalizing either the pyridine or the thiophene ring by Palladium (Pd) or Pd/Copper(Cu)-catalyzed couplings as summarized in **Scheme 1**⁸¹⁻⁸⁵. The compounds obtained in the different series were screened for their potential antitumoral activity regarding the effects on cell growth inhibition using the Sulforhodamine B (SRB) assay on several human tumor cell lines in collaboration with other research groups including the Cancer Drug Resistance group of Dr Helena Vasconcelos of i3S/IPATIMUP. The most promising compounds were also studied concerning their possible mechanisms of action (cell cycle effects and apoptosis induction).

In the following sections, the most promising compounds of each series obtained by different metal-catalyzed cross-couplings are presented.



Scheme 1. Synthesis of thieno[3,2-*b*]pyridine by C-C Suzuki and Sonogashira couplings and C-N Buchwald Hartwig coupling in the Queiroz *et al.* research group.

3.1.1.1 C-C SUZUKI COUPLING MOST PROMISING PRODUCTS

The Pd-catalyzed Suzuki-Miyaura cross-coupling products resulted from the reaction of methyl 3-amino-6-bromothieno[3,2-*b*]pyridine-2-carboxylate and several (het)aryl pinacolboranes or potassium trifluoroborates (**Scheme 1**). The effect of those compounds on the growth inhibition of three human tumor cell lines - MCF-7 (adenocarcinoma), A375-C5 (melanoma) and NCI-H460 (non-small cell lung cancer)-, was evaluated using Sulforhodamine B (SRB) assay ⁸⁶. From this series, the most promising compounds were shown to be compounds **C** and **D** (**Figure 11**) and were obtained in high yields (72 and 84%, respectively).

The bithiophene **C** presented the lowest GI₅₀ values with selectivity for MCF-7 and NCI-H460 cancer cell lines (1.0 and 0.7 μM, respectively). Compound **D**, an *o*-aniline derivative, showed GI₅₀ values below 5 μM against all the tumor cell lines studied. Further studies were then performed concerning cell cycles effects using NCI-H460 cell line. Compound **C** caused a cell cycle arrest on phases G0/G1 and compound **D** a cell cycle arrest at G2/M phase ⁸⁶.

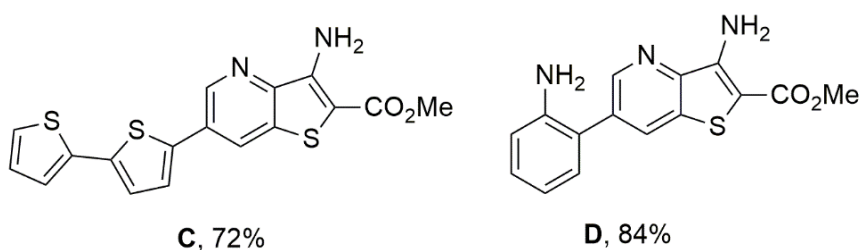


Figure 11. Most promising compounds of the C-C Suzuki Miyaura products.

3.1.1.2 C-C SONOGASHIRA COUPLING MOST PROMISING PRODUCTS

The C–C Sonogashira coupling consists in a Pd/Cu-catalyzed cross-coupling of (het)aryl halides with terminal alkynes (**Scheme 1**) and resulted in the series of products **E-P** (**Figure 12**), obtained with good yields (60-90%). The effects of the compounds were evaluated by SRB assay in several human tumor cell lines to determine the GI_{50} values. The most promising ones within the series were compounds **H**, **I** and **K** ⁸⁷.

The results showed that compound **H** presented the lowest GI_{50} values, 0.46 μ M and 0.32 μ M for MCF-7 and NCI-H460 cell lines, respectively. Compound **I** showed GI_{50} values of 3.1 μ M and 5.7 μ M and **K** of 2.6 μ M and 8.9 μ M for MCF-7 and NCI-H460 cell lines, respectively. Further studies were performed in NCI-H460 cells to evaluate possible cell cycle effects caused by the compounds. Compound **H** and **K** induced a cell cycle arrest on phase G0/G1 and **I** caused a G2/M cell cycle arrest. In addition, the compounds were also able to provoke apoptosis, mainly compound **I**, that induced a sub-G1 peak ⁸⁷.

- E** $R^1=R^2=H$, 70%
F $R^1=OMe$, $R^2=R^3=H$, 80%
G $R^2=OMe$, $R^1=R^3=H$, 75%
H $R^3=OMe$, $R^1=R^2=H$, 70%
I $R^1=NH_2$, $R^2=R^3=H$, 70%
J $R^2=NH_2$, $R^1=R^3=H$, 60%
K $R^3=NMe_2$, $R^1=R^2=H$, 75%
L $R^3=NMe_2$, $R^1=R^2=H$, 80%
M $R^1=F$, $R^2=R^3=H$, 75%
N $R^3=F$, $R^1=R^2=H$, 90%
O $R^1=R^2=R^3=H$, $X=N$, 70%
P $R^1=R^2=R^3=H$, $Y=N$, 90%
 $X=Y=CH$, unless stated

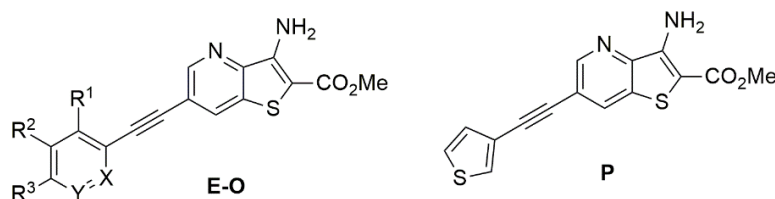


Figure 12. C-C Sonogashira coupling products.

Earlier in 2019 another series of C-C Sonogashira coupling products were synthesized and were tested concerning their possible cytotoxic effects on the growth of human tumor cell lines. This series corresponds to a functionalization on the thiophene ring, using methyl 3-bromothiopheno[3,2-*b*]pyridine-2-carboxylate and several terminal alkynes (**Scheme 1**). The antitumoral potential of the series of compounds produced was evaluated with the SRB assay in HCT-15 (colorectal adenocarcinoma) and NCI-H460 human tumor cell lines. Compound **Q** showed to be the most promising (**Figure 13**), presenting GI_{50} values of 10.8 and 17.0 μ M for

HCT-15 and NCI-H460, respectively. In addition, further assays on HCT-15 cells were performed concerning the induction of apoptosis caused by **Q** and the results indicated that the cells treated with 1.5xGI₅₀ concentration had about 30% more apoptosis than controls⁸⁵.

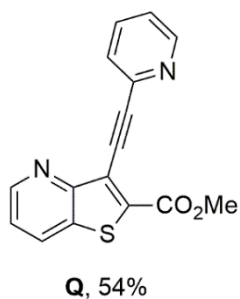


Figure 13. Most promising compound obtained by C-C Sonogashira coupling on the thiophene ring.

3.1.1.3 C-N BUCHWALD-HARTWIG COUPLING MOST PROMISING PRODUCTS

Another Pd catalyzed coupling was the Pd-catalyzed C-N Buchwald-Hartwig that forms C-N bonds by cross-coupling of (het)arylamines with (het)aryl halides (**Scheme 1**). The compounds obtained were tested in the human tumor cell lines MCF-7, A375-C5 and NCI-H460 using the SRB assay. The most promising compounds in this series were **R** and **S** (**Figure 14**) (obtained with 54 and 53% yields). The diheteroarylamine **R** presented the lowest GI₅₀ values of 6.0 μM, 3.5 μM and 6.4 μM, respectively, and the indole derivative **S** showed GI₅₀ values of 18.1 μM, 17.3 μM and 15.8 μM, respectively⁸⁴.

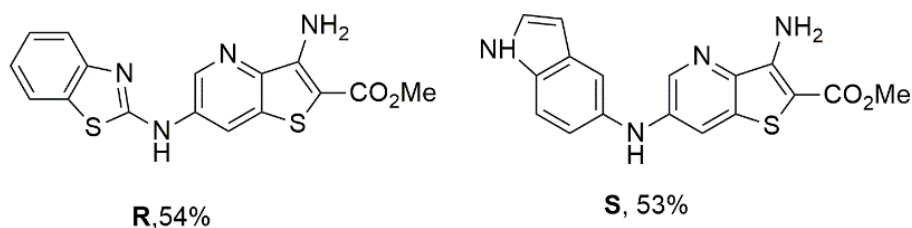


Figure 14. Most promising C-N Buchwald-Hartwig coupling compounds as potential antitumoral products.

Moreover, in 2012, nitrodi(het)arylamines were synthesized by Pd-catalyzed C-N Buchwald-Hartwig coupling functionalizing at the thiophene ring (**Scheme 1**). The resulting nitro compounds were submitted to reduction in order to give the corresponding aminodi(het)arylamine derivatives with high yields ($\geq 90\%$) (**Figure 15**)⁸⁸. These compounds were studied using the SRB assay in MCF-7, A375-C5, NCI-H460 and HepG2 (hepatocellular carcinoma), and their cytotoxicity was also evaluated in PLP1 cells (porcine liver primary culture). Compound **V** was the most promising one, presenting GI₅₀ of 1.40 μM, 1.30 μM, 1.40 μM and 1.63 μM, respectively. Furthermore, no cytotoxic effects were observed in PLP1 cell line at least at the GI₅₀ concentration⁸⁸.

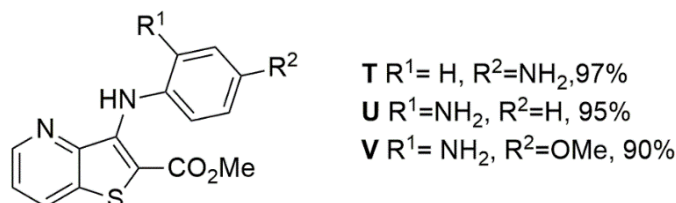


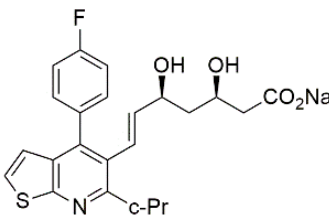
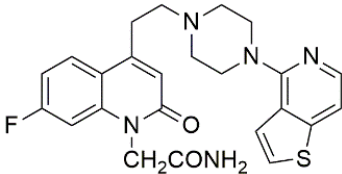
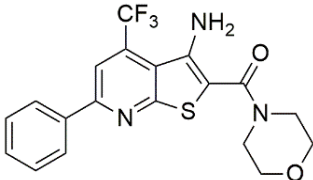
Figure 15. Aminodi(hetero)arylamines synthesized by C-N Buchwald-Hartwig coupling.

3.2 Other biological properties of thienopyridines

Thienopyridines were also recognised as class of inhibitors of the ADP P2Y₁₂ receptors, which can be found at the surface of platelets, having a determinant role in the coagulation⁸⁹. The ADP P2Y₁₂ receptors can be the target for prevention and therapy of cardiovascular diseases, such as acute coronary syndromes^{89, 90}.

Thienopyridines have shown to possess activity in the prevention of atherosclerosis⁹¹, anti-vasoconstrictor activity⁹² and, also, hepatitis C virus inhibitors⁹³, as shown in **Table 1**.

Table 1. Compounds with the thienopyridine moiety with different biological properties.

ACTIVITY	STRUCTURE
<p><u>Prevention of atherosclerosis</u> (inhibition of the 3-hydroxy-3-methylglutaryl-CoA reductase (<i>in vitro</i>), lowering the biosynthesis of cholesterol (<i>in vivo</i>)⁹¹</p>	
<p><u>Anti-vasoconstrictor activity</u> (antagonist of the receptor of serotonin 5-HT_{1B}/5HT_{2A})⁹²</p>	
<p><u>Hepatitis C virus inhibitors</u> (best compound showed EC₅₀= 3.3 μM without cytotoxicity)⁹³</p>	

4. RATIONALE AND AIMS

Synthesis of new compounds with several biological properties is crucial for countless diseases, particularly for cancer treatment. Thus, research on novel potential antitumor synthetic agents is of great importance nowadays all over the world due to cancer burden ⁹⁴.

Although the discovery of novel drugs may start with a target, it may also start with drug screening in cell lines. The present work was developed without a specific target, thus the biological studies were initiated with a screening in several human tumor cell lines.

The current work resulted from a multidisciplinary collaboration between the research group of Dr Maria João Queiroz from the Centre of Chemistry of University of Minho and Prof. Helena Vasconcelos, leader of the Cancer Drug Resistance Group at i3S/IPATIMUP, aiming to identify novel compounds with antitumour activity and low toxicity.

In recent years, Queiroz *et al.* explored the potential of several thieno[3,2-*b*]pyridine with more emphasis in functionalizing the side of the pyridine with very promising compounds ^{82-84, 88} (as shown in section 3.1.1 of this chapter). Nonetheless, the potential of the side of the thiophene ring has not been yet so explored. Although the problems concerning high lipophilicity and low water-solubility are one of the major drawbacks of the synthesis of new derivatives, it's possible to counteract this limitation since this is a frequent problem of some compounds that are currently used in the clinic, due to improvements in their lack of solubility ⁹⁵. Thus, the synthesis of novel thieno[3,2-*b*]pyridine derivatives obtained by C-C Pd-catalyzed Suzuki-Miyaura cross-coupling functionalizing on the side of the thiophene ring and evaluation of their potential antitumor activity in human tumor cell lines, was the main aim of this dissertation.

For that, the specific aims were:

- ✚ Synthesize new compounds and fully characterize them by melting point (m.p.), ¹H- and ¹³C-NMR, including bi-dimensional homonuclear ¹H-¹H (COSY) and heteronuclear correlations ¹H-¹³C (HSQC and HBMC) to attribute the signals, Low and High-resolution Mass Spectrometry (HRMS), or Elemental Analysis;
- ✚ Screen the synthesized compounds for their potential antitumor activity using different human tumor cell lines [such as pancreatic (PANC-1 and BxPC3), non-

small cell lung (NCI-H460), and triple negative breast (MDA-MD-231 and MDA-MD-468)], with the Sulforhodamine B Assay, in order to select the most promising compounds (with the lowest GI₅₀ values);

- ✚ Evaluate the cytotoxicity of the best compounds against the non-tumorigenic cell line MCF-12A, with the SRB assay (using GI₅₀ values obtained in the tumor cell lines);
- ✚ Study the possible effects of the most promising compounds on cell cycle profile, by Propidium Iodide staining and Flow Cytometry analysis;
- ✚ Evaluate the antitumoral effect of compound *p*-Cl by the Chick Chorioallantoic Membrane (CAM) assay *in ovo* inoculated with MDA-MB-231 cell line.

CHAPTER II

RESULTS AND DISCUSSION

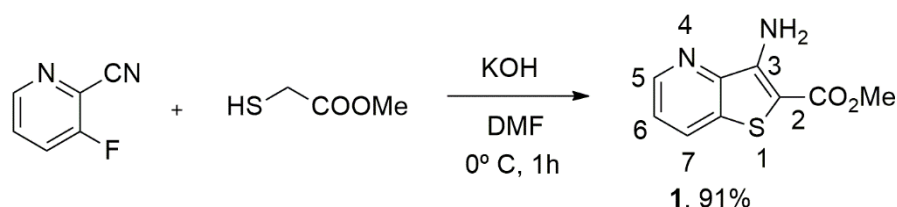
1. CHEMICAL SYNTHESIS

A series of eight new functionalized N and S fused heteroaromatic compounds, bi(het)arylthieno[3,2-*b*]pyridines were synthesized by C-C Pd-catalyzed Suzuki cross-coupling of methyl 3-bromothieno[3,2-*b*]pyridine-2-carboxylate, also prepared, with commercial (het)aryl pinacolboranes, trifluoro potassium boron salts or boronic acids, as presented and discussed below. All the new compounds were fully characterized in the Centre of Chemistry of the University of Minho by melting point (m.p.), ^1H - and ^{13}C -NMR, including bi-dimensional homonuclear ^1H - ^1H (COSY) and heteronuclear correlations ^1H - ^{13}C (HSQC and HBMC) to attribute the signals; Low and High-resolution Mass Spectrometry (HRMS) or Elemental Analysis (see Chapter IV - Experimental).

1.1 Synthesis of starting materials

1.1.1 Synthesis of methyl 3-aminothieno[3,2-*b*]pyridine-2-carboxylate (**1**)

To start the work, it was synthesized the methyl 3-aminothieno[3,2-*b*]pyridine-2-carboxylate (**1**) reacting 3-fluoropicolinonitrile with methyl thioglycolate, in excess of base (1.5 equiv. of KOH (aq)), as illustrated in **Scheme 2**. Compound **1** was the first synthesized starting material.

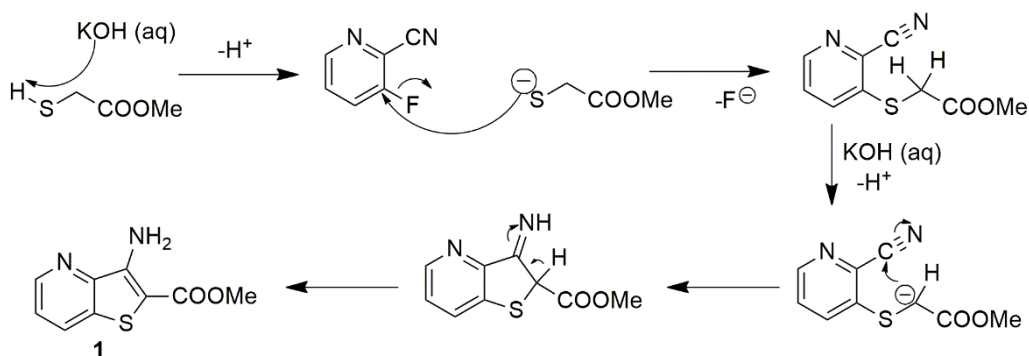


Scheme 2. Synthesis of the methyl 3-aminothieno[3,2-*b*]pyridine-2-carboxylate (**1**).

The synthesis of compound **1** was optimized earlier by our research group from 35% using 3-chloropicolinonitrile⁹⁶ to 95% of yield⁹⁷.

The mechanism of the synthesis of compound **1** is presented in **Scheme 3**. The reaction occurs in basic conditions by aromatic nucleophilic substitution ($\text{S}_{\text{N}}\text{Ar}$) of the F atom by the sulphur of the methyl thioglycolate. A carbanion is formed on the adjacent C atom to the S and to the methyl ester, which attacks the nitrile group. Then, the capture of a H atom by the

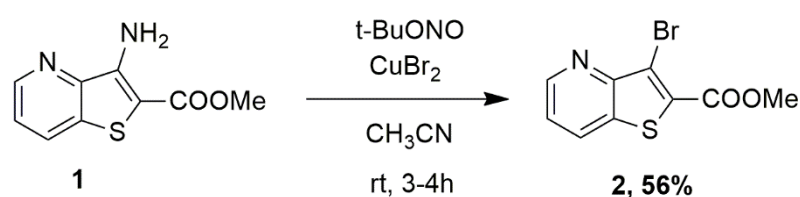
N atom and consequent aromatization with the capture of a second H atom creates a free amine at position 3⁸⁴.



Scheme 3. Mechanism for the synthesis of compound **1**.

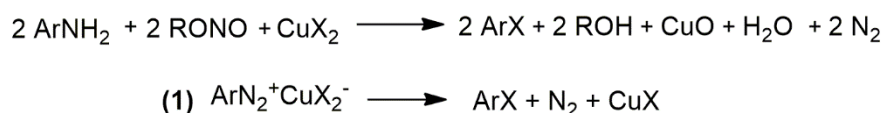
1.1.2 Synthesis of methyl 3-bromothieno[3,2-*b*]pyridine-2-carboxylate (**2**)

The next step was the synthesis of methyl 3-bromothieno[3,2-*b*]pyridine-2-carboxylate (**2**)^{85, 98} from compound **1** using *t*-BuONO and CuBr₂ in acetonitrile at room temperature (**Scheme 4**).



Scheme 4. Synthesis of the methyl 3-bromothieno[3,2-*b*]pyridine-2-carboxylate (**2**) from (**1**).

The mechanism of the synthesis of compound **2** consists in the substitution of an aromatic amino group by a bromo atom through a diazonium salt followed by a S_NAr with CuBr₂. Doyle *et al.* in 1977 reported the arylamine deamination using alkyl nitrites and copper (II) halides directly converting arylamine into aryl halides, producing copper oxide, N₂, the corresponding alkyl alcohol and aryl halides as shown in **scheme 5**⁹⁹.



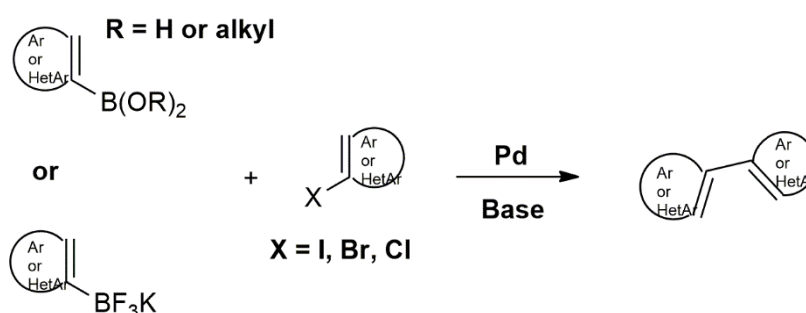
Scheme 5. Synthesis of aryl bromo compounds from arylamines using alkyl nitrites and Cu(II) salts.

Compound **2** was used as starting material in the C-C Suzuki-Miyaura cross-coupling to obtain the new bi(het)arylthieno[3,2-*b*]pyridines synthesized in this work.

1.2 C-C Suzuki-Miyaura cross-coupling

1.2.1 Introduction

The C-C Suzuki-Miyaura is a Pd-catalysed cross-coupling that forms a carbon-carbon bond to give, in our work, bi(het)aryl compounds (**Scheme 6**)¹⁰⁰. Biaryl compounds are utilized as important primary skeletons of functional materials like liquid crystals and in the scientific field as biologically active compounds¹⁰¹.

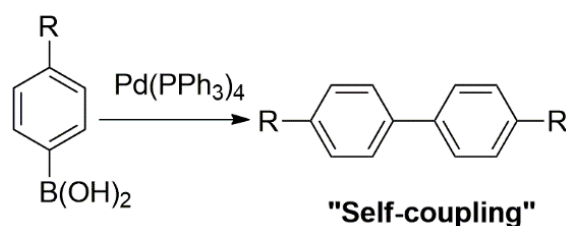


Scheme 6. General scheme for the C-C Suzuki-Miyaura cross-coupling used in this work.

The first Suzuki-Miyaura cross-coupling was discovered by reacting phenylboronic acids with haloarenes and it was published by Suzuki and Miyaura in the year of 1981. Thus, since the 80's this cross-coupling is used to functionalize several heterocyclic classes of compounds such as pyrroles¹⁰², indoles¹⁰³, pyridines¹⁰⁴, imidazoles and among others¹⁰¹. Its capacity to form C-C bonds easier between the coupling components, the reagents that are commercially available, the possible presence of water in the reaction, little formation or facile elimination of side products^{105, 106}, among other advantages such as mild reaction conditions and its less toxic nature, turns this coupling very usual nowadays. Moreover, in the last years major advancements have occurred, including expansion of the substrate scope^{107, 108}, reaction at lower temperatures^{109, 110} and reduction in the catalyst loading¹¹¹.

The previous advantages of this coupling are numerous but there are also disadvantages. One of the main drawbacks of the Suzuki-Miyaura cross-coupling is the

formation of secondary products, frequently the called "self-coupling" between two molecules of boronic acid, as shown in **Scheme 7** ¹⁰⁵.



Scheme 7. Self-coupling, the secondary product most common of the C-C Suzuki-Miyaura coupling.

To avoid this, other boron coupling components (illustrated in **Figure 16**) are preferably used nowadays namely pinacol esters ¹¹² and trifluoroborate salts ¹¹³ and then boronic acids ¹¹⁴.

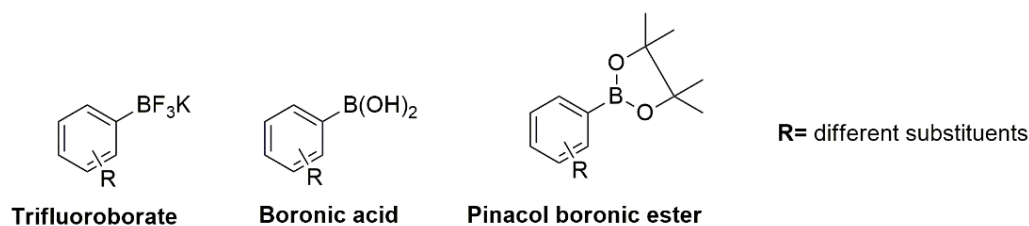
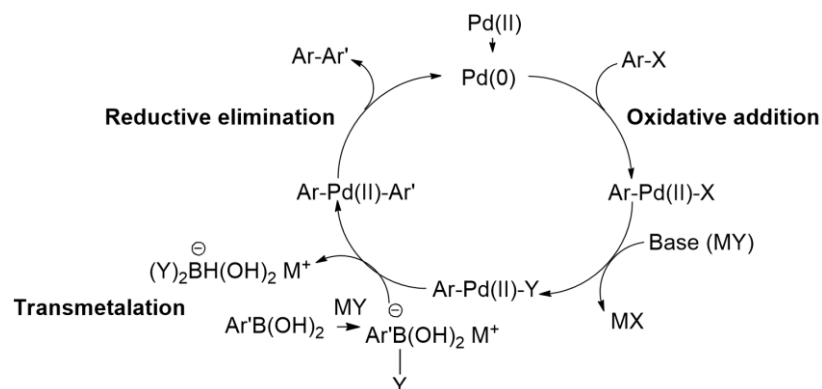


Figure 16. Examples of some of the most popular types boron reagents used as coupling components in the Suzuki reaction.

Boronic acids are more susceptible to form side products, due to the fact they are an easy target of protodeboronation, oxidation and homocoupling ¹¹⁵. On the other hand, the trifluoroborates are tetrahedral and their strong B–F bonds, together with the representative salt-like structure, offers them advantageous physical characteristics like being free-flowing crystalline solids and stable to air, making them good reagents to handle, unlike certain boronic acids that are decomposed in air or pinacol boronic esters, mostly liquids or of low melting solids ¹¹⁵.

1.2.1.1 Catalytic cycle

The Pd-catalyzed Suzuki-Miyaura coupling catalytic cycle consists in three main steps: oxidative addition, transmetalation and reductive elimination (**Scheme 8**)^{105, 116-118}.



Scheme 8. Catalytic cycle of Pd-catalyzed Suzuki-Miyaura coupling, applied to a boronic acid.

The catalytic cycle initiates with Pd(0) but Pd(II) catalysts can be used since they are more stable to air and easily reduced *in situ* to Pd(0). The main process is the oxidative addition of organic halides to the complex Pd(0) forming the organopalladium (II) halide (Ar-Pd(II)-X), through Pd electrons donation to form the new Pd–C bond. The displacement of the halide ion of the Pd(II) complex is triggered by the metal of the base and its replacement occurs by the base anion, forming a more polar bond than Pd-X, thus favouring the next step of transmetalation. In this step, the boron organometallic compound (Ar'-B-(OH)₂) reacts with the Ar-Pd(II)-Y forming the complex Ar-Pd(II)-Ar'. For this, the boron compound must be activated by the base being transformed in a tetravalent boron. Finally, reductive elimination of the Pd(II) occurs regenerating the Pd(0) and forming the bond C-C between the aryl compounds (Ar-Ar')^{105, 116-118}.

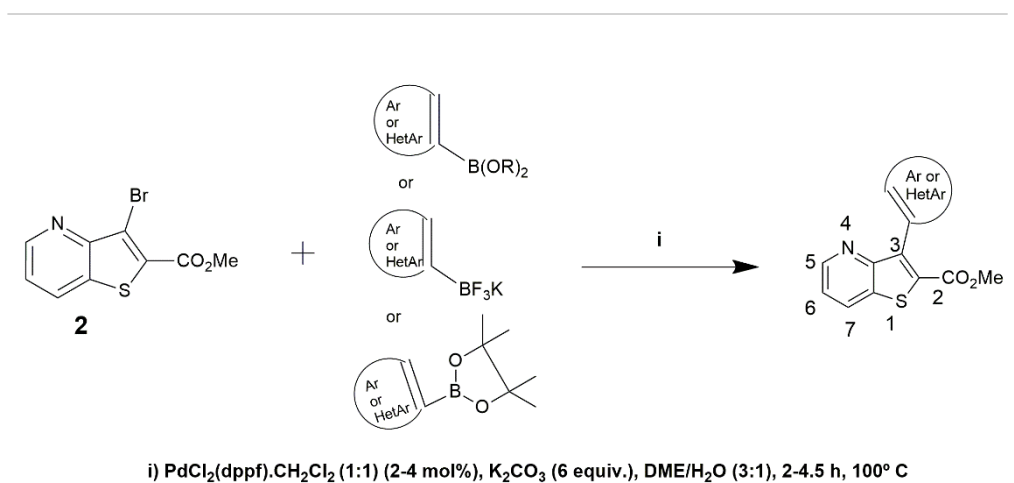
Relatively to the use of Pd(0) catalysts, the most applied is the tetrakis(triphenylphosphine)palladium(0), Pd(PPh₃)₄, but others of Pd(II) can be used, bis(triphenylphosphine)palladium(II) dichloride, PdCl₂((PPh₃)₂), [1,1'-bis(diphenylphosphino)ferrocene]dichloropalladium(II), Pd(dppf)Cl₂, and palladium(II) acetate, Pd(OAc)₂¹¹¹. In terms of base, the most common used is Na₂CO₃, but with steric hindered substrates it can be poorly achieved. Other alternative inorganic bases that can be used are NaHCO₃, Cs₂CO₃, K₂CO₃, KF, CsF or NaOH^{119, 120}.

1.2.2 Synthesis of methyl 3-(het)arylthieno[3,2-*b*]pyridine-2-carboxylates (**3-10**) by C-C

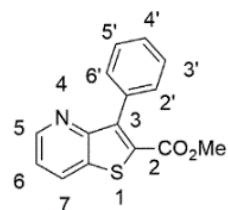
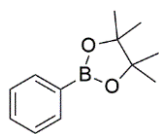
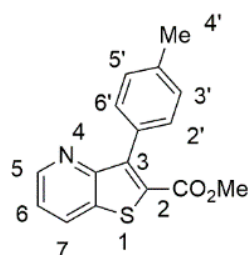
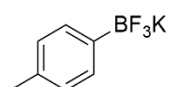
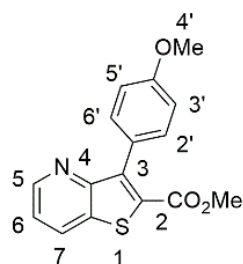
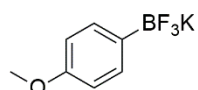
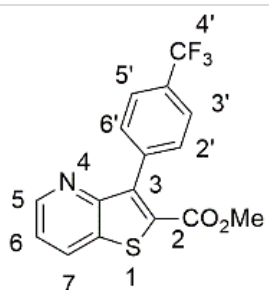
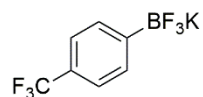
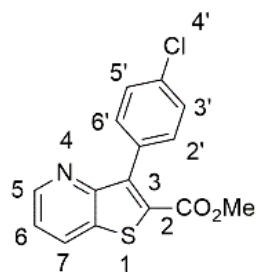
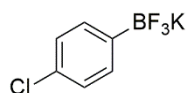
Suzuki-Miyaura cross-coupling

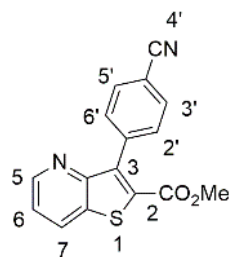
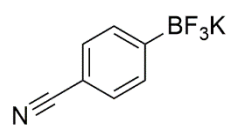
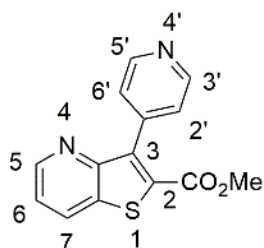
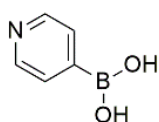
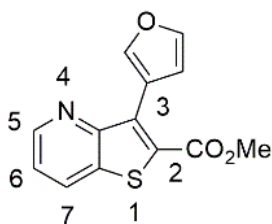
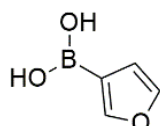
The C-C Suzuki-Miyaura cross-coupling products **3-10** were obtained from the reaction of the brominated compound **2** with aryl potassium trifluoroborates (BF₃K) salts, (het)aryl boronic acids or pinacol esters. The series of thieno[3,2-*b*]pyridine derivatives was synthesized with no substituents, with electron donating (OMe, Me) or withdrawing substituents (Cl, CN, CF₃) in the *para* position of a phenyl ring relative to the C-C bond formed, or with an electron deficient ring, pyridine, or electron-rich ring, furan, using the catalyst and the base depicted in **Table 2**. The compounds were obtained in moderate to high yields (35-84%) after purification by column chromatography and were fully characterized.

Table 2. Synthesis of compounds **3-10** by C-C Suzuki-Miyaura cross-coupling using compound **2** and (het)aryl BF₃K salts, boronic acids and/or pinacol esters. The yields (%) and reaction time (h) are shown for each compound.



STARTING MATERIAL SUZUKI COUPLING PRODUCTS

**3, 3h, 74%****4, 4.5h, 84%****5, 2h, 40%****6, 4h, 40%****7, 3h, 82%**

**8**, 3h, 35%**9**, 4h, 66%**10**, 4.5h, 52%

The compounds obtained with the best yields were **3** (Ph), **4** (*p*-Me) and **7** (*p*-Cl), followed by compound **9** (pyridine) and **10** (furan) (**Table 2**). A relation between the substituents and the yields obtained is not possible to establish and this may also be due to different boron starting reagents used.

An example of characterization by ^1H and ^{13}C -NMR using bi-dimensional heteronuclear correlations, ^{13}C and ^{19}F -NMR spectra is presented for compound **6** (**Figure 17**).

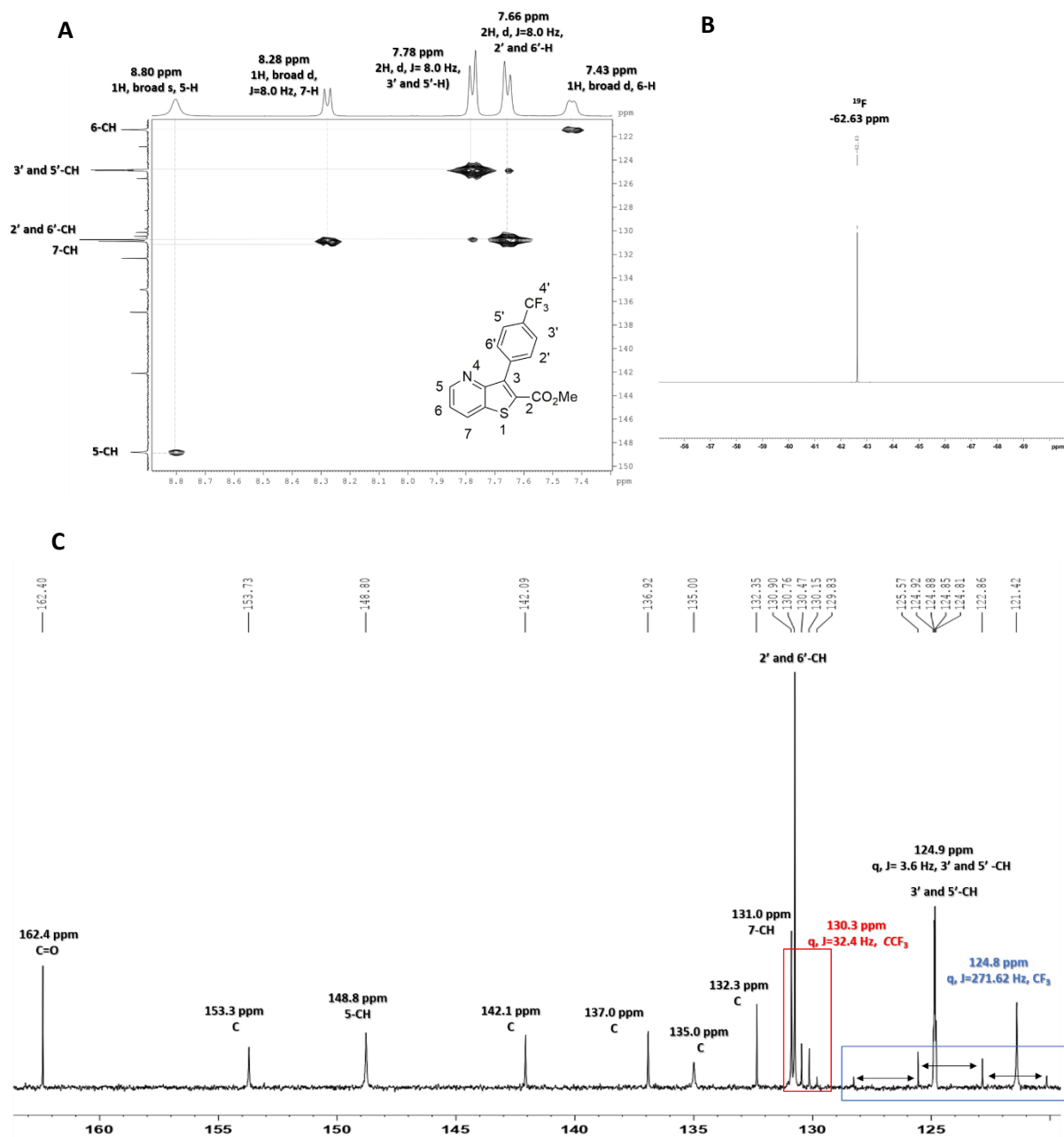


Figure 17. **A**) ^1H (CDCl_3 , 400MHz)- ^{13}C (CDCl_3 , 100.6MHz) HSQC correlations (expansion between 120 ppm and 163 ppm), **B**) ^{19}F - NMR (CDCl_3 , 376.5 MHz) and **C**) of ^{13}C -NMR (CDCl_3 , 100.6 MHz) of compound **6**.

The coupling of ^{19}F and ^{13}C in this compound appear as quartets with characteristic coupling constants, as exemplified in **Figure 17C**. The signal of ^{19}F is also characteristic in this solvent (CDCl_3). The compound was also characterized by melting-point (170-171 °C) and by elemental analysis: calculated for $\text{C}_{16}\text{H}_{10}\text{F}_3\text{NO}_2\text{S}$ (337.32): C, 56.97%, H, 2.99%, N, 4.15%, S, 9.51%; found: C, 56.62 %, H 2.65 %, N 4.35 %, S, 9.81 %. The latter are two purity criteria.

Having compounds **3-10** in hands, a screening of growth inhibition activity using human tumor cell lines was performed and for the most promising compounds further studies took place.

2. BIOLOGICAL STUDIES

The second part of this work aimed to evaluate the possible antitumoral activity of the synthesized thieno[3,2-*b*]pyridine derivatives. For that, a screening was first performed with the synthesized compounds in several human tumor cell lines, in order to select the compounds with potential antitumor effect. Then, further assays were performed, for the most promising compounds, to explore the mechanisms of action beyond the potential antitumor activity.

2.1 Screening of the synthesized compounds against several human tumor cell lines

The Sulforhodamine B (SRB) is an assay commonly used to screen compounds regarding their potential anticancer effect in several cancer cell lines⁴⁶. Briefly, SRB is a pink aminoxanthene dye able to bind to basic amino acids on fixed cells. The amount of bound dye can be used as a measurement of cell density since cellular protein content correlates linearly with the number of cells¹²¹. Therefore, this assay can easily assess cell growth being sensitive and inexpensive¹²².

The antitumor potential of all compounds was evaluated using the SRB assay, which in some cases allowed to determine the GI₅₀ concentration - concentration of each compound that inhibits 50% of the cell growth. Thus, the eight synthesized compounds were tested in five different human tumor cell lines: PDAC (PANC-1 and BxPC3), NSCLC (NCI-H460) and TNBC (MDA-MB-231 and MDA-MB-468) cell lines. Some of the features of the cancer cell lines used are presented in **Table 3** and their morphology is showed in **Figure 18**.

Table 3. Features of the different cancer cell lines used in the SRB assay (origin, cancer type, tissue, morphology and common mutations) ¹²³.

Cell line	Origin	Cancer type	Tissue	Morphology	Culture properties	Mutations
PANC-1	Human	PDAC	Pancreas-duct	Epithelial	Adherent	KRAS and TP53
BxPC3	Human	PDAC	Pancreas	Epithelial	Adherent	TP53, CDKN2A and SMAD4
NCI-H460	Human	NSCLC	Pleural effusion	Epithelial	Adherent	EGFR, PIK3CA
MDA-MB-231	Human	TNBC	Pleural effusion	Epithelial	Adherent	ER and PR negative, lacks HER-2 amplification
MDA-MB-468	Human	TNBC	Pleural effusion	Epithelial	Adherent	ER and PR negative, lacks HER-2 amplification

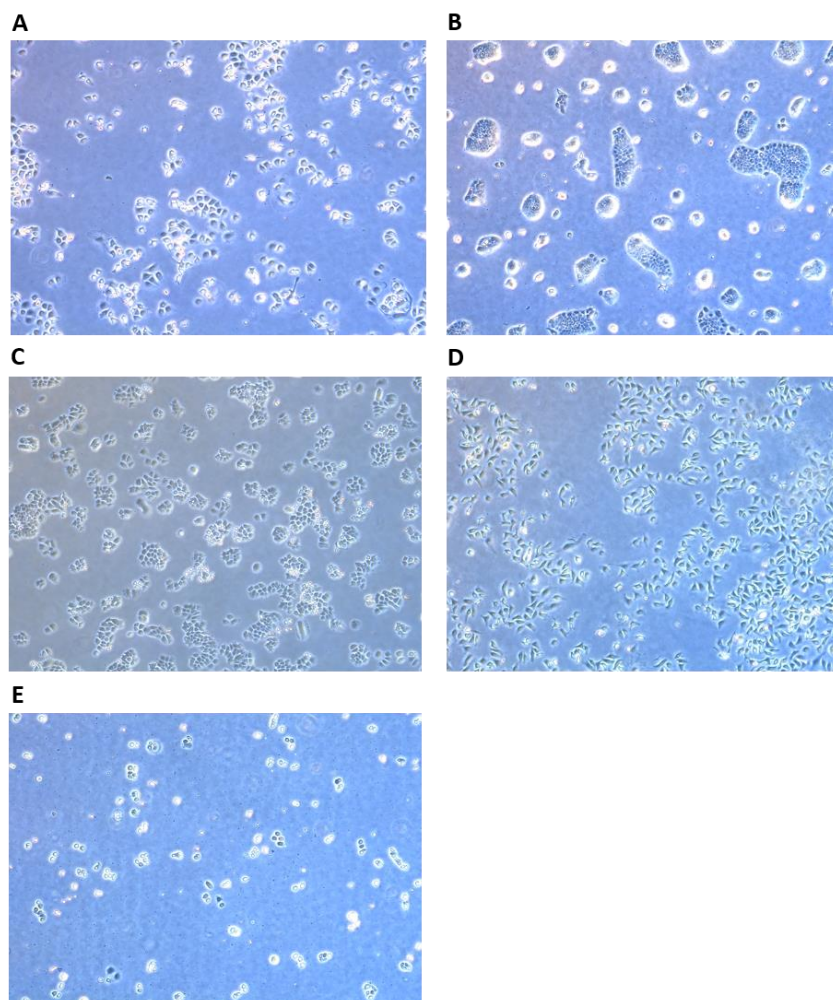


Figure 18. Microscopic images of the different tumor cell lines used in the SRB assay.

A) PANC-1; B) BxPC3; C) NCI-H460; D) MDA-MB-231 and E) MDA-MB-468 human tumor cell lines. Amplification: 20X.

Results (**Table 4**) demonstrate that none of the tested compounds had an effect in either pancreatic (BxPC3 and PANC-1) or lung (NCI-H460) cancer cell lines, at least at the concentrations tested. Interestingly, three of the compounds tested significantly inhibited the growth of both breast cancer cell lines (MDA-MB-231 and MDA-MB-468) with GI_{50} below 13 μ M. Indeed, compound **10** presented lowest GI_{50} value in the MDA-MB-468 cell line. Unfortunately, it was not possible to determine the GI_{50} values for most of the compounds, since they formed crystals at higher concentrations. Therefore, in these cases, the GI_{50} values were considered higher than the maximum concentration tested without crystal formation, once the exact value for the GI_{50} was not determined.

Table 4. GI₅₀ concentrations (GI₅₀) in different human tumor cell lines, using SRB the assay.

Cell line and respective GI ₅₀ * concentration (μM) for each compound					
Compound (μM)	<u>PANC-1</u>	<u>BxPC3</u>	<u>NCI-H460</u>	<u>MDA-MB-231</u>	<u>MDA-MB-468</u>
Compound 3	>10	>20	>20	>20	>20
Compound 4	>10	>10	>10	>10	>10
Compound 5	>10	>10	>10	>10	>10
Compound 6	>50	>30	>30	>10	>30
Compound 7	>10	>14	>10	12.56 ± 1.88	>14
Compound 8	>50	>30	>50	28.67 ± 1.34	8.73 ± 1.73
Compound 9	>50	>75	>75	>75	>75
Compound 10	>50	>75	>75	>75	4.67 ± 0.68

*GI₅₀ values correspond to the mean ± S.E.M. of at least three independent experiments, all performed in duplicated. Doxorubicin was used as a positive control on the cell lines in which the tested compounds showed activity, namely in the breast cancer cell lines MDA-MB-231 and MDA-MB-468. Doxorubicin GI₅₀ values were 68.34 ± 5.69 nM and 81.30 ± 8.99 nM in MDA-MB-231 and MDA-MB-468 cells, respectively. The concentrations tested were the ones possible without appearance of crystals or aggregates in culture.

Even though it is not possible to establish structure-activity relationships, since some GI₅₀ concentrations could not be determined, the results suggest a selectivity of compound **7** with *p*-Cl as functionalization for the breast cancer cell line MDA-MD-231. On the other hand, the furan derivative compound **10**, an electron-rich ring, seems more selective for the MDA-MB-468 cell line. Moreover, compound **8**, with a *p*-CN as functionalization, also a withdrawing group as compound **7**, was more selective for the breast cancer cell line MDA-MB-468 (lower GI₅₀).

Taking these results together, it was decided to further explore the mechanism of action of compounds **7**, **8** and **10** in MDA-MD-231 and MDA-MB-468 breast cancer cell lines. Of interest, these cancer cell lines are from TNBC presenting unique features, as presented in **Table 5**. The MDA-MB-231 cancer cell line is highly invasive and aggressive, belonging to the

class of TNBC tumors that have claudin-low genetic and molecular associated profile and poor prognosis^{40, 124-126}. On the other hand, the MDA-MB-468 cancer cell line is moderately invasive and is derived from a basal type like tumor with low response to chemotherapy, which is the only option for therapeutic approach for TNBC^{40, 124-126}.

Table 5. Molecular classification, immune-profile and typical features of the breast cancer cell lines MDA-MB-231 and MDA-MB-468^{40, 124-126}.

CLASSIFICATION	MOLECULAR IMMUNOPROFILE	FEATURES	CELL LINE
<u>Claudin-low</u>	ER–, PR–, HER2–	Ki67, E-cadherin, claudin-3, claudinin-4 and claudinin-7 low, Intermediate response to chemotherapy	MDA-MB-231
<u>Basal</u>	ER–, PR–, HER2–	EGFR+ and/or cytokeratin 5/6+, Ki67 high, endocrine nonresponsive, often chemotherapy responsive	MDA-MB-468

2.2 Effect of the selected compounds in the growth of non-tumorigenic cells

Next, the most promising compounds with effect in the inhibition of breast cancer cell growth (the ones with the lowest GI₅₀ values) were evaluated regarding their toxicity against the non-tumorigenic mammary epithelial MCF-12A cell line (**Figure 19**). For that, the SRB assay was performed using the GI₅₀ concentrations of each compound. Results presented in **Table 6** demonstrate that the compounds **7**, **8** and **10**, at the GI₅₀ concentrations in the most sensitive cancer cell line, caused a small or no effect in the growth of the non-tumorigenic MCF-12A cells. These results suggest that the three compounds are selective for cancer cells without affecting the non-tumorigenic ones, at the concentrations tested.

It is important to note that the duration of the SRB assay carried out in non-tumorigenic cells is longer than when carried out in cancer cells, since the non-tumorigenic cells have a slower cell growth rate. This longer duration of the assay allowed to evaluate possible unwanted delayed effects of the compounds in non-tumorigenic cells.

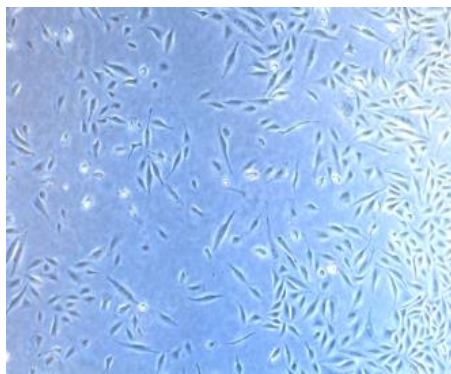
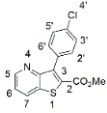
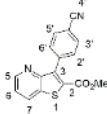
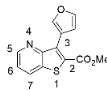


Figure 19. Morphology of MCF-12A cells (non-tumorigenic cell line) visualized under a Microscope.

Table 6. Evaluation of the toxicity of the most promising compounds in the non-tumorigenic cell line MCF-12A.

Compound	GI ₅₀ concentration (μM) in the tumor cell lines	Tumor cell line tested	% Growth of MCF-12A cell line at GI ₅₀ concentration
Compound 7 	12.56 ± 1.88	MDA-MB-231	88.62 ± 4.04
Compound 8 	8.73 ± 1.73	MDA-MB-468	117.73 ± 3.22
Compound 10 	4.67 ± 0.68	MDA-MB-468	82.13 ± 4.78

GI₅₀ concentrations values correspond to the mean ± S.E.M. of at least three independent experiments, all performed in duplicate. The % of growth of the cell line MCF-12A was achieved using the GI₅₀ concentrations of each compound in the indicated tumour cell lines.

2.3 Effect of the selected compounds on viable cell number of cancer cell lines

The effects of compounds **7**, **8** and **10** on breast cancer cell viability were determined 48 h after cell treatment, using the Trypan Blue Exclusion Assay. For that, the breast cancer cell lines (MDA-MB-231 and MDA-MB-468) were treated with the GI_{50} and $2x GI_{50}$ concentrations of the three most promising compounds, as well as with the vehicle (DMSO) at the same concentration used for the compounds (Control GI_{50} and Control $2x GI_{50}$). Results show that compound **7** at $2x GI_{50}$ concentration significantly reduced MDA-MB-231 cell viability. In addition, compound **10** at $2x GI_{50}$ concentration also reduced the cell viability of MDA-MB-468 cells. On the other hand, compound **8**, decreased MDA-MB-468 cell viability but the effect was not significant (**Figure 20**). Moreover, the vehicles (Control GI_{50} and Control $2x GI_{50}$) did not alter cancer cells viability, when compared with the blanks (cells treated only with medium), indicating that the effects observed are due to compounds treatment and not caused by DMSO toxicity. In addition, the positive control (doxorubicin), as expected, remarkably decreased cell viability in both cell lines.

It is important to take into consideration that the Trypan blue exclusion assay was performed in different conditions from the conditions used for the SRB assay. Indeed, the SRB assay was carried out in cells growing in medium with 5% FBS and in 96-well plates, while the Trypan blue exclusion assay was carried out in cells growing in medium with 10% FBS and in 6-well plates. These differences might justify why only the $2x GI_{50}$ compound treatments caused significant effects on cellular viability. Nevertheless, these results are in accordance with the previously observed inhibitory effect on cancer cell growth observed in the three selected compounds.

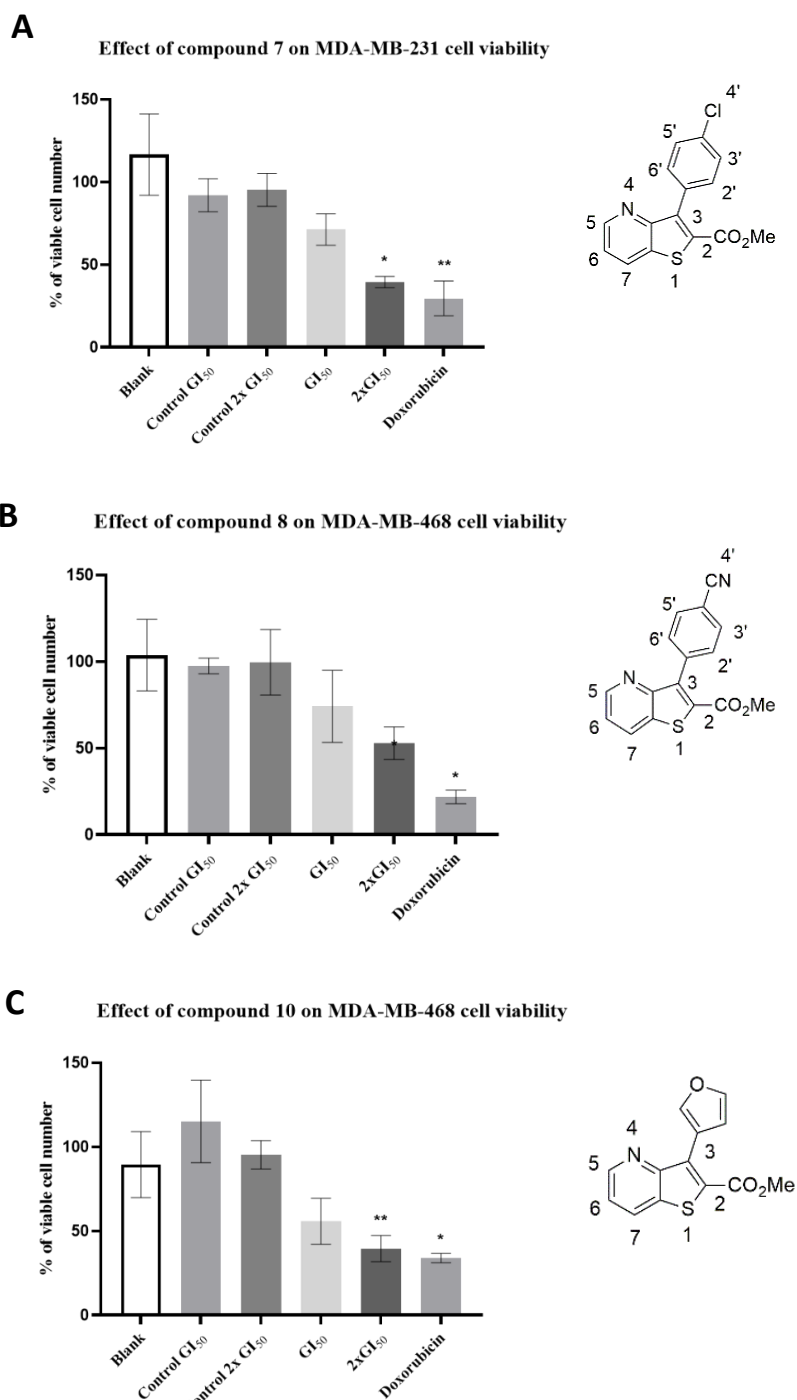


Figure 20. Effects of **compound 7** on MDA-MB-231 viable cell number.

(A) and of **compound 8 (B)** and **10 (C)** on MDA-MB-468 viable cell number, determined using the Trypan Blue Exclusion Assay. Cells were treated for 48 h with medium (Blank), with GI₅₀ concentration of each compound (13μM, 9μM and 5μM for **compounds 7, 8** and **10**, respectively) or 2xGI₅₀ concentration, and with DMSO (vehicle, at the amount used in the treatments). Results represent the mean ± SEM of at least three independent experiments. * $p \leq 0.05$, ** $p \leq 0.01$ of Controls vs. Treatments (Control GI₅₀ vs GI₅₀ and Control 2xGI₅₀ vs 2xGI₅₀) or Control GI₅₀ vs. Doxorubicin (positive control).

2.4 Effect of the selected compounds on cell cycle profile

Many antitumoral drugs are known to induce apoptosis and to target cell cycle-specific events¹²⁷. In order to understand whether the selected compounds (compounds **7**, **8** and **10**) are capable of causing alterations in the cell cycle profile, cells were treated during 48 h with the GI_{50} and $2x GI_{50}$ concentrations of each compound or with control treatments. A flow cytometry analysis of the cells was performed, after fixing and staining their DNA with Propidium Iodide (PI). This allows to measure the DNA content of the cells from different samples (treatments and controls), and to determine the percentage of cells in each of the cell-cycle phases (G1, S and G2).

Results showed that compound **7** had no effect on the cell cycle profile of MDA-MB-231 cells (**Figure 21**), although these results were from two independent experiments only. Compound **8** did also not cause any effect on the cell cycle profile of MDA-MB-468 cells (**Figure 21**). Since these two compounds inhibit cancer cell growth (already concluded from the previous data) but they do not interfere with the cell cycle profile, other possible mechanisms of action should be explored, namely a possible induction of apoptosis. This could be done with the Annexin V/PI assay¹²⁸.

Interestingly, compound **10**, at both concentrations tested (and compared with the respective controls) clearly decreased the G1/G0 and increased the G2/M phases of the cell cycle (**Figure 21**). Nevertheless, this analysis should be repeated since only two independent experiments were considered, and no statistical analysis could be performed. Thus, the effect of compound **10** in the cell cycle profile might justify the significant effect previously observed in the inhibition of MDA-MB-468 cells viability. The cell cycle arrest in the G2/M phase prevents cells to divide by mitosis and thus decreases their proliferative rate, leading to a decrease in the G1 phase. Of note, previous work by other scientists with a different compound, the 4-Hydroxynonenal, responsible for an oxidant-induced toxicity, induced a G2/M cell cycle arrest accompanied by a concomitant decrease in the G0/G1 phase and an activation of the p21 expression in HepG2 cells¹²⁹. Thus, further analysis, such as the analysis of p21 expression levels, could clarify the alterations caused in the cell cycle profile, and would help to understand the significant decrease of cancer viable cell number induced by compound **10**.

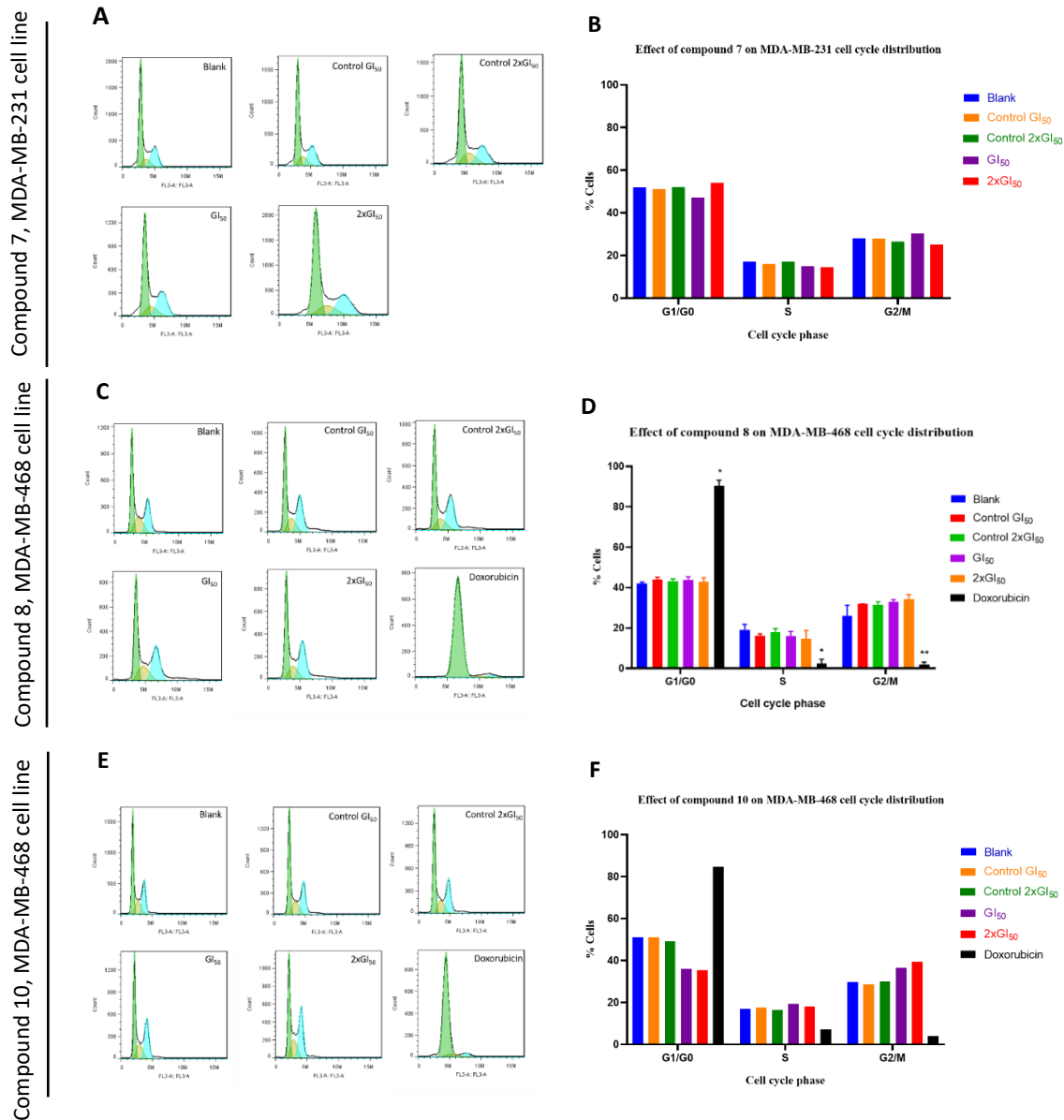


Figure 21. Cells cycle effects of **compound 7** on MDA-MB-231 cells (**panels A and B**), and of **compound 8** (**panels C and D**) and **10** (**panels E and F**) on MDA-MB-468 cells, analysed by Flow Cytometry following incubation with Propidium Iodide (PI).

Cells were treated for 48h with medium (Blank), with the GI_{50} concentration (13 μ M, 9 μ M and 5 μ M for **compounds 7, 8** and **10** respectively) or 2x GI_{50} concentration of each compound, or with DMSO (vehicle of the compounds as controls, tested at the same amount as used in the treatments). **A, C and E**) Plots from the FlowJo analysis. **B, D and F**) Statistical analysis of the data from the FlowJo, analysed on GraphPad Prism, using a two-way ANOVA followed by Tukey's multiple comparison test. Columns represent the mean \pm SEM of two (compound 7 and 10) or three (compound 8) independent experiments. * $p \leq 0.05$, ** $p \leq 0.01$ of Controls vs. Treatments (Control GI_{50} vs GI_{50} or Control 2x GI_{50} vs 2x GI_{50}) or Control GI_{50} vs. doxorubicin.

Moreover, the positive control (doxorubicin), caused a notable increase of G1 phase, as expected^{130, 131}, indicating that the experiment by itself is working. The cells treated with the vehicles (Control GI₅₀ and Control 2x GI₅₀) also showed values almost equal to the cells only treated with medium (blank), confirming that the effects observed are due to the compounds and not due to toxicity caused by the DMSO (vehicle of the compounds). Of note, treatment of MDA-MB-231 cells with the positive control (doxorubicin) reduced the number of cells drastically, therefore not being possible to read enough events in the cytometer. For this reason, the positive control is not included in the histograms of compound **7** (**Figure 21**).

2.5 Effect of the selected compounds on the expression levels of some proteins related with cell cycle, apoptosis and DNA damage

In an attempt to better understand the mechanism of action of the selected compounds (**7**, **8** and **10**) the expression levels of the apoptotic marker PARP-1¹³², the cell cycle markers p21¹³³ and cyclin-D1¹³⁴ and of the DNA damage marker γ -H2A.X¹³⁵, were analysed by Western Blot following 48h treatments. Each compound was tested in the most sensitive cell line.

Treatment with compound **7** did not cause a cleavage of PARP-1, in either of the concentrations tested in the MDA-MB-231 cells, contrarily to what was observed with the positive control, doxorubicin (**Figure 22**). These results suggest that compound **7** does not induce apoptosis. However, other analysis, such as the Annexin V/PI analysis by flow cytometry, should be performed to confirm this possibility. Moreover, a high expression level of γ -H2A.X was detected when cells were treated with 2x GI₅₀ concentration of compound **7**, suggesting that this compound induces DNA damage. The expression levels of p21 and cyclin-D1 could not be detected in this cell line (neither in cells treated with the compound nor in the positive control).

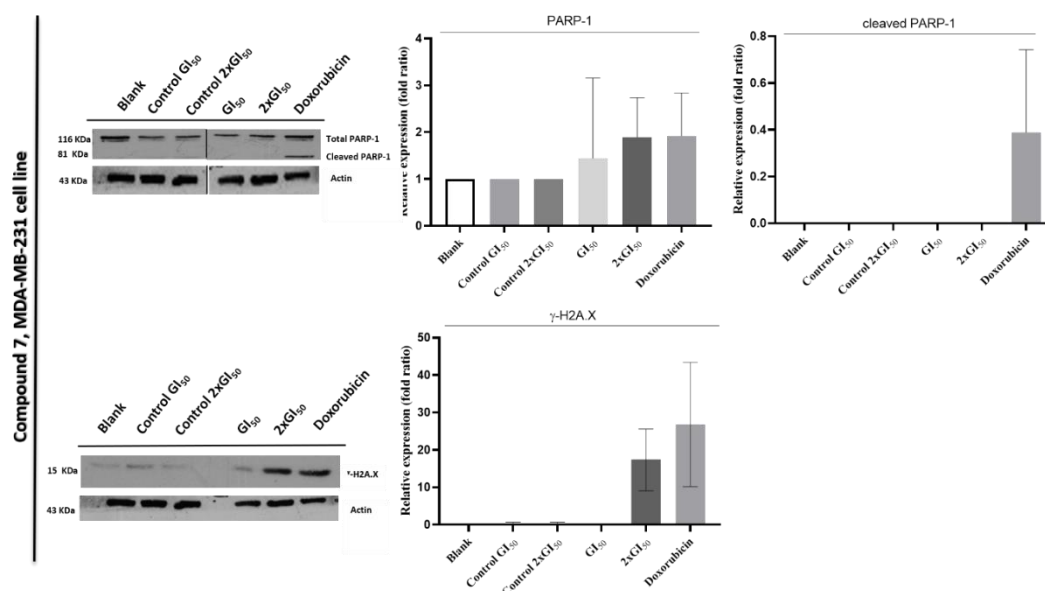


Figure 22. Expression levels of PARP-1 and γ -H2A.X in MDA-MB-231 cells, following treatment with **compound 7**, analysed by Western blot.

Cells were treated for 48 h with medium (Blank), GI₅₀ (13 μ M) and 2x GI₅₀ concentration (μ M) of the compound, or with the corresponding DMSO concentrations (control). Actin was used as a loading control. Images are representative of at least three independent experiments. The densitometer results are presented as the mean \pm S.E.M. from at least three independent experiments and expressed after the normalization for actin.

To the best of our knowledge, there are no reported studies describing thienopyridine derivatives as inducers of DNA damage. Thus, other complementary assays should be done in order to confirm the possible effect of compound **7** as inducer of DNA damage. For example, the Comet assay, a single-cell gel electrophoresis that allows measuring deoxyribonucleic acid (DNA) strand breaks in eukaryotic cells¹³⁶, could help clarifying this possibility.

Treatment of MDA-MB-468 cells with compound **8** non-significantly decreased the expression levels of total PARP-1 at 2x GI₅₀ concentration (although, surprisingly, no cleaved PARP-1 was detected, **Figure 23**). Therefore, other assays such as the Annexin V/p¹²⁸ are necessary in order to verify if compound **8** induces apoptosis. Unfortunately, the p21 and γ -H2A.X proteins were not detected in this particular cell line (including in the positive control).

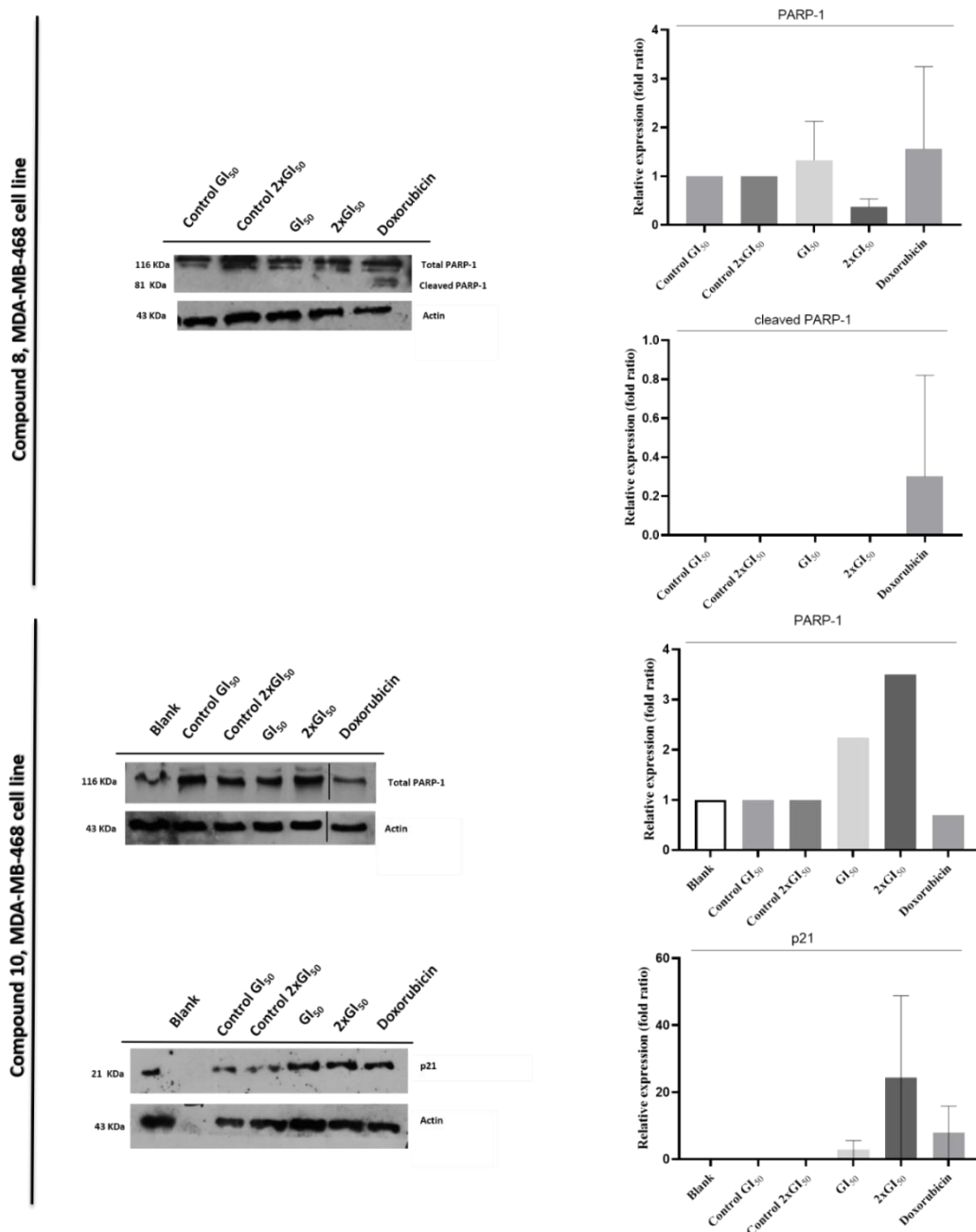


Figure 23. Expression levels of PARP-1 and p21 in MDA-MB-468 cells, following treatment with **compounds 8** or **10**, analysed by Western blot.

Cells were treated for 48 h with medium (Blank), with GI₅₀ and 2x GI₅₀ concentrations of each compound, or with the corresponding DMSO concentrations. Actin was used as a loading control. Images are representative at least three independent experiments. The densitometer results are presented as the mean \pm S.E.M. from at least three independent experiments (except for PARP-1 analysis referring to compound 10, for which only one experiment was carried out); and expressed after the normalization of the values with actin.

Treatment of MDA-MD-468 cells with compound **10** (**Figure 23**), surprisingly caused an increase in the expression levels of total PARP-1 (contrarily to what was observed with the positive control, doxorubicin, which decreased total PARP-1), but only one experiment was analysed due to time limitations and no statistical effect was verified. Moreover, the expression of cleaved PARP-1 was not detected in either controls or treatments, suggesting that the antibody did not work properly in this analysis. Therefore, other assays need to be performed (such as the Annexin V/PI staining by Flow Cytometry ¹²⁸), to clarify if this compound interferes with apoptosis. Compound **10** also caused a dose-dependent increase on the expression levels of p21, at both concentrations tested. This is in agreement with the previous data obtained from the cell cycle profile analysis (decrease in G0/G1 and increase G2/M) and effect on viable cell number. Future work should include analysis of other proteins involved in the cell cycle, such as cyclin-B (associated with G2 arrest ¹³⁷).

Unfortunately, it was not possible to detect cyclin-D1 or γ -H2A.X expressions levels in this cell line (either in treatments or in controls), with the antibodies selected for this work.

For the proteins for which no expression was detected, including in the positive control, future optimizations of the antibody incubation conditions (concentration, time and temperature) are needed, for each cell line.

2.6 Antitumoral effect of compound 7 by the Chick Chorioallantoic Membrane (CAM) assay *in ovo* inoculated with MDA-MB-231 cells

The previous data indicated that compound **7** was the most promising synthesised compound against the MDA-MD-231 cell line (representing an aggressive type of TNBC). In addition, this compound induced the expression of the DNA damage marker γ -H2A.X. Interestingly, compound **7** has also the particularity of having part of its hydrophobic tail (the phenyl ring coupled to a Cl atom) similar to Sorafenib. This specific common region is responsible for the binding to the allosteric region, which corresponds to the adjacent site where Sorafenib binds to the ATP-binding site (common sites for protein kinases) ¹³⁸. Sorafenib is an antiangiogenic drug, known as an active multikinase inhibitor ¹³⁹, approved to treat hepatocellular carcinoma patients with advance untreatable tumors ¹⁴⁰ Unfortunately, in breast cancer, the use of Sorafenib is not encouraged given its toxicity ¹⁴¹. Therefore, the

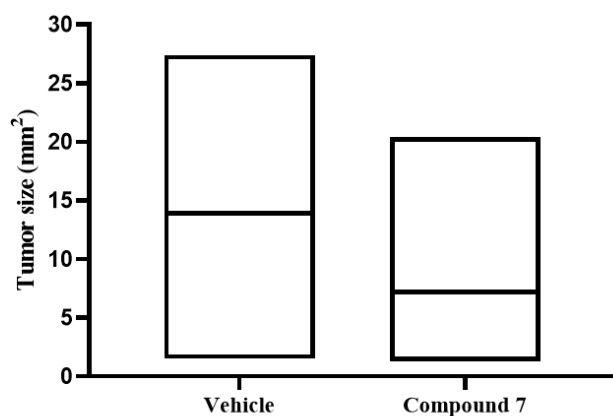
antiangiogenic and antitumor potential of compound **7** was studied using the Chick Embryo Chorioallantoic Membrane (CAM) assay.

CAM assay is used to study the effect of compounds on the angiogenesis process¹⁴², as well as to evaluate the effect on tumor growth (tumorigenic response). Since animal models are expensive and time consuming, the CAM assay has been used as a suitable *in vivo* model, alternative to mouse model, for the screening of potential novel drugs. Thus, the CAM assay was performed by inoculating MDA-MB-231 cells *in ovo*, in order to create tumors in the eggs, which was followed by testing the effect of compound **7** as potential antiangiogenic and inhibitor of tumor formation.

The obtained results (from 2 independent experiments) demonstrate that treatment of inoculated eggs for 48h with the GI₅₀ concentration of compound **7** efficiently decreased tumor formation (tumor size), when compared with the control group (vehicle) (**Figure 24**). Unfortunately, the antiangiogenic potential was not possible to analyse due to the high vascularization induced by the breast cancer cells, which lead to some degree of inflammation. Therefore, even though this needs further confirmation, the CAM assay showed promised results regarding anti-tumorigenic effect. This needs to be further confirmed in xenografts in nude mice.

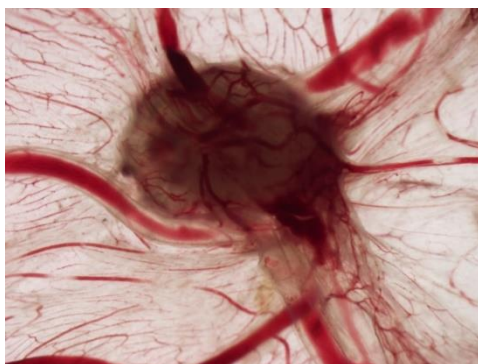
A

Effect of compound 7 on tumor formation by CAM assay



B

1



2

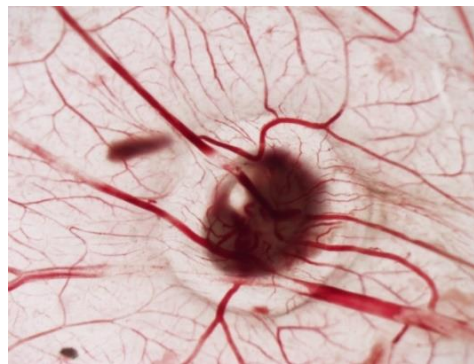


Figure 24. Chick Embryo Chorioallantoic membrane (CAM) assay. MDA-MB-231 cells were injected in the eggs, which and, after 24 h, were treated with vehicle or **compound 7** at GI_{50} concentration, for 48 h.

A) Tumor size of eggs treated with vehicle and **compound 7**. Data is from 2 independent experiments. **B)** Representative images of CAM assay (1.25X amplification): **1)** tumor size of cells treated with vehicle (DMSO) and **2)** tumor size of cells treated with **compound 7**.

CHAPTER III

CONCLUSION

1. FINAL REMARKS

The synthesis of novel compounds with potential applications in fields such as medicine, pharmacy, biology and medicinal chemistry is crucial for countless diseases, including to improve cancer treatment. Cancer is the disease of the century and the second major cause of death worldwide, just after deaths provoked by cardiovascular illnesses⁴. Thus, the screening for novel potential antitumoral drugs and the understanding of their possible mechanisms of action is of great importance to the fight against cancer.

The thieno[3,2-*b*]pyridine derivatives are one of the classes of compounds with known anticancer potential. Therefore, this work aimed the synthesis and fully characterization of novel methyl 3-(het)arylthieno[3,2-*b*]pyridine-2-carboxylates obtained by C-C Pd-catalyzed Suzuki-Miyaura cross-coupling, and the evaluation of their potential antitumor activity in several human tumor cell lines.

Considering all the specific aims of this work, it was a fulfilling year. From the first part of this work, in the synthesis process two important precursors were obtained, the methyl 3-aminothieno[3,2-*b*]pyridine-2-carboxylate (**1**) and the methyl 3-bromothieno[3,2-*b*]pyridine-2-carboxylate (**2**), using *t*-BuONO and CuBr₂, with yields of 91 and 56%, respectively. With the latter compound **2**, a series of eight novel compounds was prepared by C-C Suzuki-Miyaura cross-coupling, with moderate to high yields (from 35% to 84%). Those compounds were fully characterized by m.p., ¹H- and ¹³C-NMR, including bi-dimensional homonuclear ¹H-¹H (COSY) and heteronuclear correlations ¹H-¹³C (HSQC and HBMC) to attribute the signals; Low and High-resolution Mass Spectrometry (HRMS) or Elemental Analysis. Therefore, new synthesised compounds were generated, which makes this work innovative.

Regarding the biological part of this work, the evaluation of the effect of the series of eight compounds on cell growth (by the SRB assay) allowed to find the three most promising compounds, namely compounds **7**, **8** and **10**, with GI₅₀ values below 13 μM. Interestingly, these three compounds presented only effects against the TNBC cell lines used (MDA-MB-231 and MDA-MB-468). Moreover, and importantly, the three compounds had little or no effect against the non-tumorigenic cancer cell line MCF-12A, at the concentrations tested (that inhibited growth of the cancer cells by 50%). Therefore, these 3 best compounds seem to have selectivity for breast cancer cell lines, without toxicity effects against non-tumorigenic cells.

Although further assays are needed to understand the mechanisms of action of the best compounds, some conclusions can be taken from the work presented in this dissertation. First, compound **7** seems to cause DNA damage in MDA-MD-231 cells, since it induced high expression levels of the DNA damage marker γ -H2A.X at a concentration of $2x GI_{50}$. Regarding compound **10**, it interfered with the cell cycle-profile of MDA-MB-468 cells, increasing the % of cells in G2/M phase with a consequent decrease of the % of cells in the G0/G1 phase, at both concentrations tested (GI_{50} and $2x GI_{50}$). In addition, treatment with this compound caused an increase in the levels of expression of p21 (cell cycle related protein). Regarding compound **8**, it seemed not alter the cell cycle profile nor to induce apoptosis, at the concentrations tested.

Finally, preliminary experiments indicate that compound **7** decreased tumor size induced by inoculation of MDA-MB-231 cells *in ovo*.

2. FUTURE PERSPECTIVES

In this work, a problem of crystal formation in culture (*in vitro* studies) was verified, when higher concentrations of the compounds were tested, which indeed limited the concentration used and thus the determination of the potential antitumor effects of the compounds. One suggestion for future work is to improve the solubility of these compounds in order to allow an increase in the maximum concentration tested. For that, one option is do chemical alterations, such as make complexation and/or salt formations or use the miscellaneous methods, like the use of adjuvants surfactants and/or solubilizers¹⁴³. In fact, Zafar and co-authors¹⁴⁴ described alternatives to counteract the lack of aqueous solubility of some thieno[2,3-*b*]pyridines, by using solubilizing agents such as the cyclodextrin through the addition of the solubilizing group to the scaffold of the thieno[2,3-*b*]pyridine derivatives. Alternatively, other substitution patterns or another type of derivatives (e.g. pyrazines instead of pyridines) with the same substituents might be interesting to synthesize and test biologically.

Concerning the biological part of this work, some results could not be totally clarified due to the lack of time to finish the number of experiments required, or even the need to perform other complementary assays. Therefore, for compound **7** and **8**, since no effects were

Chapter III - Conclusion

observed on the cell cycle profile, other possible mechanism of action responsible for the inhibition of breast cancer cell growth should be explored, such as the possible induction of apoptosis (for example using Annexin V/PI) by those compounds. In addition, since high expression levels of γ -H2A.X were detected in MDA-MB-231 cells treated with compound **7**, it would be interesting to confirm those results, for example using the Comet assay¹³⁶, to clarify the effect of compound **7** in the induction of DNA damage. In addition, due to the non-conclusive results on the effect of compound **10** on apoptosis, in the future the use of other approaches, for example the Annexin V/PI analysis, would clarify if compound **10** induces or not apoptosis.

In the future, another interesting evaluation of the selected compounds would be to perform a screening using 3D cell culture. The 3D model is physiologically more relevant since it has into account the structure of the tumor, being nowadays considering a relevant *in vitro* approach to determine the cytotoxicity of new therapeutic compounds¹⁴⁵. Additionally, the use of other cancer cell line models, or even multidrug resistance cell lines (pairs of drug sensitive and drug resistant cell lines) could be studied, as well as other non-tumorigenic cell lines, such as MCF-10A, to further confirm that the compounds are only selective for cancer cells and non-toxic to non-tumor cells. Finally, since compound **7** reduced the tumor size of MDA-MB-231 cells in the CAM assay, it would be interesting to test this compound in xenografted mouse models.

CHAPTER IV

EXPERIMENTAL

1. CHEMICAL SYNTHESIS

1.1 Synthesis: General Procedure

Melting points (°C) were determined in a SMP3 Stuart apparatus. ^1H and ^{13}C NMR spectra were recorded on a Bruker Advance III at 400 and 100.6 MHz respectively, which integrates the national network of NMR (PTNMR), using the signals of the non-deuterated solvents of CHCl_3 (7.27 ppm) of the CDCl_3 or of DMSO (2.49 ppm) of the $\text{DMSO-}d_6$, as internal pattern and reference relatively to TMS (0 ppm). DEPT 135° (differential technique of ^{13}C) and bi-dimensional homo $^1\text{H-}^1\text{H}$ (COSY) and heteronuclear correlations $^1\text{H-}^{13}\text{C}$ (HSQC and HMBC) were used to attribute the signals.

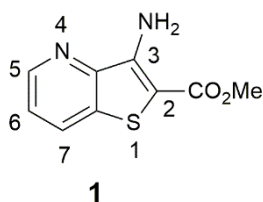
Elemental analysis was performed on a LECO CHNS 932 elemental analyser. The low-resolution MS spectra were obtained by ESI using Thermo-Finnigan LXQ at the Centre of Chemistry of University of Minho. HRMS were obtained at the external service of mass spectrometry of the University of Vigo-Spain (CACTI) using EI.

The reactions were all followed by thin layer chromatography (TLC), in plates of aluminium cover with a layer of 0.2 mm of silica gel (Macherey-Nagel) with a fluorescence indicator (UV254). Column chromatography was performed on silica gel 0.060-0.200 mm, 60 A, and dry flash chromatography on silica gel 0.035-0.070 mm, 60 A, to purify the compounds. Whenever necessary washes with ether or petroleum ether were performed after column or even a recrystallization using the same solvents or mixture of both.

Petroleum ether refers to the boiling rang 40-60 °C. Ether refers to diethylether. When a solvent gradient was used, the increase of polarity was made from petroleum ether to mixtures of ether/petroleum ether, increasing the ether proportion in 10%. DME refers to 1,2-dimethoxyethane. The catalyst $\text{PdCl}_2(\text{dppf})\cdot\text{CH}_2\text{Cl}_2$ (1:1) refers to 1,10-bis(diphenylphosphino) ferrocenedichloropalladium (II), complex with dichloromethane (1:1) and was purchased from Aldrich.

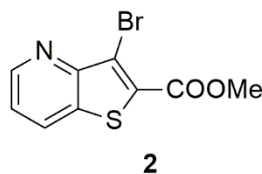
1.1.1 Synthesis of starting materials

1.1.1.1 Methyl 3-aminothieno[3,2-*b*]pyridine-2-carboxylate (**1**):



In a round flask, to a mixture of 3-fluoropicolonitrile (1.00 g, 820 μmol) in DMF (10 mL), methyl thioglycolate (1.5 equiv.) and KOH (3 equiv., aq. 30%) were added at 0 °C and it was left stirring for 1h. Then, the mixture was poured into ice and yellow solid came out, which was filtrated under vacuum and dried in the oven at 50 °C overnight (0.510 g, 92%). The $^1\text{H-NMR}$ spectrum was identical to the one earlier described by our research group ⁸³.

1.1.1.2 Methyl 3-bromothieno[3,2-*b*]pyridine-2-carboxylate (**2**):



In a round flask, to the amine **1** (0.700g, 3.36 μmol) in CH_3CN (6 mL), *t*-BuONO (1.5 equiv.) and CuBr_2 (1.2 equiv.) were added at room temperature and it was left stirring for 3 h. Then, water (10 mL) was added and the aqueous phase was extracted with CH_2Cl_2 (3x10 mL) and the organic phases were collected, dried (MgSO_4) and filtered. Removal of the solvent gave a brown solid which was purified by column chromatography using a solvent gradient till 40%-60% ether/ether petroleum. Compound **2** was obtained as a white solid (0.450 g, 57%). The $^1\text{H-NMR}$ spectrum was identical to the one earlier described by our research group ⁸⁵.

1.2 Synthesis of the C-C Suzuki-Miyaura coupling products

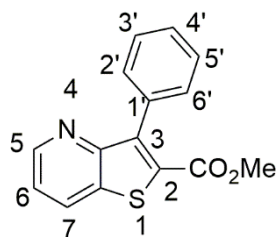
1.2.1 General procedure

In a round flask, DME (3 mL) and water (1 mL), methyl-3-bromothieno[3,2-*b*]pyridine-2-carboxylate (**2**), (het)aryl boronic acids, pinacol esters, or potassium trifluoroborates (1.2 equiv. unless stated), PdCl₂(dppf).CH₂Cl₂ (1:1) (2mol%, unless stated), K₂CO₃ (6 equiv.) were added and the mixture was heated with stirring at 100 °C for some hours. The reactions were monitored by TLC.

After cooling, the solvents were evaporated under reduced pressure giving a solid or water was added (10 mL) and extraction with ethyl acetate (3x10 mL) was performed. In the latter case, the organic phases were collected, dried (MgSO₄), filtered and the solvent removal gave a solid.

All the resulting solids were submitted to a column chromatography or to a dry flash to give the products.

1.2.1.1 Methyl 3-phenylthieno[3,2-*b*]pyridine-2-carboxylate (3)



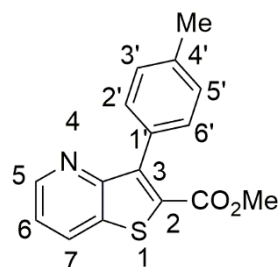
From compound **2** (0.100 g, 0.370 mmol) and phenylboronic acid pinacol ester (0.0900 g, 0.440 mmol) following the general procedure for 3 hours; purification by column chromatography using 50% ether/petroleum ether, gave compound **3** as a white solid (0.0730 g, 74% yield).

m.p.: 152-154 °C

¹H-NMR (DMSO-*d*₆, 400MHz) δ = 3.75 (3H, s, OMe), 7.43-7.48 (5H, m, Ar-H), 7.56 (1H, dd, *J*= 8.0 and 4.4 Hz, 6-H), 8.61 (1H, dd, *J*= 8.0 and 1.6 Hz, 7-H), 8.74 (1H, dd, *J*= 4.4 and 1.6 Hz, 5-H). **¹³C-NMR** (DMSO-*d*₆, 100.6 MHz) δ = 52.6 (OMe), 122.0 (6-CH), 127.4 (2×CH), 128.0 (CH), 130.5 (2×CH), 131.0 (C), 132.0 (7-CH), 133.1 (C), 134.2(C), 142.6 (C), 148.6 (5-CH), 153.3 (C), 162.1 (C=O) ppm.

MS (ESI) m/z (%): 270.03 [M+H]⁺ (100%).

Elemental Analysis Calcd. for C₁₅H₁₁NO₂S (269.32): C, 66.89%, H, 4.12%, N, 5.20%, S, 11.91%. Found: C, 67.08 %, H, 4.09 %, N, 5.46 %, S, 12.16 %.

1.2.1.2 Methyl 3-(*p*-tolyl)thieno[3,2-*b*]pyridine-2-carboxylate (**4**)

From compound **2** (0.150 g, 0.554 mmol) and potassium *p*-tolyltrifluoroborate (0.132g, 0.664 mmol) following the general procedure, using PdCl₂(dppf).CH₂Cl₂ (4%mol) and heating for 4.5 h; purification by column chromatography using 40% ether/petroleum ether, gave compound **4** as a white solid (0.132 g, 84% yield).

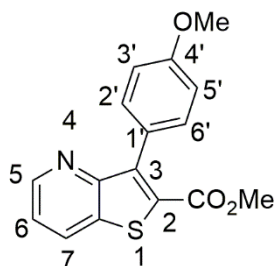
m.p.: 153-154 °C

¹H-NMR (CDCl₃, 400MHz) δ = 2.44 (3H, s, Me), 3.85 (3H, s, OMe), 7.33 (2H, d, J= 8.0 Hz, 3' and 5'-H), 7.43 (1H, dd, J= 8.4 and 4.8 Hz, 6-H), (2H, d, J= 8.0 Hz, 2' and 6'-H), 8.24 (1H, dd, J= 8.4 and 1.6 Hz, 7-H), 8.80 (1H, dd, J= 4.8 and 1.6 Hz, 5-H). **¹³C-NMR** (CDCl₃, 100.6 MHz) δ = 21.5 (Me), 52.5 (OMe), 121.1 (6-CH), 125.2 (C), 128.7 (3' and 5'-CH), 130.1 (2' and 6'-CH), 130.7 (C), 131.2 (C), 134.9 (7-CH), 138.2 (C), 144.0 (C), 148.4 (5-CH), 154.6 (C), 162.7 (C=O) ppm.

MS (ESI) m/z (%): 284.07 [M+H]⁺ (83%).

Elemental Analysis Calcd. for C₁₆H₁₃NO₂S (283.35): C, 67.82%, H, 4.62 %, N, 4.94 %, S, 11.32 %. Found: C, 68.15 %, H 4.35 %, N, 5.20 %, S, 11.69 %.

1.2.1.3 Methyl 3-(4-methoxyphenyl)thieno[3,2-*b*]pyridine-2-carboxylate (5)



From compound **2** (0.100 g, 0.370 mmol) and potassium 4-methoxyphenyltrifluoroborate (0.094 g, 0.440 mmol), following the general procedure for 2 h; purification by column chromatography using 25% ether/petroleum ether, gave compound **5** as a white solid (0.0450 g, 40% yield).

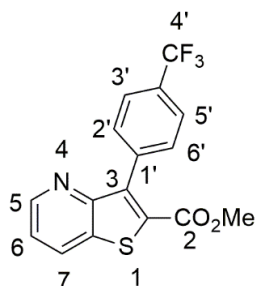
m.p.: 190-191 °C

¹H-NMR (CDCl₃, 400MHz) δ = 3.85 (3H, s, CO₂Me), 3.89 (3H, s, OMe), 7.05 (2H, d, J= 8.8 Hz, 2H, 3' and 5'-H), (1H, dd, J= 8.0 and 4.4 Hz, 6-H), 7.50 (2H, d, J= 8.8 Hz, 2' and 6'-H), 8.23 (1H, dd, J= 8.0 and 1.6 Hz, 7-H), 8.80 (1H, dd, J= 4.4 and 1.6 Hz, 5-H). **¹³C-NMR** (CDCl₃, 100.6 MHz) δ = 52.5 (COOMe), 55.2 (OMe), 113.4 (3' and 5'-CH), 121.1 (6-CH), 125.2 (C), 130.7 (7-CH), 130.9 (C), 131.6 (2' and 6'-CH), 134.9 (C), 143.6 (C), 148.5 (5-CH), 154.2 (C), 159.7 (4'-C), 162.9 (C=O) ppm.

MS (ESI) m/z (%): 300.06 [M⁺+H]⁺ (100%).

Elemental Analysis Calcd. for C₁₆H₁₃NO₃S (299.34): C, 64.20%, H, 4.38%, N, 4.68%, S, 10.71%. Found: C, 64.20 %, H, 4.45 %, N, 4.848 %, S, 10.33%.

1.2.1.4 Methyl 3-(4-(trifluoromethyl)phenyl)thieno[3,2-*b*]pyridine-2-carboxylate (**6**)



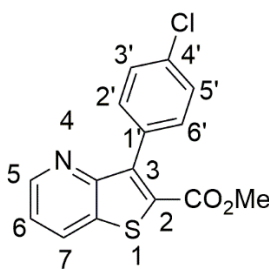
From compound **2** (0.100 g, 0.370 mmol) and potassium 4-(trifluoromethyl)phenyltrifluoroborate (0.106 g, 0.440 mmol) following the general procedure for 4 h; purification by column chromatography using 40% ether/petroleum ether, gave compound **6** as a white solid. This was recrystallized from ether to give a purer solid (0.0350 g, 40% yield).

m.p.: 170-171 °C

¹H-NMR (CDCl₃, 400MHz) δ = 3.85 (3H, s, Me), 7.43 (1H, broad d, 6-H), 7.66 (2H, d, J=8.0 Hz, 2' and 6'-H), 7.78 (2H, d, J= 8.0 Hz, 3' and 5'-H), 8.28 (1H, broad d, J=8.0 Hz, 7-H), 8.80 (1H, broad s, 5-H). **¹³C-NMR** (CDCl₃, 100.6 MHz) δ = 52.7 (OMe), 120.6 (6-CH), 124.8 (q, J=271.62 Hz, CF₃), 124.9 (q, J= 3.6 Hz, 3' and 5' -CH), 130.3 (q, J=32.4 Hz, CCF₃), 130.8 (2' and 6'- CH), 131.0 (7-CH), 132.3 (C), 135.0 (C), 137.0 (C), 142.1 (C), 148.8 (5-CH), 153.3 (C), 162.4 (C=O). **¹⁹F -NMR** (CDCl₃, 376.5 MHz): δ = - 62.63 (s, F₃) ppm.

MS (ESI) m/z (%): 338.05 [M+H]⁺ (100%).

Elemental Analysis Calcd. for C₁₆H₁₀F₃NO₂S (337.32): C, 56.97%, H, 2.99%, N, 4.15%, S, 9.51%. Found: C, 56.62 %, H 2.65 %, N 4.35 %, S, 9.81 %.

1.2.1.5 Methyl 3-(4-chlorophenyl)thieno[3,2-*b*]pyridine-2-carboxylate (7)

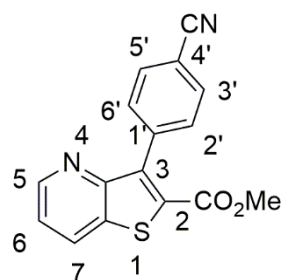
From compound **2** (0.120 g, 0.443 mmol) and potassium (4-chlorophenyl)trifluoroborate (0.116 g, 0.532 mmol) following the general procedure for 3 h; purification by column chromatography using 50% ether/petroleum ether, gave compound **7** as a white solid (0.102 g, 82% yield).

m.p.: 195–196 °C

¹H-NMR (CDCl₃, 400MHz) δ = 3.85 (3H, s, OMe), 7.43 (1H, dd, J=8.4 and 4.4 Hz, 6-H), 7.49 (4H, coalesced doublets, Ar-H), 8.27 (1H, broad d, J= 8.4 Hz, 7-H), 8.81 (1H, broad s, 5-H).
¹³C-NMR (CDCl₃, 100.6 MHz) δ = 52.6 (OMe), 121.3 (6-CH), 128.3 (2×CH), 131.2 (7-CH), 131.7 (2×CH), 132.2 (C), 134.7 (C), 135.1 (C), 142.1 (C), 148.4 (5-CH), 153.4 (C), 157.3 (C), 162.5 (C=O) ppm.

MS (ESI) m/z (%): 326.0 [M³⁵Cl+Na]⁺ (100.0%), 328.0 [M³⁷Cl+Na]⁺ (37.9%), 304.03 [M³⁵Cl+H]⁺(82.3%), 306.04 [M³⁷Cl+H]⁺(29.8%).

HRMS (EI) M⁺ ³⁵Cl Calcd. for C₁₅H₁₀³⁵ClNO₂S: 303.0121; Found: 303.0134. M⁺ ³⁷Cl Calcd. for C₁₅H₁₀³⁷ClNO₂S: 305.0091; Found: 305.0099.

1.2.1.6 Methyl 3-(4-cyanophenyl)thieno[3,2-*b*]pyridine-2-carboxylate (**8**)

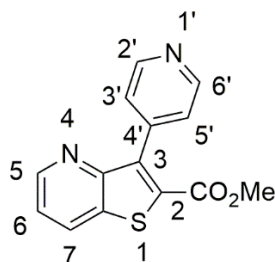
From compound **2** (0.100 g, 0.37 mmol) and 1.6 equiv. potassium (4-cyanophenyl)trifluoroborate (0.121 g, 0.592 mmol) following the general procedure for 3 h. The solid obtained was submitted to dry flash till 90% ether/petroleum ether to give compound **8** as a white (0.038 g, 35% yield).

m.p.: 198-200 °C

¹H-NMR (CDCl₃, 400MHz) δ = 3.86 (3H, s, CO₂Me), 7.44 (1H, dd, J= 8.0 and 4.4 Hz, 6-H), 7.65 (2H, d, J= 8.4 Hz, 2' and 6'-H), 7.80 (2H, d, J= 8.4 Hz, 3' and 5'-H), 8.27 (1H, broad dd, 7-H), 8.78 (1H, broad d, 5-H). **¹³C-NMR** (CDCl₃, 100.6 MHz) δ = 52.7 (OMe), 112.2 (C), 118.9 (C), 121.5 (6-CH), 131.00 (7-CH), 131.3 (3' and 5'-CH), 131.6 (2' and 6'-CH), 132.6 (C), 135.0 (C), 138.2 (C), 141.4 (C), 148.8 (5-CH), 153.4 (C), 162.2 (C=O) ppm.

HRMS (EI) M⁺ Calcd. for C₁₆H₁₀N₂O₂S: 294.0463. Found: 294.0474.

1.2.1.7 Methyl 3-(pyridin-4-yl)thieno[3,2-*b*]pyridine-2-carboxylate (9)



From compound **2** (0.120 g, 0.443 mol) and 1.6 equiv. of 4-pyridine boronic acid (0.079 g, 0.709 mmol) following the general procedure, using PdCl₂(dppf).CH₂Cl₂ (4%mol) and heating for 4 h. The solid was submitted to dry flash chromatography till 80% ether/petroleum ether to give compound **9** as a white solid (0.0400 g, 66% yield).

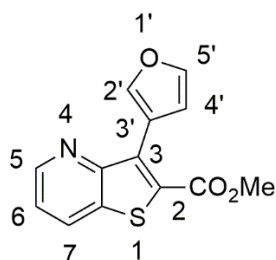
m.p.: 192-193°C

¹H-NMR (CDCl₃, 400MHz) δ = 3.90 (3H, s, OMe), 7.50 (1H, dd, J= 8.4 and 4.4 Hz, 6-H), 7.90 (2H, broad d, 3' and 5'-H), 8.32 (1H, dd, J=8.4 and 1.2 Hz, 7-H), 8.79-8.82 (3H, m, 5-H, 2' and 6'-H). **¹³C-NMR** (CDCl₃, 100.6 MHz) δ = 53.1 (OMe), 122.0 (6-CH), 127.8 (3' and 5'-CH), 131.1 (7-CH), 134.4 (C), 135.1 (C), 137.7 (C), 139.3 (C), 143.0 (2' and 6'-CH), 149.3 (5-CH), 152.6 (C), 161.7 (C=O) ppm.

MS (ESI) m/z (%): 271.0380 [M⁺+H]⁺ (100.00%).

Elemental Analysis Calcd. for C₁₄H₁₀N₂O₂S (270.31): C, 62.21%, H, 3.73%, N, 10.36%, S, 11.86%. Found: C, 61.90 %, H, 3.69 %, N, 10.06 %, S, 11.79 %.

1.2.1.8 Methyl 3-(furan-3-yl)thieno[3,2-*b*]pyridine-2-carboxylate (**10**)



From compound **2** (0.120 g, 0.443 mmol) and 1.6 equiv. potassium 3-furanylboronic acid (0.0706 g, 0.709 mmol) following the general procedure, using PdCl₂(dppf).CH₂Cl₂ (4%mol) and heating for 4.5h. The solid was submitted to dry flash chromatography till 30% ether/petroleum ether to give compound **10** as a white solid (0.0700 g, 52% yield).

m.p.: 130-132 °C

¹H-NMR (CDCl₃, 400MHz) δ = 3.94 (3H, s, OMe), 7.02-7.03 (1H, m, Ar-H), 7.40 (1H, dd, J=8.4 and 4.4 Hz, 6H), 7.56-7.57 (1H, m, Ar-H), 8.21(1H, dd, J=8.4 and 1.6 Hz, 7-H), 8.25-8.26 (1H, m, Ar-H), 8.81 (1H, dd, J= 4.4 and 1.6 Hz, 5-H). **¹³C-NMR** (CDCl₃, 100.6 MHz) δ = 52.6 (OMe), 112.3 (CH), 116.7 (C), 121.2 (6-CH), 130.0 (C), 130.6 (7-CH), 134.5 (C), 134.6 (C), 141.8 (CH), 144.3 (CH), 148.1 (5-CH), 162.8 (C=O) ppm.

MS (ESI) m/z (%): 260.04 [M⁺+H]⁺ (100.00%).

Elemental Analysis Calcd. for C₁₃H₉NO₃S (259.08): C, 60.22%, H, 3.50%, N, 5.40 %, S, 12.37 %. Found: C, 60.27 %, H, 3.33 %, N, 5.69 %, S, 12.48 %.

2. BIOLOGICAL STUDIES

2.1 Reagents and Compounds

Fetal bovine serum (FBS) and phosphate buffered saline (PBS) were purchased from Biowest and Gibco, respectively. Acetic acid, dimethyl sulfoxide (DMSO), ethylene diamine tetraacetic acid (EDTA), sulforhodamine B (SRB), trypan blue, trichloroacetic acid (TCA) and Tris base were purchased from Sigma Aldrich.

Stock solutions of the synthesized compounds were prepared with the solvent DMSO as vehicle at the concentration of 60 mM and kept at -20 °C. Stock solutions of 5 mM, 20 mM and 40 mM were also made in DMSO.

2.2 Cell culture

Five human tumor cell lines were used in this work: PANC-1 and BxPC3 (PDAC), NCI-H460 (NSCLC), MDA-MD-231 and MDA-MB-468 (TNBC).

All the cell lines were routinely maintained as adherent cell cultures and kept at 37 °C in a humidified atmosphere containing 5% CO₂. All cells used were regularly observed with a microscope and the experiments were done only when cells presented ≥90% of viability. The PANC-1 and BxPC3 cell lines were cultured in DMEM (Dulbecco's modified Eagle's medium), supplemented with 4.5 g/L of glucose with ultraglutamine (from Biowhittaker) and with 5% of FBS; the NCI-H460, MDA-MB-231 and MDA-MB-468 cell lines were cultured in RPMI 1640 (Roswell Park Memorial Institute) medium supplemented with 25 mM of glutamine and 4-(2-Hydroxyethyl)piperazine-1-ethanesulfonic acid (HEPES) buffer (from Biowest) and with 5% FBS. The non-tumorigenic cell line MCF-12A was cultured in RPMI-1640 supplemented with hEGF (Human Epidermal Growth Factor; 20 ng/μL), hydrocortisone (500 ng/μL), 5% FBS and 1% Penicillin-Streptomycin (Gibco).

All procedures concerning cell culture were carried out under a clean environment in biological safety cabinets, using sterile reagents and materials.

2.3 Trypan Blue Exclusion Assay

The cell number was counted using a haemocytometer (*Neubauer Chamber*) and the Trypan Blue reagent (Sigma-Aldrich). Trypan blue is an exclusion dye that penetrates the membrane of disrupted cells, allowing to distinguish between alive (bright) and dead cells or non-viable cells (blue ones). Therefore, trypan blue assay allows to assess cell viability and the right cell number to plate for each cell line.

2.4 Sulforhodamine B (SRB) assay

The effects of the synthesized compounds on the growth of several human tumor cell lines was evaluated using an assay based on a protein-binding dye, the sulforhodamine B (SRB).

In order to determine the GI_{50} concentration of each compound – concentration of the compound that reduced cell growth by 50 % -, dose-response curves were performed. For that, cells were plated in 96-well plates (one plate for each cell line), at the ideal cell concentration previously determined (see **Table 7**), by adding 100 μ L of cells per well. Cells were then incubated at 37 °C for 24 hours (h).

Table 7. Number of cells per mL plated, for each cell line, for the SRB assays.

PANC-1	BxPC3	NCI-H460	MDA-MB-231	MDA-MB-468	MCF-12A
5.0×10^4	7.5×10^4	5.0×10^4	5.0×10^4	5.0×10^4	5.0×10^4

Twenty-four hours later, cells were treated with 5 serial dilutions of the synthesized compounds, by adding 100 μ L of compound per well, and incubated at 37 °C for further 48 h. The effect of the vehicle (DMSO) on the growth of the cell lines was also evaluated (control), by exposing untreated control cells to the maximum concentration of DMSO used in the assays (which was never more than 0.25 % per well). The maximum concentration tested for all the compounds was 150 μ M, since precipitation was detected above this concentration.

At the end of the incubation period, cells were fixed with 10% (w/v) of cold TCA during 1 h at 4 °C. Subsequently, air-dried cells were stained with 0.4% of SRB for 30 min in the dark

at room temperature (RT). At the end, cells were washed with 1% (v/v) of acetic acid and the bound stain was solubilized with Tris base at 10 mM. The absorbance was measured at 510 nm in a microplate reader (BioTek's Synergy™ Mx) using the Gen5 software (BioTek).

The GI₅₀ concentrations were assessed from the dose-response curves and determined for each compound in each cell line. The GI₅₀ values presented are the average ± standard error (S.E.M) from at least 3 independent experiments. The layout of the plates used for the SRB assay is presented in **Figure 25**, in which panel **A** represents the layout of the plates used for screening of the synthesized compounds or the positive control (Doxorubicin), in all the tumors cell lines, and panel **B** represents the layout of the plates used for the evaluation of the cytotoxic potential of the best compounds in the non-tumorigenic cell line.

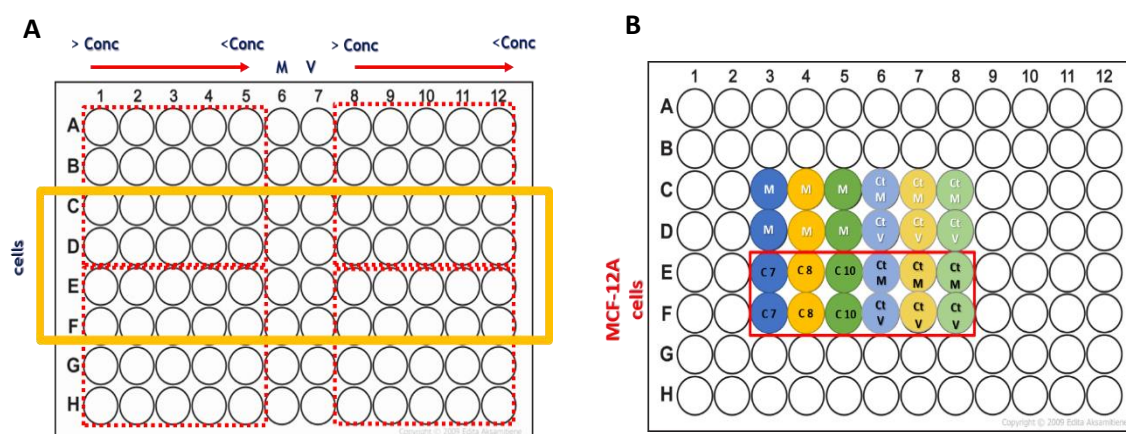


Figure 25. Layout of the plates used for the screening with the SRB assay.

A) Cells refers to all the cell lines used; **> CONC** means the highest concentration of the eight compounds or doxorubicin tested in five different serial dilutions; **< CONC** means the lowest concentration of the eight compounds or doxorubicin tested in five serial dilutions; **M** represents the medium (control); **V** means vehicle of the compounds, namely DMSO (control); the **rows 1-5 and 8-9** represent each concentration of compounds tested whereas **row 6 (M)** corresponds to the medium and **row 7** corresponds to the vehicle (DMSO); **rows A and B or G and H** had medium plus the compounds (blank) and **rows C-F** had cells plus the compounds. **B) MCF-12A cells** plated in **rows E and F**; **M** represented medium (blank) plus each compound; **Ct M** represented only medium and **Ct V** the vehicle DMSO; the wells **C7, C8 and C10** refer to **compound 7, compound 8 and compound 10**, respectively.

2.5 Flow Cytometry for cell cycle analysis with Propidium Iodide

For cell cycle distribution analysis, 1.5×10^5 cells per mL were plated from MDA-MB-231 and MDA-MB-468 cell lines, in 6-well plates for 24 h. Cells were then incubated with complete medium only (blank), medium with the vehicle (DMSO) or with the respective compounds using the previous calculated GI_{50} or $2 \times GI_{50}$ concentrations, as represented in **Figure 26**. Following 48 h incubation with the selected compounds (compound **7** for MDA-MB-231 and compounds **8** and **10** for MDA-MB-468), cells were collected, centrifuged (1200 rpm for 5 min) and then fixed with 70% cold ethanol. After being stored at 4 °C for at least 12 h, cells were centrifuged (5 min at 1200 rpm, 4 °C) and the pellets resuspended in a solution of PBS containing 5 µg/mL propidium iodide and 0.1 mg/mL RNase A, and incubated for at least 30 min in the dark on ice, prior to each analysis on the flow cytometer.

Cellular DNA content for cell cycle distribution was analysed by flow cytometry using the BD Accuri™ C6 Flow cytometer (BD Biosciences). The exclusion of cell debris and aggregates was performed for each analysis, and at least 20,000 events per sample were plotted for all the acquisitions. The percentage of cells in the G0/G1, S, and G2/M phases of the cell cycle was subsequently determined using the FlowJo 7.2 software (Tree Star, Inc. version 7.6.5, Tree Star, Inc., Ashland, OR, US). The results were from two or three independent experiments, and are presented as mean \pm SEM.

2.6 Expression of specific proteins

2.6.1 Extraction of total protein

For protein extraction, MDA-MB-231 and MDA-MB-468 cells were plated 1.5×10^5 cells/mL in 6-well plates and treated with the selected compounds, compound **7** (for MDA-MB-231) and compounds **8** and **10** (for MDA-MB-468), at concentrations of GI_{50} and $2 \times GI_{50}$, for 48 h, as illustrated in **Figure 26**.

After an incubation period of 48 h, culture medium containing floating cells was recovered to a 15 mL falcon tube. Adherent cells were washed with PBS, trypsinized and collected to the same falcon. Then, cells (floating and adherent) were centrifuged (1200 rpm, 5 min) and the pellets resuspended in PBS. After another centrifugation step (1200 rpm, 5 min,

4 °C) the supernatant was discarded, and the pellet was kept on ice to continue immediately for lysis (or kept at -20 °C if lysis was not done immediately). To lysate the cells, 30 µL of ice-cold Winman's buffer (5 mM EDTA, 0.15 M NaCl, 1% NP-40, 0.1 M Tris-HCl pH 8) supplemented with protease inhibitor cocktail (Roche Applied Sciences) was added to each sample during 30 min at 4 °C with agitation. Then, cell lysates were centrifuged at 13 000 rpm for 10 min at 4 °C and the supernatants (corresponding to the proteins) were collected and stored at -20°C.

2.6.2 Protein quantification

The determination of the protein concentration was performed using the colorimetric method based on the Lowry protocol (Bio-Rad DC™ Protein assay). Briefly, protein concentration was determined using a standard curve made with bovine serum albumin (BSA, from Sigma-Aldrich, Co). The absorbance was read in a microplate reader (Biotek (Synergy Mx) at 655 nm. Ultrapure H₂O was used as Blank. The total protein concentration was determined as µg/mL.

2.6.3 Western blot assay

A total amount of 20 µg of protein was mixed with Loading Buffer (Tris-HCl 1 M, 5% SDS, 12% glycerol, 12% β-mercaptoethanol and 0.024% bromophenol blue) and boiled for 5 min at 95 °C (for protein denaturation). The protein samples were then separated in 10% Tris-glycine SDS-Page polyacrylamide gel (at 70 V for about 30 min, followed by 1 h and 30 min at 100 V). The molecular weight marker (Precision Plus Protein™ Standards Dual Color, BioRad) was used to determinate the size of the proteins run in the gel. The running buffer used was 10x Tris/Glycine/SDS buffer solution (Bio-Rad). After protein separation, proteins were transferred onto a nitrocellulose membrane (Amersham Protran 0.45NC, GE Healthcare) during 1 h and 30 min at 100 V on ice, with agitation. The transfer buffer used was 10x Tris/Glycine buffer solution (Bio-Rad) containing 20 % of methanol. All the procedure was done in a Bio-Rad Western Blot System. After that, membranes were stained with Ponceau solution (Sigma Aldrich) in order to verify the successful protein transfer and the correct loading of the same amount of protein. Membranes were then blocked in TBS-T (a Tris-buffered saline solution with 0.1 % Tween-20 (Promega), containing 5 % (w/v) non-fat dry milk (Molico), for at least 1 h and 30 min with agitation at RT. After this period, the membranes

Chapter IV - Experimental

were incubated with the primary antibodies overnight at 4 °C with agitation. The primary antibodies used and their corresponding dilutions were: PARP-1 (1:1000; sc-7150), Cyclin D1 (1:1000, sc-8396) and γ -H2A.X (1:250, sc-101696) from Santa Cruz Biotechnology and p21 (1:1000, ab7960) from Abcam. The loading control used was actin (Actin (1:2000; sc-1616) from Santa Cruz Biotechnology. The primary antibodies were prepared using TBS-T solution and kept at -20°C. Then, membranes were washed 3 times in TBS-T during 10 min with agitation and incubated with the corresponding secondary antibodies for 1 h at RT. The following secondary antibodies were used: anti-rabbit IgG-HRP (sc-2004); anti-mouse IgG-HRP (sc-2031) and anti-goat IgG-HRP (sc-2020), all from Santa Cruz Biotechnology at dilution of 1:2000. The Amersham™ ECL Western Blotting Detection Reagents (GE Healthcare), the High Performance Chemiluminescence Film (GE Healthcare) and the Kodak GBX developer and fixer (Sigma-Aldrich, Co.) were used to detect the signal (bands). The intensity of the bands was analysed using the software Quantity One – ID Analysis (Bio-Rad) and actin was used as internal control (for protein loading). Results are from three independent experiments unless stated.

In order to reprobe the membranes with other antibodies, whenever it was necessary, membranes were stripped with a stripping solution (10 % methanol and 10 % acetic acid in H₂O) for 15 min at 50 °C, followed by several washes with TBS-T and then blocking for further primary antibody incubation.

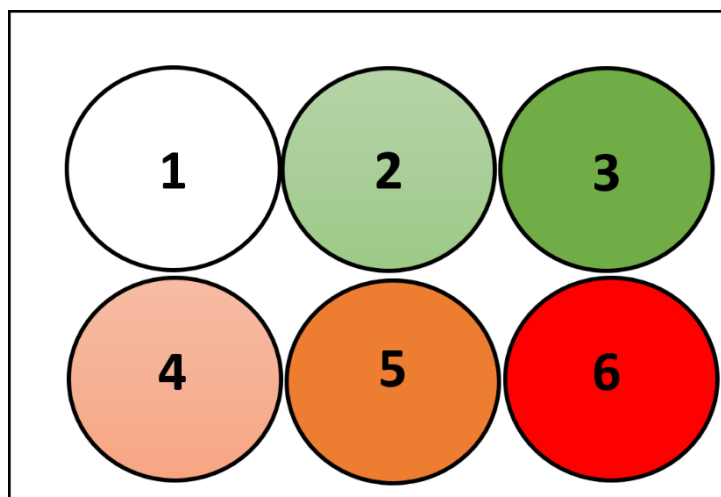


Figure 26. Layout of the 6-well plates for the Cell cycle and Western Blot experiments performed in MDA-MB-231 and MDA-MB-468 human tumor cell lines.

Well 1: cells with only medium (blank); wells **2 and 3:** cells incubated with DMSO (control) at the same concentration used for the GI_{50} and $2x GI_{50}$ of each compound wells **4 and 5:** cells treated with the compounds at GI_{50} and $2x GI_{50}$ concentrations; well **6:** cells treated with doxorubicin (positive control).

2.7 Chick Chorioallantoic Membrane (CAM) assay

The experimental procedure for the CAM assays was performed by the i3S facilities (Dr. Marta Pinto). The aim of this experiment was to evaluate the effect of the best compound on xenografted tumor's induced angiogenesis and formation. The cell line MDA-MB-231 (the most aggressive TNBC subtype cell lines used in this work) was inoculated in fertilized chicken eggs in order to make the xenografts. The experimental procedure is illustrated in **Figure 27**.

Briefly, MDA-MB-231 cells were inoculated, pairwise, into a total of 10 to 12 eggs for each of replica (were made two) for two different tested conditions: A (vehicle) and B (compound). Thus, Chick Chorioallantoic Membranes (CAM's) were inoculated at embryonic development day (EDD) 9 with the cells resuspended in matrigel to allow them to become adherent (between 6.0×10^5 to 1.0×10^6 cells were used). After 24h (EDD 10), the xenografted tumors were treated with the following tested conditions: group A treated with DMSO and group B treated with compound **7**. The experiment ended at EDD13, in order to mimetize the 48h treatment performed *in vitro*. At this endpoint, CAM's were fixed with paraformaldehyde,

the embryo was excised *ex ovo* and photographed. The readouts analysed were used to evaluate the tumorigenic response (pictures were used to determine tumor area). The angiogenic response was not possible to be measured due to inflammation issues.

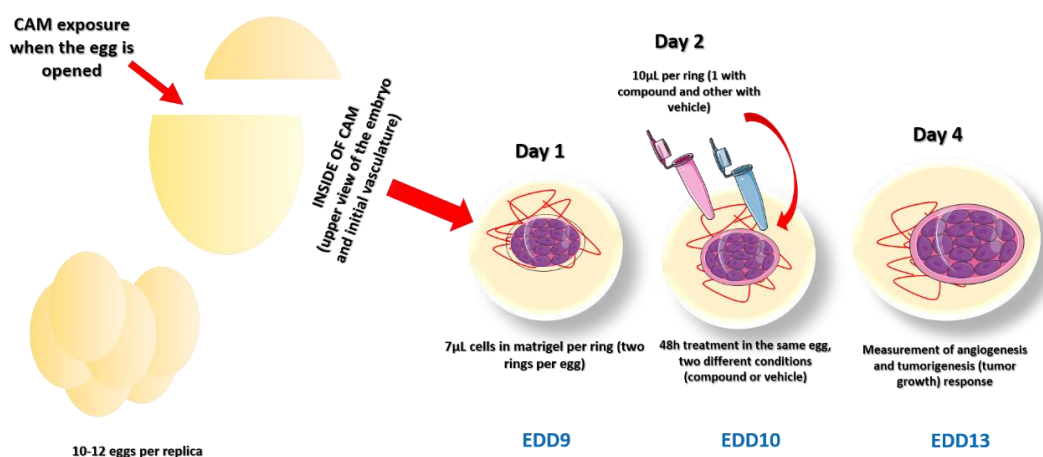


Figure 27. Illustration of CAM (Chick Chorioallantoic Membrane) assay procedure.

Fertilized chicken eggs were opened at day 9 of EDD (embryonic development day), when the developing vasculature is identified and a “window” is opened on the egg in order to seed, in each of the two rings, the tumor cells in a matrigel suspension. On the following day (EDD10), the vehicle (control on ring A) and the compound (treatment on ring B) are given. After 48h of incubation it should be possible to assess tumor growth and angiogenic response.

2.8 Statistical analysis of the results

Data is presented as mean \pm standard error of mean (SEM). All data was analysed using the software GraphPad Prism 8.0 (GraphPad Software, Inc., CA, USA). Statistical analysis was performed using the Student’s *t*-test and two-way ANOVA followed by Tukey’s multiple comparison tests. *p*-values less than 0.05 ($p < 0.05$) were considered statistically significant.

CHAPTER V

REFERENCES

1. REFERENCES

1. Dai, X.; Cheng, H.; Bai, Z.; Li, J. Breast Cancer Cell Line Classification and Its Relevance with Breast Tumor Subtyping. *Journal of Cancer* **2017**, *8*, 3131-3141.
2. Metzger-Filho, O.; Tutt, A.; de Azambuja, E.; Saini, K. S.; Viale, G.; Loi, S.; Bradbury, I.; Bliss, J. M.; Azim, H. A.; Ellis, P.; Di Leo, A.; Baselga, J.; Sotiriou, C.; Piccart-Gebhart, M. Dissecting the Heterogeneity of Triple-Negative Breast Cancer. *Journal of Clinical Oncology* **2012**, *30*, 1879-1887.
3. Hanahan, D.; Weinberg, Robert A. Hallmarks of Cancer: The Next Generation. *Cell* **2011**, *144*, 646-674.
4. Ghorab, M. M.; Alsaid, M. S.; Al-Dosari, M. S.; Ragab, F. A.; Al-Mishari, A. A.; Almoqbil, A. N. Novel quinolines carrying pyridine, thienopyridine, isoquinoline, thiazolidine, thiazole and thiophene moieties as potential anticancer agents. *Acta Pharm* **2016**, *66*, 155-71.
5. Cancer. <http://www.who.int/cancer/en/> (28 February).
6. Hassan, F. A. Y., K. W. ; AL-Qaisi A. H. . In *Antitumoral effect of 1 , 2 , 4-Triazole derivatives on prostate carcinoma (DU 145) , Human Liver carcinoma (HEPG 2) , and Human Breast Cancer (MCF 7) cell Lines* , Australian Journal of Basic and Applied Sciences, 2013; 2013; pp 133-140.
7. Strahm, B.; Capra, M. Insights into the molecular basis of cancer development. *Current Paediatrics* **2005**, *15*, 333-338.
8. Malarkey, D. E.; Hoenerhoff, M.; Maronpot, R. R. Carcinogenesis. In *Haschek and Rousseaux's Handbook of Toxicologic Pathology*, 2013; pp 107-146.
9. Keating, G. M.; Santoro, A. Sorafenib: a review of its use in advanced hepatocellular carcinoma. *Drugs* **2009**, *69*, 223-40.
10. Devita, V. T.; Young, R. C.; Canellos, G. P. Combination versus single agent chemotherapy: A review of the basis for selection of drug treatment of cancer. *Cancer* **1975**, *35*, 98-110.
11. Hanahan, D.; Weinberg, R. A. Hallmarks of cancer: the next generation. *Cell* **2011**, *144*, 646-74.
12. Lieu, C. H.; Tan, A. C.; Leong, S.; Diamond, J. R.; Eckhardt, S. G. From bench to bedside: lessons learned in translating preclinical studies in cancer drug development. *J Natl Cancer Inst* **2013**, *105*, 1441-56.
13. Hanahan, D.; Weinberg, R. A. The Hallmarks of Cancer. *Cell* **2000**, *100*, 57-70.
14. Fouad, Y. A.; Aanei, C. Revisiting the hallmarks of cancer. *Am J Cancer Res* **2017**, *7*, 1016-1036.
15. Malumbres, M.; Barbacid, M. Cell cycle, CDKs and cancer: a changing paradigm. *Nature Reviews Cancer* **2009**, *9*, 153-166.
16. Vogelstein, B.; Papadopoulos, N.; Velculescu, V. E.; Zhou, S.; Diaz, L. A.; Kinzler, K. W. Cancer Genome Landscapes. *Science* **2013**, *339*, 1546-1558.
17. Aubrey, B. J.; Strasser, A.; Kelly, G. L. Tumor-Suppressor Functions of the TP53 Pathway. *Cold Spring Harbor Perspectives in Medicine* **2016**, *6*.
18. Fernald, K.; Kurokawa, M. Evading apoptosis in cancer. *Trends in Cell Biology* **2013**, *23*, 620-633.
19. Koff, J.; Ramachandiran, S.; Bernal-Mizrachi, L. A Time to Kill: Targeting Apoptosis in Cancer. *International Journal of Molecular Sciences* **2015**, *16*, 2942-2955.
20. Warburg, O. On the Origin of Cancer Cells. *Science* **1956**, *123*, 309-314.

21. Swann, J. B.; Smyth, M. J. Immune surveillance of tumors. *Journal of Clinical Investigation* **2007**, 117, 1137-1146.
22. Witz, I. P. The Tumor Microenvironment: The Making of a Paradigm. *Cancer Microenvironment* **2009**, 2, 9-17.
23. Siegel, R. L.; Miller, K. D.; Jemal, A. Cancer statistics, 2019. *CA: A Cancer Journal for Clinicians* **2019**, 69, 7-34.
24. Wolfgang, C. L.; Herman, J. M.; Laheru, D. A.; Klein, A. P.; Erdek, M. A.; Fishman, E. K.; Hruban, R. H. Recent progress in pancreatic cancer. *CA Cancer J Clin* **2013**, 63, 318-48.
25. Waddell, N.; Pajic, M.; Patch, A. M.; Chang, D. K.; Kassahn, K. S.; Bailey, P.; Johns, A. L.; Miller, D.; Nones, K.; Quek, K.; Quinn, M. C.; Robertson, A. J.; Fadlullah, M. Z.; Bruxner, T. J.; Christ, A. N.; Harliwong, I.; Idrisoglu, S.; Manning, S.; Nourse, C.; Nourbakhsh, E.; Wani, S.; Wilson, P. J.; Markham, E.; Cloonan, N.; Anderson, M. J.; Fink, J. L.; Holmes, O.; Kazakoff, S. H.; Leonard, C.; Newell, F.; Poudel, B.; Song, S.; Taylor, D.; Waddell, N.; Wood, S.; Xu, Q.; Wu, J.; Pinese, M.; Cowley, M. J.; Lee, H. C.; Jones, M. D.; Nagrial, A. M.; Humphris, J.; Chantrill, L. A.; Chin, V.; Steinmann, A. M.; Mawson, A.; Humphrey, E. S.; Colvin, E. K.; Chou, A.; Scarlett, C. J.; Pinho, A. V.; Giry-Laterriere, M.; Rooman, I.; Samra, J. S.; Kench, J. G.; Pettitt, J. A.; Merrett, N. D.; Toon, C.; Epari, K.; Nguyen, N. Q.; Barbour, A.; Zeps, N.; Jamieson, N. B.; Graham, J. S.; Niclou, S. P.; Bjerkvig, R.; Grutzmann, R.; Aust, D.; Hruban, R. H.; Maitra, A.; Iacobuzio-Donahue, C. A.; Wolfgang, C. L.; Morgan, R. A.; Lawlor, R. T.; Corbo, V.; Bassi, C.; Falconi, M.; Zamboni, G.; Tortora, G.; Tempero, M. A.; Australian Pancreatic Cancer Genome, I.; Gill, A. J.; Eshleman, J. R.; Pilarsky, C.; Scarpa, A.; Musgrove, E. A.; Pearson, J. V.; Biankin, A. V.; Grimmond, S. M. Whole genomes redefine the mutational landscape of pancreatic cancer. *Nature* **2015**, 518, 495-501.
26. Pettazoni, P.; Viale, A.; Shah, P.; Carugo, A.; Ying, H.; Wang, H.; Genovese, G.; Seth, S.; Minelli, R.; Green, T.; Huang-Hobbs, E.; Corti, D.; Sanchez, N.; Nezi, L.; Marchesini, M.; Kapoor, A.; Yao, W.; Francesco, M. E. D.; Petrocchi, A.; Deem, A. K.; Scott, K.; Colla, S.; Mills, G. B.; Fleming, J. B.; Heffernan, T. P.; Jones, P.; Toniatti, C.; DePinho, R. A.; Draetta, G. F. Genetic Events That Limit the Efficacy of MEK and RTK Inhibitor Therapies in a Mouse Model of KRAS-Driven Pancreatic Cancer. *Cancer Research* **2015**, 75, 1091-1101.
27. Cicenas, J.; Kvederaviciute, K.; Meskinyte, I.; Meskinyte-Kausiliene, E.; Skeberdyte, A.; Cicenas, J. KRAS, TP53, CDKN2A, SMAD4, BRCA1, and BRCA2 Mutations in Pancreatic Cancer. *Cancers (Basel)* **2017**, 9.
28. Infante, J. R.; Somer, B. G.; Park, J. O.; Li, C. P.; Scheulen, M. E.; Kasubhai, S. M.; Oh, D. Y.; Liu, Y.; Redhu, S.; Stepkowski, K.; Le, N. A randomised, double-blind, placebo-controlled trial of trametinib, an oral MEK inhibitor, in combination with gemcitabine for patients with untreated metastatic adenocarcinoma of the pancreas. *Eur J Cancer* **2014**, 50, 2072-81.
29. Makohon-Moore, A.; Iacobuzio-Donahue, C. A. Pancreatic cancer biology and genetics from an evolutionary perspective. *Nat Rev Cancer* **2016**, 16, 553-65.
30. Brauswetter, D.; Gurbi, B.; Varga, A.; Varkondi, E.; Schwab, R.; Banhegyi, G.; Fabian, O.; Keri, G.; Valyi-Nagy, I.; Petak, I. Molecular subtype specific efficacy of MEK inhibitors in pancreatic cancers. *PLoS One* **2017**, 12, e0185687.
31. Latest global cancer data: Cancer burden rises to 18.1 million new cases and 9.6 million cancer deaths in 2018. In WHO: International Agency for Cancer Research
32. Molina, J. R.; Yang, P.; Cassivi, S. D.; Schild, S. E.; Adjei, A. A. Non-small cell lung cancer: epidemiology, risk factors, treatment, and survivorship. *Mayo Clin Proc* **2008**, 83, 584-94.
33. Lovly, C., L. Horn, W. Pao. Molecular Profiling of Lung Cancer. <https://www.mycancergenome.org/content/disease/lung-cancer/> (14 june).

34. What Is Non-Small Cell Lung Cancer? <https://www.cancer.org/cancer/non-small-cell-lung-cancer/about/what-is-non-small-cell-lung-cancer.html> (30 March 2019).
35. Prabhakar, C. N. Epidermal growth factor receptor in non-small cell lung cancer. *Transl Lung Cancer Res* **2015**, 4, 110-8.
36. Pao, W.; Hutchinson, K. E. Chipping away at the lung cancer genome. *Nat Med* **2012**, 18, 349-51.
37. Vnencak-Jones CL, B. M., Pao W. Types of Molecular Tumor Testing. <http://www.mycancergenome.org/content/molecular-medicine/types-of-molecular-tumortesting>
38. Akram, M.; Iqbal, M.; Daniyal, M.; Khan, A. U. Awareness and current knowledge of breast cancer. *Biol Res* **2017**, 50, 33.
39. Fragomeni, S. M.; Sciallis, A.; Jeruss, J. S. Molecular Subtypes and Local-Regional Control of Breast Cancer. *Surgical Oncology Clinics of North America* **2018**, 27, 95-120.
40. Prat, A.; Parker, J. S.; Karginova, O.; Fan, C.; Livasy, C.; Herschkowitz, J. I.; He, X.; Perou, C. M. Phenotypic and molecular characterization of the claudin-low intrinsic subtype of breast cancer. *Breast Cancer Research* **2010**, 12.
41. Dai, X.; Li, T.; Bai, Z.; Yang, Y.; Liu, X.; Zhan, J.; Shi, B. Breast cancer intrinsic subtype classification, clinical use and future trends. *Am J Cancer Res* **2015**, 5, 2929-43.
42. Perou, C. M.; Sørlie, T.; Eisen, M. B.; van de Rijn, M.; Jeffrey, S. S.; Rees, C. A.; Pollack, J. R.; Ross, D. T.; Johnsen, H.; Akslen, L. A.; Fluge, Ø.; Pergamenschikov, A.; Williams, C.; Zhu, S. X.; Lønning, P. E.; Børresen-Dale, A.-L.; Brown, P. O.; Botstein, D. Molecular portraits of human breast tumours. *Nature* **2000**, 406, 747-752.
43. Holliday, D. L.; Speirs, V. Choosing the right cell line for breast cancer research. *Breast Cancer Res* **2011**, 13, 215.
44. Huang, E.; Cheng, S. H.; Dressman, H.; Pittman, J.; Tsou, M. H.; Horng, C. F.; Bild, A.; Iversen, E. S.; Liao, M.; Chen, C. M.; West, M.; Nevins, J. R.; Huang, A. T. Gene expression predictors of breast cancer outcomes. *Lancet* **2003**, 361, 1590-6.
45. Cheang, M. C. U.; Chia, S. K.; Voduc, D.; Gao, D.; Leung, S.; Snider, J.; Watson, M.; Davies, S.; Bernard, P. S.; Parker, J. S.; Perou, C. M.; Ellis, M. J.; Nielsen, T. O. Ki67 Index, HER2 Status, and Prognosis of Patients With Luminal B Breast Cancer. *JNCI: Journal of the National Cancer Institute* **2009**, 101, 736-750.
46. Monks, A.; Scudiero, D.; Skehan, P.; Shoemaker, R.; Paull, K.; Vistica, D.; Hose, C.; Langley, J.; Cronise, P.; Vaigro-Wolff, A.; Gray-Goodrich, M.; Campbell, H.; Mayo, J.; Boyd, M. Feasibility of a High-Flux Anticancer Drug Screen Using a Diverse Panel of Cultured Human Tumor Cell Lines. *JNCI Journal of the National Cancer Institute* **1991**, 83, 757-766.
47. Kondo, J.; Inoue, M. Application of Cancer Organoid Model for Drug Screening and Personalized Therapy. *Cells* **2019**, 8.
48. Kim, H. S.; Devarenne, T. P.; Han, A. A high-throughput microfluidic single-cell screening platform capable of selective cell extraction. *Lab on a Chip* **2015**, 15, 2467-2475.
49. Baker, B. M.; Chen, C. S. Deconstructing the third dimension – how 3D culture microenvironments alter cellular cues. *Journal of Cell Science* **2012**, 125, 3015-3024.
50. Kondo, J.; Endo, H.; Okuyama, H.; Ishikawa, O.; Iishi, H.; Tsujii, M.; Ohue, M.; Inoue, M. Retaining cell-cell contact enables preparation and culture of spheroids composed of pure primary cancer cells from colorectal cancer. *Proceedings of the National Academy of Sciences* **2011**, 108, 6235-6240.
51. Pampaloni, F.; Reynaud, E. G.; Stelzer, E. H. K. The third dimension bridges the gap between cell culture and live tissue. *Nature Reviews Molecular Cell Biology* **2007**, 8, 839-845.

52. Wilding, J. L.; Bodmer, W. F. Cancer Cell Lines for Drug Discovery and Development. *Cancer Research* **2014**, *74*, 2377-2384.
53. Alimbetov, D.; Askarova, S.; Umbayev, B.; Davis, T.; Kipling, D. Pharmacological Targeting of Cell Cycle, Apoptotic and Cell Adhesion Signaling Pathways Implicated in Chemoresistance of Cancer Cells. *International Journal of Molecular Sciences* **2018**, *19*.
54. Lundberg, A. S.; Weinberg, R. A. Control of the cell cycle and apoptosis. *European Journal of Cancer* **1999**, *35*, 1886-1894.
55. Johnstone, R. W.; Ruefli, A. A.; Lowe, S. W. Apoptosis. *Cell* **2002**, *108*, 153-164.
56. Wong, R. S. Y. Apoptosis in cancer: from pathogenesis to treatment. *Journal of Experimental & Clinical Cancer Research* **2011**, *30*.
57. Ricci, M. S. Chemotherapeutic Approaches for Targeting Cell Death Pathways. *The Oncologist* **2006**, *11*, 342-357.
58. Mannhold, R.; Fulda, S.; Carosati, E. IAP antagonists: promising candidates for cancer therapy. *Drug Discovery Today* **2010**, *15*, 210-219.
59. Gabrielli, B.; Brooks, K.; Pavey, S. Defective Cell Cycle Checkpoints as Targets for Anti-Cancer Therapies. *Frontiers in Pharmacology* **2012**, *3*.
60. Dominguez-Brauer, C.; Thu, Kelsie L.; Mason, Jacqueline M.; Blaser, H.; Bray, Mark R.; Mak, Tak W. Targeting Mitosis in Cancer: Emerging Strategies. *Molecular Cell* **2015**, *60*, 524-536.
61. Jingwen, B.; Yaochen, L.; Guojun, Z. Cell cycle regulation and anticancer drug discovery. *Cancer Biology & Medicine* **2017**, *14*.
62. Fisher, R.; Pusztai, L.; Swanton, C. Cancer heterogeneity: implications for targeted therapeutics. *British Journal of Cancer* **2013**, *108*, 479-485.
63. Gomtsyan, A. Heterocycles in drugs and drug discovery. *Chemistry of Heterocyclic Compounds* **2012**, *48*, 7-10.
64. Martins, P.; Jesus, J.; Santos, S.; Raposo, L. R.; Roma-Rodrigues, C.; Baptista, P. V.; Fernandes, A. R. Heterocyclic Anticancer Compounds: Recent Advances and the Paradigm Shift towards the Use of Nanomedicine's Tool Box. *Molecules* **2015**, *20*, 16852-91.
65. Vitaku, E.; Smith, D. T.; Njardarson, J. T. Analysis of the structural diversity, substitution patterns, and frequency of nitrogen heterocycles among U.S. FDA approved pharmaceuticals. *J Med Chem* **2014**, *57*, 10257-74.
66. Rangra, N. *Pyridine derivatives as potential anticancer agents: A review*. 2014.
67. HONG-KE LIU, A. P. J. S. Metal Complexes as DNA Intercalators. *Accounts of Chemical Research* **2011**, *44*, 311-392.
68. Rodrigues, K. A. d. F.; Dias, C. N. d. S.; N ris, P. L. d. N.; Rocha, J. d. C.; Scotti, M. T.; Scotti, L.; Mascarenhas, S. R.; Veras, R. C.; Medeiros, I. A. d.; Keesen, T. d. S. L.; Oliveira, T. B. d.; Lima, M. d. C. A. d.; Balliano, T. L.; Aquino, T. M. d.; Moura, R. O. d.; Mendonça Junior, F. J. B.; Oliveira, M. R. d. 2-Amino-thiophene derivatives present antileishmanial activity mediated by apoptosis and immunomodulation in vitro. *European Journal of Medicinal Chemistry* **2015**, *106*, 1-14.
69. Mohareb, R. M.; Megally Abdo, N. Y. Synthesis and Cytotoxic Evaluation of Pyran, Dihydropyridine and Thiophene Derivatives of 3-Acetylcoumarin. *Chemical & Pharmaceutical Bulletin* **2015**, *63*, 678-687.
70. Ghorab, M. M.; Bashandy, M. S.; Alsaid, M. S. Novel thiophene derivatives with sulfonamide, isoxazole, benzothiazole, quinoline and anthracene moieties as potential anticancer agents. *Acta Pharmaceutica* **2014**, *64*, 419-431.

71. Romagnoli, R.; Baraldi, P. G.; Kimatrai Salvador, M.; Preti, D.; Aghazadeh Tabrizi, M.; Bassetto, M.; Brancale, A.; Hamel, E.; Castagliuolo, I.; Bortolozzi, R.; Basso, G.; Viola, G. Synthesis and Biological Evaluation of 2-(Alkoxy-carbonyl)-3-Anilinobenzo[b]thiophenes and Thieno[2,3-b]pyridines as New Potent Anticancer Agents. *Journal of Medicinal Chemistry* **2013**, 56, 2606-2618.
72. Pharma, D.; Almulla, A. ISSN 0975-413X CODEN (USA): PCHHAX A Review: Biological Importance of Heterocyclic Compounds. **2017**, 2017, 141-147.
73. Hayakawa, I.; Shioya, R.; Agatsuma, T.; Furukawa, H.; Sugano, Y. Thienopyridine and benzofuran derivatives as potent anti-tumor agents possessing different structure-activity relationships. *Bioorg Med Chem Lett* **2004**, 14, 3411-4.
74. Munchhof, M. J.; Beebe, J. S.; Casavant, J. M.; Cooper, B. A.; Doty, J. L.; Higdon, R. C.; Hillerman, S. M.; Soderstrom, C. I.; Knauth, E. A.; Marx, M. A.; Rossi, A. M.; Sobolov, S. B.; Sun, J. Design and SAR of thienopyrimidine and thienopyridine inhibitors of VEGFR-2 kinase activity. *Bioorg Med Chem Lett* **2004**, 14, 21-4.
75. Strawn, L. M.; McMahon, G.; App, H.; Schreck, R.; Kuchler, W. R.; Longhi, M. P.; Hui, T. H.; Tang, C.; Levitzki, A.; Gazit, A.; Chen, I.; Keri, G.; Orfi, L.; Risau, W.; Flamme, I.; Ullrich, A.; Hirth, K. P.; Shawver, L. K. Flk-1 as a target for tumor growth inhibition. *Cancer Res* **1996**, 56, 3540-5.
76. Frame, M. C. Src in cancer: deregulation and consequences for cell behaviour. *Biochim Biophys Acta* **2002**, 1602, 114-30.
77. Irby, R. B.; Yeatman, T. J. Role of Src expression and activation in human cancer. *Oncogene* **2000**, 19, 5636-42.
78. Boschelli, D. H.; Wu, B.; Barrios Sosa, A. C.; Chen, J. J.; Golas, J. M.; Boschelli, F. Inhibition of Src kinase activity by 7-[(2,4-dichloro-5-methoxyphenyl)amino]-2-heteroaryl-thieno[3,2-b]pyridine-6-carbonitriles. *Bioorg Med Chem Lett* **2005**, 15, 4681-4.
79. Claridge, S.; Raepel, F.; Granger, M. C.; Bernstein, N.; Saavedra, O.; Zhan, L.; Llewellyn, D.; Wahhab, A.; Deziel, R.; Rahil, J.; Beaulieu, N.; Nguyen, H.; Dupont, I.; Barsalou, A.; Beaulieu, C.; Chute, I.; Gravel, S.; Robert, M. F.; Lefebvre, S.; Dubay, M.; Pascal, R.; Gillespie, J.; Jin, Z.; Wang, J.; Besterman, J. M.; MacLeod, A. R.; Vaisburg, A. Discovery of a novel and potent series of thieno[3,2-b]pyridine-based inhibitors of c-Met and VEGFR2 tyrosine kinases. *Bioorg Med Chem Lett* **2008**, 18, 2793-8.
80. Heyman, H. R.; Frey, R. R.; Bousquet, P. F.; Cunha, G. A.; Moskey, M. D.; Ahmed, A. A.; Soni, N. B.; Marcotte, P. A.; Pease, L. J.; Glaser, K. B.; Yates, M.; Bouska, J. J.; Albert, D. H.; Black-Schaefer, C. L.; Dandliker, P. J.; Stewart, K. D.; Rafferty, P.; Davidsen, S. K.; Michaelides, M. R.; Curtin, M. L. Thienopyridine urea inhibitors of KDR kinase. *Bioorg Med Chem Lett* **2007**, 17, 1246-9.
81. Calhelha, R. C.; Ferreira, I. C. F. R.; Peixoto, D.; Abreu, R. M. V.; Vale-Silva, L. A.; Pinto, E.; Lima, R. T.; Alvelos, M. I.; Vasconcelos, M. H.; Queiroz, M.-J. R. P. Aminodi(hetero)arylamines in the Thieno[3,2-b]pyridine Series: Synthesis, Effects in Human Tumor Cells Growth, Cell Cycle Analysis, Apoptosis and Evaluation of Toxicity Using Non-Tumor Cells. *Molecules* **2012**, 17, 3834-3843.
82. Queiroz, M.-J. R. P.; Calhelha, R. C.; Vale-Silva, L. A.; Pinto, E.; Almeida, G. M.; Vasconcelos, M. H. Synthesis and evaluation of tumor cell growth inhibition of methyl 3-amino-6-[(hetero)arylethynyl]thieno[3,2-b]pyridine-2-carboxylates. Structure-activity relationships, effects on the cell cycle and apoptosis. *European Journal of Medicinal Chemistry* **2011**, 46, 236-240.

83. Queiroz, M.-J. R. P.; Calhelha, R. C.; Vale-Silva, L. A.; Pinto, E.; Lima, R. T.; Vasconcelos, M. H. Efficient synthesis of 6-(hetero)arylthieno[3,2-b]pyridines by Suzuki–Miyaura coupling. Evaluation of growth inhibition on human tumor cell lines, SARs and effects on the cell cycle. *European Journal of Medicinal Chemistry* **2010**, *45*, 5628-5634.
84. Queiroz, M.-J. R. P.; Calhelha, R. C.; Vale-Silva, L. A.; Pinto, E.; São-José Nascimento, M. Novel 6-[(hetero)arylamino]thieno[3,2-b]pyridines: Synthesis and antitumoral activities. *European Journal of Medicinal Chemistry* **2010**, *45*, 5732-5738.
85. Rodrigues, J. M.; Buisson, P.; Pereira, J. M.; Pinheiro, I. M.; Fernández-Marcelo, T.; Vasconcelos, M. H.; Berteina-Raboin, S.; Queiroz, M.-J. R. P. Synthesis of novel 8-(het)aryl-6H-pyrano[4',3':4,5]thieno[3,2-b]pyridines by 6-endo-dig cyclization of Sonogashira products and halolactonizations with Cu salts/NXS. Preliminary antitumor evaluation. *Tetrahedron* **2019**, *75*, 1387-1397.
86. Queiroz, M. J.; Calhelha, R. C.; Vale-Silva, L. A.; Pinto, E.; Lima, R. T.; Vasconcelos, M. H. Efficient synthesis of 6-(hetero)arylthieno[3,2-b]pyridines by Suzuki-Miyaura coupling. Evaluation of growth inhibition on human tumor cell lines, SARs and effects on the cell cycle. *Eur J Med Chem* **2010**, *45*, 5628-34.
87. Queiroz, M. J.; Calhelha, R. C.; Vale-Silva, L. A.; Pinto, E.; Almeida, G. M.; Vasconcelos, M. H. Synthesis and evaluation of tumor cell growth inhibition of methyl 3-amino-6-[(hetero)arylethynyl]thieno[3,2-b]pyridine-2-carboxylates. Structure-activity relationships, effects on the cell cycle and apoptosis. *Eur J Med Chem* **2011**, *46*, 236-40.
88. Calhelha, R. C.; Ferreira, I. C.; Peixoto, D.; Abreu, R. M.; Vale-Silva, L. A.; Pinto, E.; Lima, R. T.; Alvelos, M. I.; Vasconcelos, M. H.; Queiroz, M. J. Aminodi(hetero)arylamines in the thieno[3,2-b]pyridine series: synthesis, effects in human tumor cells growth, cell cycle analysis, apoptosis and evaluation of toxicity using non-tumor cells. *Molecules* **2012**, *17*, 3834-43.
89. Dorsam, R. T.; Kunapuli, S. P. Central role of the P2Y12 receptor in platelet activation. *J Clin Invest* **2004**, *113*, 340-5.
90. Gachet, C. Regulation of platelet functions by P2 receptors. *Annu Rev Pharmacol Toxicol* **2006**, *46*, 277-300.
91. Suzuki, M.; Iwasaki, H.; Fujikawa, Y.; Sakashita, M.; Kitahara, M.; Sakoda, R. Synthesis and biological evaluations of condensed pyridine and condensed pyrimidine-based HMG-CoA reductase inhibitors. *Bioorg Med Chem Lett* **2001**, *11*, 1285-8.
92. McCort, G.; Hoornaert, C.; Aletru, M.; Denys, C.; Duclos, O.; Cadilhac, C.; Guilpain, E.; Dellac, G.; Janiak, P.; Galzin, A. M.; Delahaye, M.; Guilbert, F.; O'Connor, S. Synthesis and SAR of 3- and 4-substituted quinolin-2-ones: discovery of mixed 5-HT(1B)/5-HT(2A) receptor antagonists. *Bioorg Med Chem* **2001**, *9*, 2129-37.
93. Wang, N. Y.; Zuo, W. Q.; Xu, Y.; Gao, C.; Zeng, X. X.; Zhang, L. D.; You, X. Y.; Peng, C. T.; Shen, Y.; Yang, S. Y.; Wei, Y. Q.; Yu, L. T. Discovery and structure-activity relationships study of novel thieno[2,3-b]pyridine analogues as hepatitis C virus inhibitors. *Bioorg Med Chem Lett* **2014**, *24*, 1581-8.
94. Cancer. <https://www.who.int/news-room/fact-sheets/detail/cancer> (30 set 2019).
95. Narvekar, M.; Xue, H. Y.; Eoh, J. Y.; Wong, H. L. Nanocarrier for Poorly Water-Soluble Anticancer Drugs—Barriers of Translation and Solutions. *AAPS PharmSciTech* **2014**, *15*, 822-833.
96. Dunn, A. D.; Norrie, R. Nucleophilic displacements in pyridine rings. *Journal of Heterocyclic Chemistry* **1987**, *24*, 85-89.

97. Calhelha, R. C.; Queiroz, M.-J. R. P. Synthesis of new thieno[3,2-b]pyridine derivatives by palladium-catalyzed couplings and intramolecular cyclizations. *Tetrahedron Letters* **2010**, 51, 281-283.
98. Kamata, M.; Yamashita, T.; Kina, A.; Funata, M.; Mizukami, A.; Sasaki, M.; Tani, A.; Funami, M.; Amano, N.; Fukatsu, K. Design, synthesis, and structure–activity relationships of novel spiro-piperidines as acetyl-CoA carboxylase inhibitors. *Bioorganic & Medicinal Chemistry Letters* **2012**, 22, 3643-3647.
99. Doyle, M. P.; Dellaria, J. F.; Siegfried, B.; Bishop, S. W. Reductive deamination of arylamines by alkyl nitrites in N,N-dimethylformamide. A direct conversion of arylamines to aromatic hydrocarbons. *The Journal of Organic Chemistry* **1977**, 42, 3494-3498.
100. Miyaura, N.; Yanagi, T.; Suzuki, A. The Palladium-Catalyzed Cross-Coupling Reaction of Phenylboronic Acid with Haloarenes in the Presence of Bases. *Synthetic Commun* **1981**, 11, 513-519.
101. Sołoducho, J.; Olech, K.; Świst, A.; Zając, D.; Cabaj, J. Recent Advances of Modern Protocol for C-C Bonds—The Suzuki Cross-Coupling. *Advances in Chemical Engineering and Science* **2013**, 03, 19-32.
102. A. Zolewicz, J.; P. Cruskie, M. Strategies for the synthesis of unsymmetrical quaterpyridines using palladium-catalyzed cross-coupling reactions. *Tetrahedron* **1995**, 51, 11393-11400.
103. Li, J.; Song Yue, W. *Synthesis of 3-aryl and 3-heterocyclic quinoxalin-2-ylamines via Pd-catalyzed cross-coupling reactions*. 1999; Vol. 40, p 4507-4510.
104. Peters, D.; Hörnfeldt, A.-B.; Gronowitz, S. Synthesis of various 5-substituted uracils. *Journal of Heterocyclic Chemistry* **1990**, 27, 2165-2173.
105. Miyaura, N.; Suzuki, A. Palladium-Catalyzed Cross-Coupling Reactions of Organoboron Compounds. *Chemical Reviews* **1995**, 95, 2457-2483.
106. Casalnuovo, A. L.; Calabrese, J. C. Palladium-catalyzed alkylations in aqueous media. *Journal of the American Chemical Society* **1990**, 112, 4324-4330.
107. Altenhoff, G.; Goddard, R.; Lehmann, C. W.; Glorius, F. Sterically Demanding, Bioxazoline-Derived N-Heterocyclic Carbene Ligands with Restricted Flexibility for Catalysis. *Journal of the American Chemical Society* **2004**, 126, 15195-15201.
108. Littke, A. F.; Fu, G. C. Palladium-Catalyzed Coupling Reactions of Aryl Chlorides. *Angewandte Chemie International Edition* **2002**, 41, 4176-4211.
109. Zim, D.; Gruber, A. S.; Ebeling, G.; Dupont, J.; Monteiro, A. L. Sulfur-Containing Palladacycles: Efficient Phosphine-Free Catalyst Precursors for the Suzuki Cross-Coupling Reaction at Room Temperature. *Organic Letters* **2000**, 2, 2881-2884.
110. Littke, A. F.; Dai, C.; Fu, G. C. Versatile Catalysts for the Suzuki Cross-Coupling of Arylboronic Acids with Aryl and Vinyl Halides and Triflates under Mild Conditions. *Journal of the American Chemical Society* **2000**, 122, 4020-4028.
111. Wolfe, J. P.; Singer, R. A.; Yang, B. H.; Buchwald, S. L. Highly Active Palladium Catalysts for Suzuki Coupling Reactions. *Journal of the American Chemical Society* **1999**, 121, 9550-9561.
112. Murata, M.; Oyama, T.; Watanabe, S.; Masuda, Y. Palladium-Catalyzed Borylation of Aryl Halides or Triflates with Dialkoxyborane: A Novel and Facile Synthetic Route to Arylboronates. *The Journal of Organic Chemistry* **2000**, 65, 164-168.
113. Stefani, H. A.; Amaral, M. F. Z. J.; Juaristi, E. Synthesis of (2S)-isopropyl-5-alkynylpyrimidin-2-ones: precursors of β -aminoacids. *Tetrahedron Letters* **2011**, 52, 1014-1019.

114. Lennox, A. J. J.; Lloyd-Jones, G. C. Selection of boron reagents for Suzuki–Miyaura coupling. *Chem. Soc. Rev.* **2014**, 43, 412-443.
115. Lennox, A. J. J.; Lloyd-Jones, G. C. The Slow-Release Strategy in Suzuki-Miyaura Coupling. *Israel Journal of Chemistry* **2010**, 50, 664-674.
116. Kotha, S.; Lahiri, K.; Kashinath, D. Recent applications of the Suzuki–Miyaura cross-coupling reaction in organic synthesis. *Tetrahedron* **2002**, 58, 9633-9695.
117. Stanforth, S. P. Catalytic cross-coupling reactions in biaryl synthesis. *Tetrahedron* **1998**, 54, 263-303.
118. Suzuki, A. Recent advances in the cross-coupling reactions of organoboron derivatives with organic electrophiles, 1995–1998. *Journal of Organometallic Chemistry* **1999**, 576, 147-168.
119. Moore, L. R.; Shaughnessy, K. H. Efficient Aqueous-Phase Heck and Suzuki Couplings of Aryl Bromides Using Tri(4,6-dimethyl-3-sulfonatophenyl)phosphine Trisodium Salt (TXPTS). *Organic Letters* **2004**, 6, 225-228.
120. Thompson, D. P.; Boudjouk, P. A convenient synthesis of alkali metal selenides and diselenides in tetrahydrofuran and the reactivity differences exhibited by these salts toward organic bromides. Effect of ultrasound. *The Journal of Organic Chemistry* **1988**, 53, 2109-2112.
121. Skehan, P.; Storeng, R.; Scudiero, D.; Monks, A.; McMahon, J.; Vistica, D.; Warren, J. T.; Bokesch, H.; Kenney, S.; Boyd, M. R. New Colorimetric Cytotoxicity Assay for Anticancer-Drug Screening. *JNCI Journal of the National Cancer Institute* **1990**, 82, 1107-1112.
122. Vichai, V.; Kirtikara, K. Sulforhodamine B colorimetric assay for cytotoxicity screening. *Nat Protoc* **2006**, 1, 1112-6.
123. Cell lines. https://www.lgcstandards-atcc.org/Products/Cells_and_Microorganisms/Cell_Lines.aspx?geo_country=ro (30 may 2019).
124. Thompson, A.; Brennan, K.; Cox, A.; Gee, J.; Harcourt, D.; Harris, A.; Harvie, M.; Holen, I.; Howell, A.; Nicholson, R.; Steel, M.; Streuli, C. Evaluation of the current knowledge limitations in breast cancer research: a gap analysis. *Breast Cancer Research* **2008**, 10.
125. Lacroix, M.; Leclercq, G. Relevance of Breast Cancer Cell Lines as Models for Breast Tumours: An Update. *Breast Cancer Research and Treatment* **2004**, 83, 249-289.
126. Vargo-Gogola, T.; Rosen, J. M. Modelling breast cancer: one size does not fit all. *Nat Rev Cancer* **2007**, 7, 659-72.
127. Côte-Real, M., Sansonetty, F., Ludovico, P., Prudêncio, C., Rodrigues, F., Fortuna, M., Sousa, M. Contributos da citologia analítica para estudos de biologia de leveduras. *Boletim de Biotecnologia* **2002**, 71.
128. Rieger, A. M.; Nelson, K. L.; Konowalchuk, J. D.; Barreda, D. R. Modified Annexin V/Propidium Iodide Apoptosis Assay For Accurate Assessment of Cell Death. *Journal of Visualized Experiments* **2011**.
129. Chaudhary, P.; Sharma, R.; Sahu, M.; Vishwanatha, J. K.; Awasthi, S.; Awasthi, Y. C. 4-Hydroxynonenal Induces G2/M Phase Cell Cycle Arrest by Activation of the Ataxia Telangiectasia Mutated and Rad3-related Protein (ATR)/Checkpoint Kinase 1 (Chk1) Signaling Pathway. *Journal of Biological Chemistry* **2013**, 288, 20532-20546.
130. Lüpertz, R.; Wätjen, W.; Kahl, R.; Chovolou, Y. Dose- and time-dependent effects of doxorubicin on cytotoxicity, cell cycle and apoptotic cell death in human colon cancer cells. *Toxicology* **2010**, 271, 115-121.
131. Siu, W. Y.; Yam, C. H.; Poon, R. Y. C. G1 versus G2 cell cycle arrest after adriamycin-induced damage in mouse Swiss3T3 cells. *FEBS Letters* **1999**, 461, 299-305.

132. Kaufmann, S. H.; Desnoyers, S.; Ottaviano, Y.; Davidson, N. E.; Poirier, G. G. Specific proteolytic cleavage of poly(ADP-ribose) polymerase: an early marker of chemotherapy-induced apoptosis. *Cancer Res* **1993**, *53*, 3976-85.
133. Karimian, A.; Ahmadi, Y.; Yousefi, B. Multiple functions of p21 in cell cycle, apoptosis and transcriptional regulation after DNA damage. *DNA Repair (Amst)* **2016**, *42*, 63-71.
134. Gillett, C.; Smith, P.; Gregory, W.; Richards, M.; Millis, R.; Peters, G.; Barnes, D. Cyclin D1 and prognosis in human breast cancer. *Int J Cancer* **1996**, *69*, 92-9.
135. Kuo, L. J.; Yang, L. X. Gamma-H2AX - a novel biomarker for DNA double-strand breaks. *In Vivo* **2008**, *22*, 305-9.
136. Collins, A. R. The Comet Assay for DNA Damage and Repair: Principles, Applications, and Limitations. *Molecular Biotechnology* **2004**, *26*, 249-261.
137. Scaife, R. M. G2 cell cycle arrest, down-regulation of cyclin B, and induction of mitotic catastrophe by the flavoprotein inhibitor diphenylethidium. *Mol Cancer Ther* **2004**, *3*, 1229-37.
138. Traxler, P.; Furet, P. Strategies toward the Design of Novel and Selective Protein Tyrosine Kinase Inhibitors. *Pharmacology & Therapeutics* **1999**, *82*, 195-206.
139. Keating, G. M.; Santoro, A. Sorafenib. *Drugs* **2009**, *69*, 223-240.
140. Marisi, G.; Cucchetti, A.; Ulivi, P.; Canale, M.; Cabibbo, G.; Solaini, L.; Foschi, F. G.; Matteis, S. D.; Ercolani, G.; Valgiusti, M.; Frassinetti, G. L.; Scartozzi, M.; Gardini, A. C. Ten years of sorafenib in hepatocellular carcinoma: Are there any predictive and/or prognostic markers? *World Journal of Gastroenterology* **2018**, *24*, 4152-4163.
141. Bronte, G.; Andreis, D.; Bravaccini, S.; Maltoni, R.; Cecconetto, L.; Schirone, A.; Farolfi, A.; Fedeli, A.; Serra, P.; Donati, C.; Amadori, D.; Rocca, A. Sorafenib for the treatment of breast cancer. *Expert Opinion on Pharmacotherapy* **2017**, *18*, 621-630.
142. Folkman, J. What Is the Evidence That Tumors Are Angiogenesis Dependent? *JNCI: Journal of the National Cancer Institute* **1990**, *82*, 4-7.
143. Savjani, K. T.; Gajjar, A. K.; Savjani, J. K. Drug Solubility: Importance and Enhancement Techniques. *ISRN Pharmaceutics* **2012**, *2012*, 1-10.
144. Zafar, A.; Pilkington, L.; Haverkate, N.; van Rensburg, M.; Leung, E.; Kumara, S.; Denny, W.; Barker, D.; Alsuraifi, A.; Hoskins, C.; Reynisson, J. Investigation into Improving the Aqueous Solubility of the Thieno[2,3-b]pyridine Anti-Proliferative Agents. *Molecules* **2018**, *23*.
145. Zanoni, M.; Piccinini, F.; Arienti, C.; Zamagni, A.; Santi, S.; Polico, R.; Bevilacqua, A.; Tesei, A. 3D tumor spheroid models for in vitro therapeutic screening: a systematic approach to enhance the biological relevance of data obtained. *Scientific Reports* **2016**, *6*.